

THE SOLUTION OF THE CAUCHY PROBLEM WITH LARGE DATA FOR A MODEL OF A MIXTURE OF GASES

HELGE HOLDEN, NILS HENRIK RISEBRO, AND HILDE SANDE

ABSTRACT. In this paper we study mixture of gases, each governed by a gamma law. The system is modeled by the p -system with variable gamma. We use this model to study immiscible gas flow. The main result is that the Cauchy problem with large data is shown to have a solution. We use the Glimm scheme for the proof. The result is illustrated by numerical examples.

1. INTRODUCTION

We want to describe the one dimensional flow for several isentropic gases. The different gases are initially separated, and the pressure is for all gases given by a γ -law, that is, $p = \rho^\gamma$, where ρ is the density and γ is the adiabatic gas constant for each gas. The different gases cannot mix, therefore, in Lagrangian coordinates γ only depends on x and does not change in time. The flow of these gases is thus in Lagrangian coordinates described for $x \in \mathbb{R}$ and $t \in (0, \infty)$ by the system

$$(1.1) \quad \begin{aligned} v_t - u_x &= 0, \\ u_t + p(v, \gamma)_x &= 0, \\ \gamma_t &= 0, \end{aligned}$$

where $v = 1/\rho$ is the specific volume, u is the velocity, and $p(v, \gamma) = v^{-\gamma}$ is the pressure function. We assume $\gamma(x, t) > 1$. This 3×3 system of hyperbolic conservation laws is strictly hyperbolic. The first and third family are genuinely nonlinear and the second family is linearly degenerate.

We consider the Cauchy problem for this system, that is, the system (1.1) with general initial data

$$(1.2) \quad v(x, 0) = v_0(x), \quad u(x, 0) = u_0(x), \quad \gamma(x, 0) = \gamma_0(x), \quad x \in \mathbb{R}.$$

Glimm [9] proved global existence of a weak solution of the Cauchy problem with small initial data for strictly hyperbolic systems where each family is either genuinely nonlinear or linearly degenerate, thus including the present system. This solution is found by using the Glimm scheme [9, 19, 20] or by using front tracking [11] by which one can prove stability of the Cauchy problem. Here we extend the existence result to large initial data for (1.1).

System (1.1) is an extension of the 2×2 system known as the p -system,

$$(1.3) \quad \begin{aligned} v_t - u_x &= 0, \\ u_t + p(v)_x &= 0, \end{aligned}$$

which describes the flow of an isentropic gas, with only one gas is present here, thus γ is constant and the pressure, still given by a γ -law, is a function of v only.

For the p -system with $\gamma = 1$, Nishida [15] showed existence of a global solution for arbitrary bounded initial data. For $\gamma > 1$, Nishida and Smoller [16] proved existence of a solution for initial data where $(\gamma - 1)$ times the total variation of the initial data is sufficiently small. The case with large initial data for 2×2 systems is also discussed in [6, 4].

System (1.1) does not have a coordinate system of Riemann invariants, only a 2-Riemann coordinate. Therefore we do not have the advantage of changing variables to Riemann invariants as for the p -system and other 2×2 systems. Liu [12] proved existence of a solution for the full Euler system with large initial data, another 3×3 system without a coordinate system of Riemann invariants. Liu's change of variables is inspired by the use of Riemann invariants, but a similar approach does not simplify system (1.1), because γ is a function of x . The general results by Temple [21] includes both the results of [16] and [12]. In [21] one considers the flux function as a smooth one parameter family of functions where one has existence of a solution for arbitrary large initial data for the system with the parameter, ϵ , equal to zero. Then the system with $0 \leq \epsilon \leq 1$ has a unique solution if ϵ times the total variation of the initial data is sufficiently small. Letting $\epsilon = \gamma - 1$ for the p -system and the Euler equations, one obtains similar results as in [16] and [12]. However, this cannot be used for system (1.1) since γ is one of the variables. Wissman proves in [25] a large data existence theorem for the 3×3 system of relativistic Euler equations in the ultra-relativistic limit. Applying a change of coordinates the shock waves become translation invariant and a Nishida-type of analysis is used.

For 3×3 systems with a 2-Riemann coordinate, Temple and Young [22] showed existence of a solution for initial data with arbitrary large total variation, provided that the oscillations are small. This result applies to our system as well, but we want to avoid this restriction on the oscillations. Peng [18, 17] also considered certain 3×3 systems (Lagrangian gas dynamics for a perfect gas and a model originating in multiphase flow modeling) with large initial data.

All these existence results are proved using the Glimm scheme. Asakura applies front tracking to show existence of a solution for the p -system [3] and for the Euler equations [2] with large initial data. The conditions on the initial data are the same as obtained in [16] and [12].

Amadori and Corli [1] extend the p -system with an extra equation, $\lambda_t = 0$, to model multiphase flow, and they use front tracking to prove existence of a weak solution. As for system (1.1), the pressure function in [1] is a function of both v and the new variable, λ , making the two systems similar. However, since the adiabatic gas constant, γ , is equal to one in [1], vacuum can never occur for their system as it can for system (1.1). Furthermore, the wave curves in [1] are monotone in λ , resulting in a considerably simpler analysis of the wave interactions compared to the system considered here. The system treated in [1] is a simplified version of the model discussed by Fan in [8]. Similar models, but with a rather different pressure law, are also considered in [7] and [14] applying completely different methods. A model in the context of the Navier–Stokes equation with finitely many independent pressure laws has been studied in [5].

System (1.1) can also be rewritten as a 2×2 system with discontinuous flux. We get

$$\begin{aligned} v_t - u_x &= 0, \\ u_t + p(v, \gamma(x))_x &= 0, \end{aligned}$$

where the adiabatic gas constant of the different gases is given by the discontinuous function $\gamma(x)$.

This paper is organized as follows: In Section 2 we discuss the wave curves of the system. The variable γ is constant along the rarefaction and shock waves of the first and third family, therefore these curves are similar to the wave curves of the p -system. However, these curves are not monotone in γ , which considerably complicates the interactions of waves with different values of γ . The second family is linearly degenerate and gives rise to a contact discontinuity along which p and u are constant. Thus, by changing variables to p , u and γ , the Riemann problem is easy to describe. The invariant region for the Riemann problem includes vacuum. This is a problem since the interaction estimates are not valid when p tends to zero, see [13].

In Section 3 we describe the Glimm scheme and discuss all possible interactions before we define the Glimm functional. In Lemma 3.3 we give the conditions needed on the initial data for the Glimm functional to be decreasing in time. The main part of this paper is the proof of Lemma 3.3, and we devote Section 4 to this. Here all possible interactions are discussed, estimates are found and we show that the Glimm functional is decreasing for each of them. The presentation aims at being self-contained.

In Section 5 we show convergence, and Lemma 5.1 states that given some conditions on the total variation of the initial data, we have stability of the total variation. This follows from the decreasing Glimm functional and is only valid when the approximate solution is bounded away from vacuum. The conditions for this is given by Lemma 5.2. The main result reads as follows:

Theorem 5.3. *The Cauchy problem for system (1.1) has a global, weak solution if $(\sup(\gamma) - 1)\text{T.V.}(p(\cdot, 0), u(\cdot, 0))$ and $\text{T.V.}(\gamma(\cdot, 0))$ are sufficiently small.*

Observe that by reducing the total variation of γ and reducing its supremum, one can allow for large total variation of p and u . Due to Wagner [23], this result translates into existence for the system in Eulerian coordinates as stated in Theorem 5.4.

In the last section we study two examples numerically. In the first example we have one gas confined to an interval, surrounded by another gas. The two gases have distinct but constant gammas. The constants that limit the total variation of the initial data are computed, and the initial data are chosen so that they satisfy the conditions in the theorem. The Glimm functional is explicitly computed, and shown to decay in accordance with the theorem. In the second example we consider a case with a continuously varying gamma. Again the initial data are chosen so that they satisfy the explicitly computed constants that appear in Theorem 5.3. Finally, the decaying Glimm functional is computed and displayed for this example.

Further numerical experiments reveal that, as expected, the Glimm functional decays also in cases where the fairly stringent restrictions on the initial data are violated. A necessary condition for the Glimm scheme to work is that the Riemann problems that occur all are solvable, but no conjecture as to the maximum size of the Glimm functional can be made at this stage.

We intend to discuss the same system using the front-tracking method in a subsequent paper. The basic interactions between two waves (fronts) in front-tracking are similar to those of the Glimm scheme. Interactions between more waves (fronts) are different from the interactions discussed in Section 4, but the

same methods apply. In addition, the front-tracking method requires a close control of the number of fronts at all times, possibly by removing weak fronts according to some measure. These issues are not yet fully resolved for our system, therefore we choose to use the Glimm scheme in this paper.

2. THE SYSTEM

It is well-known that systems of hyperbolic conservation laws such as (1.1) do not in general have smooth solutions, even for smooth initial data. Thus, by a solution of (1.1) with the initial data (1.2) we mean a *weak solution* in the distributional sense with $v, u, \gamma \in L^\infty(\mathbb{R} \times [0, \infty))$ so that

$$\begin{aligned} \iint_{\mathbb{R} \times [0, \infty)} (v\phi_t - u\phi_x) \, dxdt + \int_{\mathbb{R}} v_0(x)\phi(x, 0) \, dx &= 0, \\ \iint_{\mathbb{R} \times [0, \infty)} (u\phi_t + p\phi_x) \, dxdt + \int_{\mathbb{R}} u_0(x)\phi(x, 0) \, dx &= 0, \\ \iint_{\mathbb{R} \times [0, \infty)} \gamma\phi_t \, dxdt + \int_{\mathbb{R}} \gamma_0(x)\phi(x, 0) \, dx &= 0, \end{aligned}$$

for all infinitely differentiable functions $\phi(x, t)$ with compact support.

If the specific volume, v , becomes infinite, which corresponds to zero density and zero pressure, we have *vacuum*. At vacuum, the properties of the system change and the methods used here do not apply, therefore we only consider system (1.1) for $v(x, t) < \infty$. Furthermore, we assume $\gamma(x, t) > 1$.

We write $U(x, t) = (v(x, t), u(x, t), \gamma(x, t))$. Often we will work with p instead of v , and then also write $U(x, t) = (p(x, t), u(x, t), \gamma(x, t))$.

For $v < \infty$, or equivalently, $p > 0$, the system (1.1) is strictly hyperbolic with eigenvalues

$$(2.1) \quad \lambda_1 = -\lambda, \quad \lambda_2 = 0, \quad \lambda_3 = \lambda,$$

where $\lambda := \sqrt{-p_v} = \sqrt{\gamma v^{-\gamma-1}}$, and corresponding eigenvectors

$$(2.2) \quad r_1 = (1, \lambda, 0), \quad r_2 = (-p_\gamma, 0, p_v), \quad r_3 = (-1, \lambda, 0).$$

Note that the eigenvalues and eigenvectors do not depend on u . The first and the third family are genuinely nonlinear, while the second family is linearly degenerate. Moreover, the system does not possess a coordinate system of Riemann invariants, but γ is a Riemann coordinate for the second family.

Before we can turn to solving system (1.1) for general initial data, we need to solve the Riemann problem for (1.1), that is, when the initial data consists of two constant states separated by a jump, cf. (2.26). The solution of the Riemann problem consists of up to three elementary *waves*, one from each family, and up to two intermediate constant states separating these waves. Thus, we start by looking at the wave curves.

2.1. Wave curves. For a genuinely nonlinear family there are two types of waves; *rarefaction waves* which are continuous waves of the form $U(x, t) = w(x/t)$ satisfying

$$(2.3) \quad \dot{w}(x/t) = r_j(w(x/t)), \quad \lambda_j(w(x/t)) = x/t, \quad j = 1, 3,$$

where λ_j is increasing along the wave, and *shock waves* which are solutions

$$(2.4) \quad U(x, t) = \begin{cases} U_l, & \text{if } x < \sigma t, \\ U_r, & \text{if } x > \sigma t, \end{cases}$$

satisfying the Rankine–Hugoniot condition

$$(2.5) \quad \sigma(U_r - U_l) = f(U_r) - f(U_l),$$

for a shock velocity σ . The admissible shock waves are those satisfying the Lax entropy conditions

$$(2.6) \quad \lambda_{j-1}(U_l) < \sigma < \lambda_j(U_l), \quad \lambda_j(U_r) < \sigma < \lambda_{j+1}(U_r), \quad j = 1, 3.$$

For the linearly degenerate family $j = 2$ there is only one type of waves called *contact discontinuities*. These waves are solutions of the form (2.4) that satisfy the Rankine–Hugoniot condition (2.5) with $\sigma = \lambda_2$.

We fix a left state U_l . For each family the *wave curve* consists of all states U that can be connected to the given left state by a wave of this family. The rarefaction solution is of the form

$$(2.7) \quad U(x, t) = \begin{cases} U_l, & \text{if } x < \lambda_j(U_l)t, \\ w(x/t), & \text{if } \lambda_j(U_l)t < x < \lambda_j(U)t, \\ U, & \text{if } x > \lambda_j(U)t. \end{cases}$$

The rarefaction wave curve is the set of all right states U that can be connected to the left state by a rarefaction wave. For system (1.1) these are

$$\begin{aligned} R_1(v, U_l) &:= \left(v, u_l - \frac{2\sqrt{\gamma l}}{\gamma l - 1} \left(v^{\frac{1-\gamma l}{2}} - v_l^{\frac{1-\gamma l}{2}} \right), \gamma l \right), & v > v_l, \\ R_3(v, U_l) &:= \left(v, u_l + \frac{2\sqrt{\gamma l}}{\gamma l - 1} \left(v^{\frac{1-\gamma l}{2}} - v_l^{\frac{1-\gamma l}{2}} \right), \gamma l \right), & v < v_l. \end{aligned}$$

The shock curves of all states which can be connected to U_l by an admissible shock wave are

$$\begin{aligned} S_1(v, U_l) &:= \left(v, u_l - ((v_l - v)(v^{-\gamma} - v_l^{-\gamma}))^{1/2}, \gamma l \right), & v < v_l, \\ S_3(v, U_l) &:= \left(v, u_l - ((v_l - v)(v^{-\gamma} - v_l^{-\gamma}))^{1/2}, \gamma l \right), & v > v_l, \end{aligned}$$

with the shock velocities

$$(2.8) \quad \sigma_1(U_l, U_r) = -\sqrt{\frac{v_l^{-\gamma} - v^{-\gamma}}{v - v_l}} = -\sqrt{\frac{p_l - p}{p^{-1/\gamma_l} - p^{-1/\gamma}}},$$

$$(2.9) \quad \sigma_3(U_l, U_r) = \sqrt{\frac{v^{-\gamma} - v_l^{-\gamma}}{v_l - v}} = \sqrt{\frac{p - p_l}{p_l^{-1/\gamma_l} - p^{-1/\gamma}}},$$

respectively. Note that the shock velocities do not depend on u . The curve of all right states which can be connected to U_l by a contact discontinuity is

$$C_2(\gamma, U_l) := \left(v_l^{\gamma/\gamma}, u_l, \gamma \right), \quad \gamma > 1,$$

with the velocity $\sigma_2 = \lambda_2 = 0$.

Note that γ only changes along the contact discontinuities. Furthermore, both u and $p = v^{-\gamma}$ are constant along a contact discontinuity, and we therefore choose to

work with p , u and γ . A shock or a rarefaction curve through U_l lies in the plane $\gamma = \gamma_l$ and is equal to the corresponding wave curve for the p -system (1.3) with $\gamma = \gamma_l$. We proceed by defining the wave curves using p , u , and γ ;

$$(2.10) \quad \Phi_1(p, U_l) := \begin{cases} (p, u_l - r(p, p_l, \gamma_l), \gamma_l), & p < p_l, \\ (p, u_l - s(p, p_l, \gamma_l), \gamma_l), & p > p_l, \end{cases}$$

$$(2.11) \quad \Phi_2(\gamma, U_l) := (p_l, u_l, \gamma), \quad \gamma > 1,$$

$$(2.12) \quad \Phi_3(p, U_l) := \begin{cases} (p, u_l + r(p, p_l, \gamma_l), \gamma_l), & p > p_l, \\ (p, u_l - s(p, p_l, \gamma_l), \gamma_l), & p < p_l, \end{cases}$$

where

$$(2.13) \quad r(p, p_l, \gamma_l) := \frac{2\sqrt{\gamma_l}}{\gamma_l - 1} \left(p^{\frac{\gamma_l - 1}{2\gamma_l}} - p_l^{\frac{\gamma_l - 1}{2\gamma_l}} \right),$$

$$(2.14) \quad s(p, p_l, \gamma_l) := \left(\left(p_l^{-\frac{1}{\gamma_l}} - p^{-\frac{1}{\gamma_l}} \right) (p - p_l) \right)^{1/2}.$$

Recall that if $p = 0$, we have vacuum, and thus the wave curves are only well-defined for $p > 0$ and $p_l > 0$. All results are for waves contained in

$$(2.15) \quad \mathcal{D} = \{(p, u, \gamma) \mid p \in [p_{\min}, p_{\max}], |u| < \infty, \gamma \in (1, \bar{\gamma}]\},$$

where $p_{\min} > 0$, $p_{\max} < \infty$ and $\bar{\gamma} \in (1, \infty)$ are constants. For initial data given by (1.2) we will later establish the upper and lower bound on p and argue that

$$(2.16) \quad \bar{\gamma} := \sup_x (\gamma_0(x)),$$

for all waves.

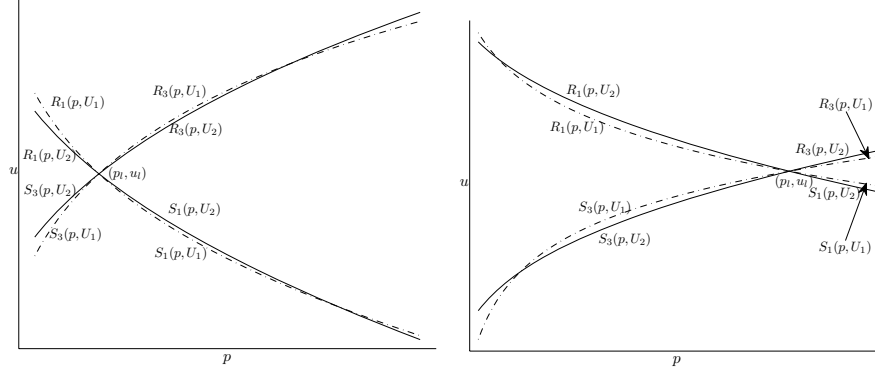
The projection onto the (p, u) -plane of two wave curves with different γ 's are shown in Fig. 1. Note that the projected curves intersect. Before we discuss this and other important properties of the wave curves, we mention the *backward wave curves*. These are the curves of all left states U that can be connected to a given right state U_r by a wave of the given family. We denote these wave curves by $\tilde{\Phi}_i$. We will use the backward 3-wave curve several times and this is given by

$$(2.17) \quad \tilde{\Phi}_3(p, U_r) := \begin{cases} (p, u_r - r(p_r, p, \gamma_r), \gamma_r), & p < p_r, \\ (p, u_r + s(p_r, p, \gamma_r), \gamma_r), & p > p_r, \end{cases}$$

where r and s are given by (2.13) and (2.14). We now turn to the properties of the wave curves.

Lemma 2.1. *Assume that the wave curves are contained in \mathcal{D} . Then they have the following properties:*

- (i) *Viewed as functions of p , Φ_1 is strictly decreasing and Φ_3 is strictly increasing.*
- (ii) *Given two wave curves, $\Phi_j(p, U_1)$ and $\Phi_j(p, U_2)$ where $j \in \{1, 3\}$, so that U_1 is not on $\Phi_j(p, U_2)$ and U_2 is not on $\Phi_j(p, U_1)$. Then the two wave curves never intersect. Moreover, if $\gamma_1 = \gamma_2$, then also the projected wave curves onto the (p, u) -plane never intersect. However, if $\gamma_1 \neq \gamma_2$, then the projected wave curves can intersect.*



- (a) The projected curves going to the left do not intersect, while the curves going to the right do.
- (b) The projected curves going to the left intersect, while the curves going to the right do not.

FIGURE 1. The wave curves through $U_1 = (p_l, u_l, \gamma_1)$ (dotted line) and $U_2 = (p_l, u_l, \gamma_2)$, where $\gamma_1 < \gamma_2$, projected onto the (p, u) -plane are depicted for two different values of the parameters.

- (iii) Consider the projections onto the (p, u) -plane of the wave curves through $U_1 = (p_l, u_l, \gamma_1)$ and $U_2 = (p_l, u_l, \gamma_2)$ where $\gamma_1 \leq \gamma_2$. If

$$\frac{\partial}{\partial p} r(p_l, p_l, \gamma_1) < \frac{\partial}{\partial p} r(p_l, p_l, \gamma_2),$$

then the projected wave curves going to the right (with respect to p) will never intersect, while the projected wave curves going to the left will intersect as p decreases. If

$$\frac{\partial}{\partial p} r(p_l, p_l, \gamma_1) > \frac{\partial}{\partial p} r(p_l, p_l, \gamma_2),$$

then the projected wave curves going to the right will intersect, while the projected wave curves going to the left will not. If

$$\frac{\partial}{\partial p} r(p_l, p_l, \gamma_1) = \frac{\partial}{\partial p} r(p_l, p_l, \gamma_2),$$

then none of the projected wave curves will intersect.

- (iv) The slope of a rarefaction wave in the plane $\gamma = \gamma_l$, $\partial r / \partial p$, only depends on p and γ_l , not on p_l . Furthermore, there exist two constants r'_{\min} and r'_{\max} only depending on p_{\min} , p_{\max} and $\bar{\gamma}$ so that

$$r'_{\min} \leq \frac{\partial}{\partial p} r(p, p_l, \gamma_l) \leq r'_{\max}.$$

- (v) The slope of a shock wave in the plane $\gamma = \gamma_l$, $\partial s / \partial p$, depends on p , γ_l and p_l . Furthermore, there exist two constants s'_{\min} and s'_{\max} only depending on p_{\min} , p_{\max} and $\bar{\gamma}$ so that

$$s'_{\min} \leq \frac{\partial}{\partial p} s(p, p_l, \gamma_l) \leq s'_{\max}.$$

(vi) The wave curves have a continuous derivative at U_l ,

$$\lim_{p \rightarrow p_l} \frac{\partial}{\partial p} s(p, p_l, \gamma_l) = \frac{\partial}{\partial p} r(p_l, p_l, \gamma_l).$$

Furthermore,

$$\frac{\partial}{\partial p} s(p, p_l, \gamma_l) \geq \frac{\partial}{\partial p} r(p, p_l, \gamma_l),$$

for all p_l . Hence, a shock wave is always steeper than a rarefaction wave at a given $p \neq p_l$ provided both waves lie in the plane $\gamma = \gamma_l$.

(vii) Rarefaction waves are additive; if a rarefaction wave connects U_1 to U_2 and another rarefaction wave of the same family connects U_2 to U_3 , then the rarefaction wave connecting U_1 to U_3 equals the sum of the other two rarefaction waves.

(viii) Given two 1-shock waves starting at (p_1, u, γ) and (p_2, u, γ) , respectively, and assume $p_1 < p_2$. Then the shock wave starting at p_1 is steeper than the shock wave starting at p_2 at any given point p , that is,

$$\frac{\partial}{\partial p} s(p, p_2, \gamma) < \frac{\partial}{\partial p} s(p, p_1, \gamma),$$

for all $p \geq p_2 > p_1$.

(ix) Given two 3-shock waves starting at (p_1, u, γ) and (p_2, u, γ) , respectively, and assume $p_1 < p_2$. Then the shock wave starting at p_2 is steeper than the shock wave starting at p_1 at any given point p , that is,

$$\frac{\partial}{\partial p} s(p, p_1, \gamma) < \frac{\partial}{\partial p} s(p, p_2, \gamma),$$

for all $p \leq p_1 < p_2$.

Proof. All the properties follows from differentiating the wave curves. \square

According to the above lemma, the slopes of the projected wave curves onto the (p, u) -plane depend on γ . The next lemma gives an estimate on how different two waves with different γ 's are.

Lemma 2.2. *Let ϵ_1 and ϵ_2 be 1-waves of the same type such that ϵ_1 connects (p_0, u_0, γ_1) to (p, u_1, γ_1) and ϵ_2 connects (p_0, u_0, γ_2) to (p, u_2, γ_2) , or let η_1 and η_2 be 3-waves of the same type such that η_1 connects (p, u_1, γ_1) to (p_0, u_0, γ_1) and η_2 connects (p, u_2, γ_2) to (p_0, u_0, γ_2) . Assume that all waves are contained in \mathcal{D} and furthermore that $u_1 < u_2$. Then*

$$(2.18) \quad u_2 - u_1 \leq c_2 |p - p_0| |\gamma_2 - \gamma_1|,$$

where c_2 only depends on p_{\min} , p_{\max} and $\bar{\gamma}$.

Note that for 1-waves we compare two waves where the projected waves start at the same point in the (p, u) -plane, while we for 3-waves compare two waves where the projected waves end at the same point. The proof is based on the same techniques as used in [24].

Proof. Since the projection of the 3-waves end at the same point, we make use of the 3-backward wave curves. The projected (backward) wave curves can be described

by a function of two variables,

$$(2.19) \quad u(p, \gamma) = \begin{cases} u_0 - s(p, p_0, \gamma), & p > p_0, & \text{for 1-shock waves,} \\ u_0 - r(p, p_0, \gamma), & p < p_0, & \text{for 1-rarefaction waves,} \\ u_0 + s(p_0, p, \gamma), & p > p_0, & \text{for 3-shock waves,} \\ u_0 - r(p_0, p, \gamma), & p < p_0, & \text{for 3-rarefaction waves,} \end{cases}$$

where $u(p_0, \gamma_1) = u(p_0, \gamma_2) = u_0$, $u(p, \gamma_1) = u_1$ and $u(p, \gamma_2) = u_2$ for all cases. Figure 2 illustrates this when the waves are 1-shocks. If the two wave curves do

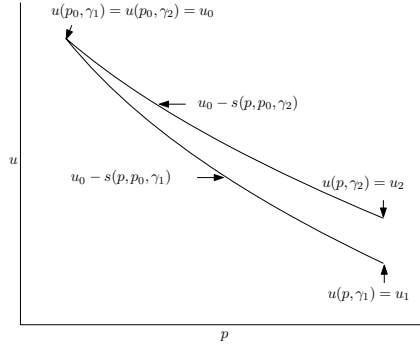


FIGURE 2. When ϵ_1 and ϵ_2 of Lemma 2.2 are 1-shocks.

not intersect between p_0 and p , then

$$(2.20) \quad \int_{\gamma_1}^{\gamma_2} \int_{p_0}^p u_{p\gamma}(s, t) \, ds \, dt = u(p, \gamma_2) - u(p, \gamma_1) - u(p_0, \gamma_2) + u(p_0, \gamma_1),$$

where $u_{p\gamma}$ denotes the second order partial derivative with respect to p and γ . If the two wave curves intersect at $p = p_m$, then we integrate from p_m to p and replace p_0 by p_m at the right-hand side. This will give us an even stronger estimate than (2.18), and therefore we can assume for the rest of the proof that the wave curves do not intersect.

If we can show that $|u_{p\gamma}| \leq c_2$, where c_2 is a constant only depending on p_{\min} , p_{\max} and $\bar{\gamma}$, then

$$\begin{aligned} u_2 - u_1 &= u(p, \gamma_2) - u(p, \gamma_1) - u(p_0, \gamma_2) + u(p_0, \gamma_1) \\ &= \int_{\gamma_1}^{\gamma_2} \int_{p_0}^p u_{p\gamma}(s, t) \, ds \, dt \leq c_2 |\gamma_2 - \gamma_1| |p - p_0|, \end{aligned}$$

and we have proved (2.18).

Let us first consider when the waves are either 1- or 3-rarefaction waves. Then we find that

$$(2.21) \quad \frac{\partial^2 r}{\partial p \partial \gamma}(p, p_0, \gamma) = -\frac{\partial^2 r}{\partial p \partial \gamma}(p_0, p, \gamma) = \frac{1}{2} \gamma^{-5/3} p^{-(1+\gamma)/2\gamma} (\ln p - \gamma).$$

For a fixed γ , we see that (2.21) is negative for $\ln p < \gamma$. By differentiating (2.21) with respect to p , we find that it is increasing in p until it reaches its maximum value,

$$0 < \gamma^{-\frac{2}{3}} \exp\left(-\frac{3+\gamma}{2}\right) \leq 1,$$

at $\ln p = \gamma(3+\gamma)/(1+\gamma)$. After this point, (2.21) is strictly decreasing towards zero as p grows large. Thus, if $\ln p_{\min} \leq \gamma$, then the minimum value of (2.21) is obtained at $p = p_{\min}$, otherwise (2.21) is positive for all $p_{\min} \leq p \leq p_{\max}$. Define

$$(2.22) \quad c := \max_{\gamma \in (1, \bar{\gamma})} \frac{1}{2} \gamma^{-5/3} p_{\min}^{-(1+\gamma)/2\gamma} |\ln p_{\min} - \gamma|,$$

which is a constant depending only on p_{\min} and $\bar{\gamma}$. We conclude that when the waves are either 1- or 3-rarefaction waves, then

$$|u_{p\gamma}| \leq \max\{c, 1\}.$$

For shock waves we have

$$(2.23) \quad \frac{\partial^2 s}{\partial p \partial \gamma}(p, p_0, \gamma) = -\frac{\partial^2 s}{\partial p \partial \gamma}(p_0, p, \gamma) = f,$$

where

$$(2.24) \quad f := \frac{-s p^{-\frac{\gamma+1}{\gamma}}(p-p_0) + \gamma(p_0^{-\frac{1}{\gamma}} \ln p_0 - p^{-\frac{1}{\gamma}} \ln p)((p-p_0)\frac{\partial s}{\partial p} + s)}{2\gamma^3 s^2},$$

and $s = s(p, p_0, \gamma)$. By differentiating with respect to p , we find that (2.24) does in general behave similar to (2.21); its minimum value is obtained at the limit when p tends to p_0 , and this limit equals the value of (2.21) at $p = p_0$. Furthermore, also (2.24) increases until it reaches its maximum value, which is positive and less than one, before it decreases towards zero as p grows large. However, (2.24) does depend on p_0 while (2.21) does not, therefore the two expressions behave different for small p_0 . Then (2.24) is negative and increasing for all p , but still its minimum value is obtained at the limit when p goes to p_0 . Therefore,

$$|u_{p\gamma}| \leq \max\{c, 1\},$$

also when the waves are shock waves where c is given by (2.22). We define

$$(2.25) \quad c_2 := \max\{c, 1\},$$

and conclude that $|u_{p\gamma}| \leq c_2$ for u given by any of the cases in (2.19), and for all $p \in [p_{\min}, p_{\max}]$ and $\gamma \in (1, \bar{\gamma}]$. This ends the proof of the lemma. \square

2.2. The Riemann Problem. We have the following fundamental definition.

Definition 2.3. The Riemann problem for (1.1) is the Cauchy problem with initial data

$$(2.26) \quad U(x, 0) = \begin{cases} U_l, & \text{if } x < 0, \\ U_r, & \text{if } x > 0, \end{cases}$$

where $U = (v, u, \gamma)$ and $U_l, U_r \in \mathbb{R}^3$ are constants.

Lemma 2.4. *The Riemann problem for (1.1) where U_l and U_r are contained in \mathcal{D} , cf. (2.15), has a unique solution with no vacuum if*

$$(2.27) \quad u_r - u_l < r(p_r, 0, \gamma_r) - r(0, p_l, \gamma_l).$$

Proof. Note that if $\gamma_l = \gamma_r$, then the Riemann problem for (1.1) reduces to the Riemann problem for the p -system (1.3). The solution of this problem is described in detail in [20, Ch. 17, §A], and it is unique if (2.27) is satisfied with $\gamma_l = \gamma_r$.

A 2-wave takes us from one plane, $\gamma = \gamma_1$, to another plane, $\gamma = \gamma_2$, while p and u remain constant. Therefore, the Riemann problem has a unique solution if the projections onto the (p, u) -plane of the 1-wave curve, $\Phi_1(p, U_l)$, and the backward 3-wave curve, $\tilde{\Phi}_3(p, U_r)$, have a unique intersection point. From property (i) we have that the projection of Φ_1 is strictly decreasing in p and it follows that the projection of $\tilde{\Phi}_3$ is strictly increasing in p . Hence, the projected curves intersect at most once. The only case where the two curves do not intersect is if the projection of the backward 3-rarefaction wave from U_r always lies above the projection of the 1-rarefaction wave from U_l . Thus, if

$$u_r - r(p_r, 0, \gamma_r) < u_l - r(0, p_l, \gamma_l),$$

then the projections of $\tilde{\Phi}_3(p, U_r)$ and $\Phi_1(p, U_l)$ onto the (p, u) -plane have a unique intersection point, and the Riemann problem has a unique solution. \square

The solution of the Riemann problem (U_l, U_r) is constructed as follows: Let (\tilde{p}, \tilde{u}) be the unique intersection between the projections of $\Phi_1(p, U_l)$ and $\tilde{\Phi}_3(p, U_r)$ onto the (p, u) -plane. We connect $U_l = (p_l, u_l, \gamma_l)$ to $\tilde{U}_1 = (\tilde{p}, \tilde{u}, \gamma_l)$ by a 1-curve, then we go from \tilde{U}_1 to $\tilde{U}_2 = (\tilde{p}, \tilde{u}, \gamma_r)$ along a contact discontinuity, and finally connect \tilde{U}_2 to $U_r = (p_r, u_r, \gamma_r)$ by a 3-wave.

2.3. Invariant region and vacuum. A region Ω is invariant for the Riemann problem if for any Riemann problem with initial data in Ω , its solution is also in Ω . For the p -system we know from [10, Ex. 3.5] that the convex region in the (v, u) -plane between the integral curves of the eigenvectors is invariant. This region bounds v from below, but not from above, thus vacuum is included in the invariant region. In the (p, u) -plane this corresponds to the region bounded by $p = 0$ and the two integral curves. Since γ cannot take any other values than those of the initial data, we find the invariant region for the p -system for each γ and take the union of these. This gives us an invariant region for (1.1). Moreover, this gives us the upper bound on p , p_{\max} , which we need, but p is still not bounded away from vacuum.

3. DECREASING GLIMM FUNCTIONAL

In order to prove existence of a unique weak solution of (1.1) with the initial data (1.2), we first find a sequence of approximate solutions of (1.1), and then show that this converges to a weak solution. We use the Glimm scheme to obtain the approximate solutions, for details on the Glimm scheme see, e.g., [20, Ch. 19]. If we can show that the total variation of the approximate solution is bounded, convergence to a weak solution of (1.1) follows. To do this we use a Glimm functional and therefore need interaction estimates which are quadratic in the incoming waves for all possible interactions. As discussed for the p -system by Liu and Smoller [13], it is not possible to find such estimates if the approximate solution is not bounded away from vacuum. Fortunately, using the Glimm scheme we have a region \mathcal{U} which

contains the approximate solution and this region is bounded by the total variation of the initial data. Therefore, given some assumptions on the initial data, we can show that this region does not contain vacuum.

3.1. The Glimm Scheme. Before we define the Glimm functional and prove it is decreasing, we need to introduce the Glimm scheme and some more notation.

Choose the spatial mesh size $\Delta x = h$ and the temporal mesh size Δt so that

$$(3.1) \quad \frac{h}{\Delta t} > \max_{U \in \mathcal{U}} |\lambda_j(U)|, \quad j = 1, 2, 3,$$

and define $x_i := ih$ for $i = 0, \pm 1, \pm 2, \dots$, and $t_n := n\Delta t$ for $n = 0, 1, 2, \dots$. The *mesh points* (x_i, t_n) with $i + n$ even, $n = 0, 1, 2, \dots$, make up a staggered grid, see Fig. 3. Let furthermore $a = \{a_0, a_1, \dots\}$ be a random sequence, equidistributed in

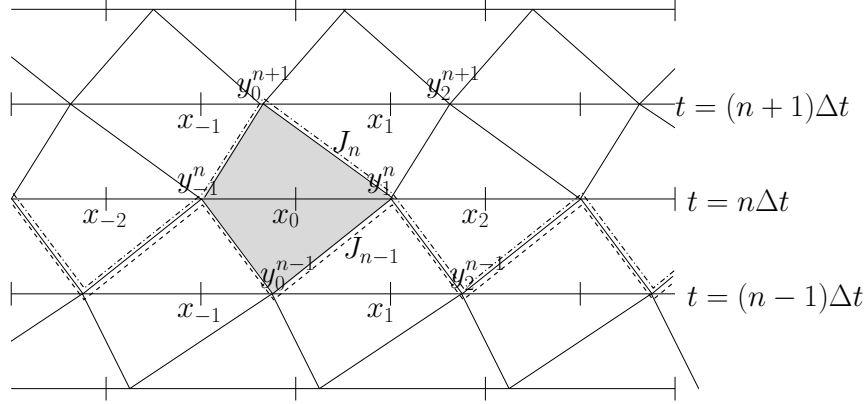


FIGURE 3. The staggered grid with the diamonds and two successive mesh curves indicated by dotted lines. Here n is even.

the interval $[-1, 1]$, and let

$$(3.2) \quad y_i^n := x_i + a_n h, \quad i + n \text{ odd},$$

be the *sampling points*. Figure 3 shows the characteristic diamonds we get by drawing the lines between the sampling points, each diamond containing exactly one mesh point. A curve going from the left to the right along the edges of the diamonds, connecting y_i^n to either y_{i-1}^{n-1} or y_{i+1}^{n+1} , is called a *mesh curve*. Two mesh curves, J_{n-1} and J_n , are indicated by dotted lines in Fig. 3. These curves are called *successive mesh curves* since they only differ at one point.

We approximate the initial data by piecewise constants,

$$(3.3) \quad U_h(x, 0) = U_0(y_i^0-), \quad (i-1)h \leq x \leq (i+1)h, \quad i \text{ odd},$$

and at each time step we use the solution already found for $0 \leq t < t_n$ to define $U_h(x, t_n)$ as a piecewise constant function by

$$(3.4) \quad U_h(x, t_n) = U_h(y_i^n-, t_n-), \quad (i-1)h \leq x \leq (i+1)h, \quad i + n \text{ odd},$$

i.e., by using the values of the solution at the sampling points. We solve all Riemann problems at $t = t_n$ and together these waves give the approximate solution for $t_n \leq t < t_{n+1}$. None of the waves will interact before the next time step because

the ratio between the spatial mesh and the temporal mesh is larger than the speed of any of the waves, cf. (3.1).

We now turn to what happens inside one diamond. Waves may enter a diamond through its lower left or lower right edge. A shock wave or a contact discontinuity either enters the diamond or not. For a rarefaction wave one part of the wave can enter one diamond, while the rest of the rarefaction wave enters the nearby diamond. As stated in property (vii), rarefaction waves are additive and therefore this corresponds to one rarefaction wave entering each diamond. We call waves that are entering a diamond *incoming waves*.

At the grid point inside the diamond we solve the Riemann problem (U_l, U_r) where U_l and U_r are the values at the sampling points. Since the sampling points are the corners of the diamond, U_l is the leftmost state (with respect to x) among the incoming waves and U_r is the rightmost state. The solution of the Riemann problem (U_l, U_r) consists of up to three waves. These waves are called *outgoing waves* and are the only waves leaving the diamond. Let U_i , $i = 1, \dots, 3$, be the intermediate states among the incoming waves and \tilde{U}_j , $j = 1, 2$, the intermediate states among the outgoing waves. Note that $\tilde{p}_1 = \tilde{p}_2$ and $\tilde{u}_1 = \tilde{u}_2$, and we refer to them by \tilde{p} and \tilde{u} .

We define an *interaction* between incoming waves as solving the Riemann problem with the leftmost state among the incoming waves as the left state and the rightmost state among the incoming waves as the right state. We also say that two or more *waves interact* meaning the interaction between these waves. In other words, the waves entering one diamond interacts and the result of this interaction is the outgoing waves. Note that there is no actual interaction in the Glimm scheme because the grid is constructed so that no waves can collide at any time.

The goal is to estimate the *total strength* of the outgoing waves, that is, the sum of the strengths of the outgoing waves, in terms of the strengths of the incoming waves. First we define *the strength of a 1-wave or a 3-wave* as the jump in p across the wave, and *the strength of a 2-wave* as the jump in γ across the wave. Furthermore, we let

ϵ define a 1-wave,	α a 1-shock wave,	μ a 1-rarefaction wave,
η a 3-wave,	β a 3-shock wave,	ν a 3-rarefaction wave,
ζ a 2-wave,	δ a 1- or 3-wave.	

The strength of a wave is written $|\delta|$. We use a prime, like δ' , to indicate an outgoing wave and write an interaction as $\delta_1 + \delta_2 \rightarrow \delta'_1 + \delta'_2$ where δ_1 enters the diamond through its left edge and δ_2 through its right edge. If more than two waves interact, we use parentheses to indicate which waves enter the diamond through the left and the right edge.

Since γ only changes along ζ -waves, the incoming and outgoing ζ -waves will always be equal and we write them all as ζ . Moreover, the incoming and outgoing ζ -waves have the same strength and we therefore omit them from the interaction estimates.

3.2. Possible interactions in a diamond. Due to the staggered grid used in the Glimm scheme, the number of possible interactions in one diamond is limited. All contact discontinuities have zero speed, therefore at most one contact discontinuity can enter one diamond. Moreover, it follows from the wave speeds that two rarefaction waves of the same family can only enter the same diamond if there is another

wave between them. Furthermore, it is not possible to have both a 1-wave and a 3-wave entering through both the left and the right edge. Therefore we do not get interactions between more than four waves.

We divide all possible interactions into four main types:

- (A) Waves entering through only one edge, see Fig. 4: $(\epsilon + \zeta + \eta)$ where one or two of the waves can be absent.
- (B) Two waves entering the diamond through different edges, see Fig. 5:
 - (a) Both waves are of the same family: $\epsilon_1 + \epsilon_2$ or $\eta_1 + \eta_2$ where at least one wave is a shock wave.
 - (b) Different families, but no contact discontinuity: $\eta + \epsilon$.
 - (c) With a contact discontinuity: $\zeta + \epsilon$ or $\eta + \zeta$.
- (C) Three waves entering the diamond, see Fig. 6:
 - (a) No contact discontinuity: $(\epsilon + \eta) + \epsilon$ or $\eta + (\epsilon + \eta)$.
 - (b) A contact discontinuity as the leftmost or rightmost wave: $(\zeta + \eta) + \epsilon$ or $\eta + (\epsilon + \zeta)$.
 - (c) A contact discontinuity as the middle wave: $(\epsilon_1 + \zeta) + \epsilon_2$ or $\eta_1 + (\zeta + \eta_2)$.
- (D) Four waves entering the diamond, see Fig. 7: $(\epsilon_1 + \zeta + \eta) + \epsilon_2$ or $\eta_1 + (\epsilon + \zeta + \eta_2)$.
 - (a) Waves of the same family are also of the same type.
 - (b) Waves of the same family are not of the same type.

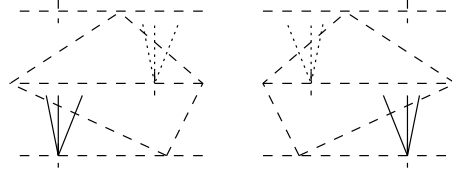


FIGURE 4. Interactions of type A.

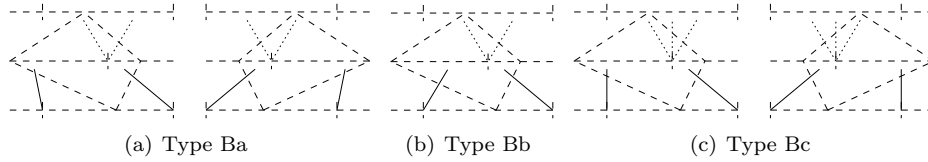


FIGURE 5. Interactions of type B.

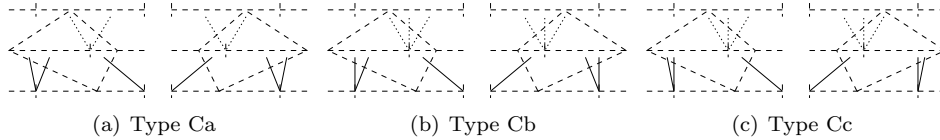


FIGURE 6. Interactions of type C.

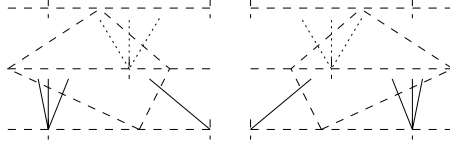


FIGURE 7. Interactions of type D.

Even though we have at most four interacting waves, we get a notable number of interactions. However, symmetries of the system considerably reduce the number of cases that need to be discussed. The symmetries are summarized in the following lemma.

Lemma 3.1 (Symmetry property). *By letting x go to $-x$, a 1-wave connecting U_l to U_r becomes a 3-wave connecting U_r to U_l , and vice versa. A 2-wave is unchanged under this transformation. Furthermore, the leftmost wave with respect to x will be the rightmost wave with respect to $-x$.*

Proof. Consider first a 1-rarefaction wave connecting U_l to U_r . In the (x, t) -plane this wave is the fan between the lines $x = \lambda_1(U_l)t$ and $x = \lambda_1(U_r)t$ where $\lambda_1(U_l) \leq \lambda_1(U_r)$. Recall that $\lambda_1 = -\lambda_3$. Changing variables from x to $y = -x$, we get

$$\frac{dy}{dt} = \frac{dy}{dx} \frac{dx}{dt} = -\frac{dx}{dt},$$

thus, in the new variables, we have the fan between $y = -\lambda_1(U_r)t = \lambda_3(U_r)t$ and $y = -\lambda_1(U_l)t = \lambda_3(U_l)t$, or in other words, we have obtained the 3-rarefaction wave connecting U_r to U_l .

In the (x, t) -plane, a 1-shock wave connecting U_l to U_r is given by the line $x = \sigma_1(U_l, U_r)t$. Note that $p_l < p_r$ according to (2.10) and that the shock velocity $\sigma_1(U_l, U_r)$ satisfies the Rankine–Hugoniot condition (2.5). Changing variables from x to $y = -x$, we get

$$\sigma = \frac{dy}{dt} = \frac{dy}{dx} \frac{dx}{dt} = -\frac{dx}{dt} = -\sigma_1(U_l, U_r) = \sigma_3(U_r, U_l),$$

where the last equality follows from (2.8) and (2.9). Thus, the 1-shock wave changes into the line $x = \sigma t = \sigma_3(U_r, U_l)t$. The Rankine–Hugoniot condition must still be satisfied after the change of variables, thus

$$\begin{aligned} \sigma(U_r - U_l) &= f(U_r) - f(U_l), \\ \Leftrightarrow -\sigma_1(U_l, U_r)(U_r - U_l) &= f(U_r) - f(U_l), \\ \Leftrightarrow \sigma_3(U_r, U_l)(U_l - U_r) &= f(U_l) - f(U_r). \end{aligned}$$

Hence, we have a wave connecting U_r to U_l with the shock velocity $\sigma_3(U_r, U_l)$ satisfying the Rankine–Hugoniot condition. Furthermore, $p_r > p_l$, therefore it is an admissible 3-shock wave connecting U_r to U_l .

The fact that a 3-wave becomes a 1-wave under this transformation follows by the same arguments.

For a 2-wave we have $\sigma = \lambda = 0$, therefore a 2-wave is unchanged when sending x to $-x$. \square

For instance, it follows from Lemma 3.1 that $\zeta + \nu + \alpha$ becomes $\beta + \mu + \zeta$ under the transformation from x to $-x$ and therefore the two interactions are symmetric.

This means that all estimates found for $\zeta + \nu + \alpha$ will apply to $\beta + \mu + \zeta$ as well, and we only need to consider one of them.

3.3. The Glimm functional. Our Glimm functional is defined on a mesh curve J by

$$(3.5) \quad G(J) := F(J) + 3C_1(\bar{\gamma} - 1)Q_1(J) + 3C_2Q_2(J),$$

where C_1 is the constant appearing in the estimates given by (4.3) for the interaction between two shock waves, cf. the case Bb-ii (see Subsection 4.2.2), and

$$(3.6) \quad C_2 := \frac{c_2}{\min\{r'_{\min}, s'_{\min}\}} = kc_2,$$

where c_2 is the constant from Lemma 2.2 defined by (2.25) and

$$(3.7) \quad k := \frac{1}{\min\{r'_{\min}, s'_{\min}\}}.$$

Note that both C_1 and C_2 are constants only depending on p_{\min} , p_{\max} and $\bar{\gamma}$. The linear functional F and the two quadratic functionals Q_1 and Q_2 are defined by

$$(3.8) \quad F(J) := \sum\{|\delta| \mid \text{all shock waves } \delta \text{ crossing } J\},$$

$$(3.9) \quad Q_1(J) := \sum\{|\alpha| |\beta| \mid \text{all approaching 1- and 3-shock waves crossing } J\},$$

$$(3.10) \quad Q_2(J) := \sum\{|\zeta| |\delta| \mid \text{all approaching pairs of } \zeta \text{ and } \delta \text{ crossing } J\},$$

where two waves of different families are *approaching* if the wave of the lowest family is the rightmost wave with respect to x . Note that F and Q_1 only sum over shock waves.

Remark 3.2. The Glimm functional used in [16] is similar to the two first terms of our Glimm functional (3.5), only the constants differ slightly.

We need two more functionals, one summing over all shock and rarefaction waves crossing a mesh curve J and one summing over the contact discontinuities crossing J . We define

$$(3.11) \quad L(J) := \sum\{|\delta| \mid \text{all } \delta \text{ crossing } J\},$$

and

$$(3.12) \quad F_\gamma(J) = F_\gamma := \sum\{|\zeta| \mid \text{all } \zeta \text{ crossing } J\}.$$

Note that the sum of all contact discontinuities, F_γ , is constant for all mesh curves.

The key point in order to show convergence, is to prove that this Glimm functional is a decreasing functional in time. Define the constant

$$(3.13) \quad C = \min\{\tilde{C}, 1\},$$

where the minimum is taken over all the constants \tilde{C} appearing in the estimates for interactions of type Ba considered in Subsection 4.2.1. Note that $0 < C \leq 1$ depends only on p_{\min} , p_{\max} and $\bar{\gamma}$. We can now state the following lemma.

Lemma 3.3. *Assume that all waves are contained in \mathcal{D} and let $G(J)$ be the Glimm functional defined by (3.5). If*

$$(3.14) \quad (\bar{\gamma} - 1)L(J_0) \leq \frac{C}{9C_1},$$

$$(3.15) \quad F_\gamma \leq \frac{C}{9C_2},$$

then $G(J)$ is a decreasing functional, that is, $G(J_N) \leq G(J_{N-1}) \leq \dots \leq G(J_0)$. Furthermore, $F(J_N) \leq \frac{5}{3}L(J_0)$.

We prove this lemma by going through every possible interaction we can get in the Glimm scheme, and we devote the next section to this.

4. PROOF OF LEMMA 3.3

We prove that the Glimm functional (3.5) is decreasing by induction on successive mesh curves. Since two successive mesh curves only differ at the edges of one diamond, we have to consider all possible interactions that can take place in one diamond and show that G is decreasing across these.

Before we start on the induction, we prove the last part of Lemma 3.3. Assume that G is decreasing for successive mesh curves up to J_n and assume furthermore that $L_0 = L(J_0)$ and F_γ satisfy (3.14) and (3.15), respectively. To simplify the notation we write $G_j = G(J_j)$, $F_j = F(J_j)$, and $Q_{k,j} = Q_k(J_j)$. We get

$$(4.1) \quad \begin{aligned} F_n &\leq G_n \leq G_{n-1} \leq \dots \leq G_0 = F_0 + 3C_1(\bar{\gamma} - 1)Q_{1,0} + 3C_2Q_{2,0} \\ &\leq F_0 + 3C_1(\bar{\gamma} - 1)(F_0)^2 + 3C_2L_0F_\gamma \\ &\leq (1 + 3C_1(\bar{\gamma} - 1)F_0 + 3C_2F_\gamma)L_0 \\ &\leq (1 + 3C_1(\bar{\gamma} - 1)L_0 + 3C_2F_\gamma)L_0 \\ &\leq \left(1 + \frac{C}{3} + \frac{C}{3}\right)L_0 \leq \frac{5}{3}L_0, \end{aligned}$$

where we have used that $C \leq 1$. This proves that if G is decreasing, then $F(J_N) \leq \frac{5}{3}L(J_0)$.

We now turn to the induction argument. The first step is to show that $G_1 - G_0 \leq 0$ where J_0 is the unique mesh curve connecting the sampling points at $t = 0$ to the sampling points at $t = \Delta t$. Then we assume that G is decreasing for successive mesh curves up to J_n , that is, $G_n \leq G_{n-1} \leq \dots \leq G_0$. The induction step is to show that $\Delta G := G_{n+1} - G_n \leq 0$. For a given interaction, the calculations needed to estimate $G_1 - G_0$ and ΔG are the same. The sum over all shock waves or all contact discontinuities crossing the first of the two successive mesh curves most often show up in the estimates, and we use conditions (3.14) and (3.15) in addition to (4.1) to show that the estimates are nonpositive. Thus, the only difference in the estimates for $G_1 - G_0$ and ΔG is that for the first one we might get terms with $F_0 \leq L_0$, while for the second one these terms involve $F_n \leq \frac{5}{3}L_0$. We only include the calculations for ΔG .

In Section 3.2 we discussed all the possible interactions and divided them into four main types. Recall that the projection of 1- or 3-wave curves onto the (p, u) -plane can intersect if they have different γ 's, cf. property (ii) in Lemma 2.1, therefore each interaction has up to four possible outcomes and they all have to be considered. Fortunately, the symmetry properties of system (1.1) stated in Lemma 3.1 nearly halve the number of interactions we have to consider.

Before we start considering each interaction, we describe our general approach. We start by proving that the Glimm functional is decreasing for all interactions of type B, that is, interactions between two waves. This is either done by using

estimates and properties of the wave curves given in [16] and translating these into estimates using p and u as the variables, or by applying Lemma 2.2.

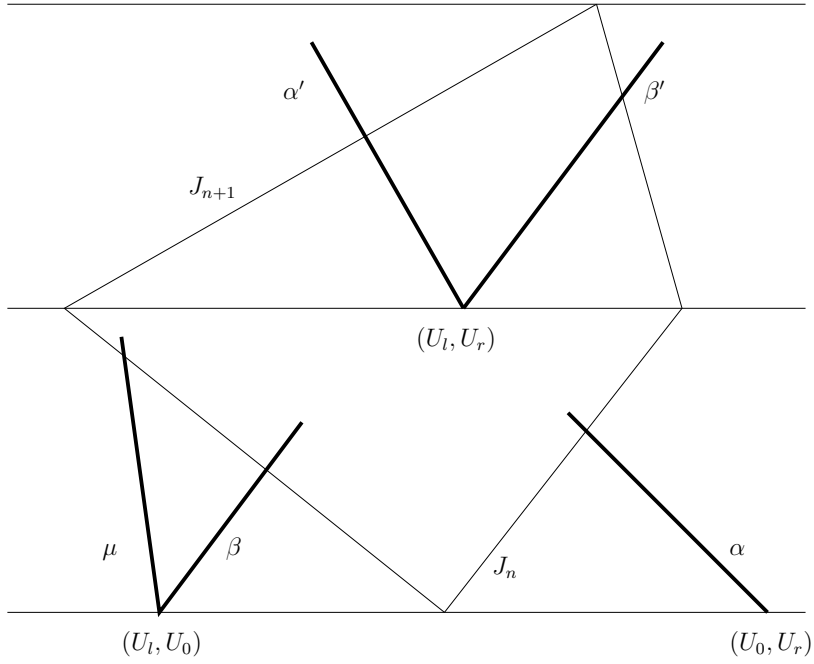
To show that $\Delta G \leq 0$ for interactions between more than two waves, we use a strategy of dividing the interaction into several steps. As long as we can show that G is decreasing across each step, it follows that G is decreasing going from the first to the last step and that $\Delta G \leq 0$ across the interaction. Based on this, we divide the interaction into steps for which we already know that G is decreasing. Thus, at each step we let two (or sometimes three) waves interact. As long as this is an interaction already analyzed, we know that G decreases across this step. We continue this until we at some point easily can show that G is decreasing across the last step, that is, we are able to find sufficiently strong estimates of the outgoing waves in terms of the collection of waves obtained through the previous steps.

Formally, we can describe the division of the interaction into k steps using inner diamonds and intermediate mesh curves. Start by identifying two (or three) nearby waves among the incoming waves for which we already have established that the Glimm functional is decreasing across the interaction. Introduce an *intermediate mesh curve*, J_1^* , which coincides with J_n everywhere except near the lower corner of the original diamond. Near the lower corner J_1^* lies above J_n so that J_1^* and J_n enclose a small *inner diamond* inside the original diamond. This is done so that the waves interacting at the first step enter the inner diamond, while the waves left unchanged at this step cross J_n and J_1^* outside the inner diamond. Observe that J_n and J_1^* act as successive mesh curves. Since the waves entering this inner diamond correspond to an interaction already analyzed, we have $\Delta G_1 := G(J_1^*) - G(J_n) \leq 0$. Note that J_1^* is not a real mesh curve by the definition given above, since it inside the original diamond does not consist of lines connecting sampling points. However, the outcome of the interaction inside an inner diamond is found by solving the Riemann problem where the left and right states are the values at the corners of the inner diamond, so the corners act as sampling points. Let the fan of the outgoing waves be situated somewhere on the line between the left and the right corner of the inner diamond in such a way that the waves interacting at the next step enter the next inner diamond while the rest of the waves do not. Thus, both the intermediate mesh curves and the inner diamonds resemble the real mesh curves and diamonds. One example of an interaction divided into steps and the introduced intermediate mesh curves and inner diamonds is shown in Fig. 8.

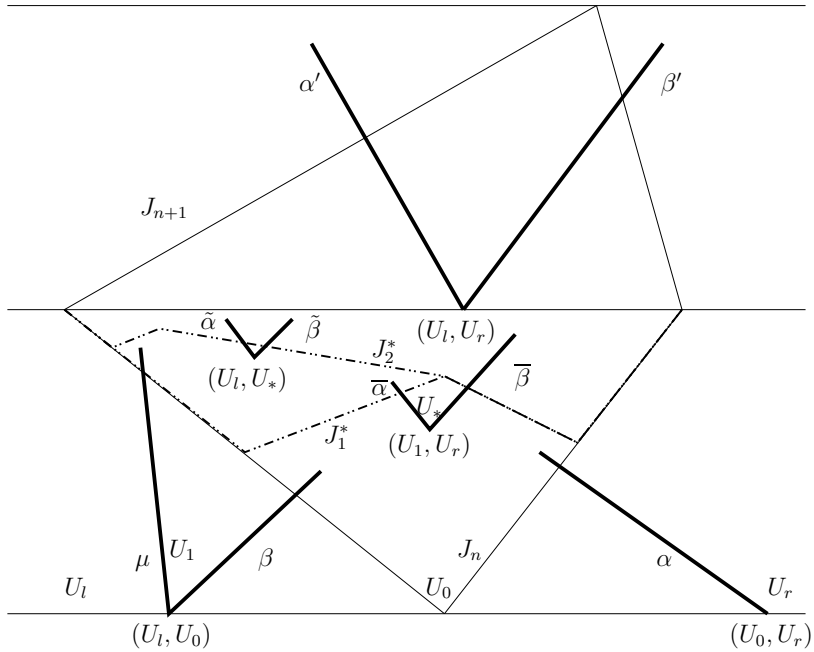
For each step $i = 2, \dots, k-1$ we introduce a new mesh curve J_i^* which acts as a successive mesh curve to J_{i-1}^* , that is, the two intermediate mesh curves enclose an inner diamond which the interacting waves enter. Since the waves entering an inner diamond correspond to an interaction already analyzed, we have that $\Delta G_i := G(J_i^*) - G(J_{i-1}^*) \leq 0$ for $i = 2 \dots k-1$. We stop this process when we after step $k-1$ are able to show that $\Delta G_k := G(J_{n+1}) - G(J_{k-1}^*) \leq 0$. In other words, we divide the interaction into steps until we after step $k-1$ have a collection of waves which are easy to compare (possibly using Lemma 2.2) with the outgoing waves so that we are able show that $\Delta G_k \leq 0$. Then we have $G(J_{n+1}) \leq G(J_{k-1}^*) \leq \dots \leq G(J_i^*) \leq \dots \leq G(J_1^*) \leq G(J_n)$, thus, $\Delta G = G(J_{n+1}) - G(J_n) \leq 0$.

In most cases only a few extra steps are needed in order to show $\Delta G \leq 0$. However, for the cases where many steps are required, we change our strategy slightly. At the first step¹ we replace the incoming waves with a new set of waves

¹For the last case of interaction Db-iv we actually do this replacement at the second step.



(a) The interaction before division.



(b) The interaction divided into three steps with two new mesh curves, J_1^* and J_2^* , and two inner diamonds.

FIGURE 8. An interaction divided into three steps: $\mu + \beta + \alpha \rightarrow \alpha' + \beta'$ which is the second case of Ca-v. The projection onto the (p, u) -plane is shown in Fig. 16(b).

connecting U_l to U_r . We introduce inner diamonds and intermediate mesh curves as before, thus, all the incoming waves enter the first inner diamond and the introduced waves leave this diamond. The only difference from before is that these outgoing waves of the first diamond is not a result of some known interaction. Therefore, we have to obtain estimates on these introduced waves in terms of the original incoming waves, so that we can show $\Delta G_1 \leq 0$. After this step of replacing one interaction with a new one, we carry on as before. We identify nearby waves among the introduced waves for which we already have analyzed the corresponding interaction, and then carry on as above. The advantage of this method is that it requires only a few extra steps for an interaction where we otherwise would need many steps.

We use the notation $\xrightarrow{\Delta G_i}$ to indicate the different steps of an interaction and square brackets to group the waves that interact at each step. Recall that we use ordinary parentheses to indicate which waves enter through the same edge. In the figures displaying the interactions we see the projection of the interaction onto the (p, u) -plane. The left and right states are drawn as circles, the incoming waves are drawn by dashed lines and the outgoing waves with dash-dotted lines. The contact discontinuities, ζ , are indicated by asterisks. For most of the interactions that are divided into steps, we have included the intermediate waves drawn by dotted lines. Furthermore, any wave drawn by a solid line is a introduced wave which is not a result of an interaction.

We are now ready to prove that $\Delta G \leq 0$ across all possible interactions.

4.1. Type A: Waves entering through only one edge. These interactions are trivial: If one, two or three waves all enter one diamond through the same edge, then they are by definition the solution of a Riemann problem (U_l, U_r) . If no more waves enter the diamond, then the Riemann problem to be solved inside the diamond is also (U_l, U_r) . Thus we have

$$(\epsilon + \zeta + \eta) \rightarrow \epsilon' + \zeta + \eta', \quad \text{where} \quad \epsilon = \epsilon', \quad \eta = \eta',$$

and since the incoming and outgoing waves are equal, so are their strengths and $\Delta G = 0$ for all interactions of type A.

4.2. Type B: Two waves entering the diamond. The interactions between two waves that do not include a contact discontinuity, are the same interactions as for the p -system and are discussed in [16] where the waves are measured by the jumps in the Riemann invariants for the p -system, r and s , defined by [16, Eq. (5)]. We use the estimates given in [16] and transform these into estimates using the jump in p to measure the strength of the waves. The map from (p, u) to (r, s) is one-to-one and onto for all $p > 0$. We state the estimates and skip the detailed transformations going from the estimates and properties in (r, s) -coordinates to estimates in (p, u) -coordinates. Note that the constants appearing in [16] depend on p_{\min} , p_{\max} and γ . However, for a given p_{\min} and p_{\max} we take the maximum or minimum over all γ and find an upper bound of these constants that only depend on p_{\min} , p_{\max} and $\bar{\gamma}$. For the interactions involving a contact discontinuity, we obtain the needed estimates using Lemma 2.2.

Recall that for all interactions of type B we have one wave entering through each edge, otherwise the interaction is a trivial interaction of type A.

4.2.1. *Type Ba: Two waves of the same family.*

(i) $\alpha_1 + \alpha_2 \rightarrow \alpha' + \nu'$ (and $\beta_1 + \beta_2 \rightarrow \mu' + \beta'$): Property (viii) implies that α_2

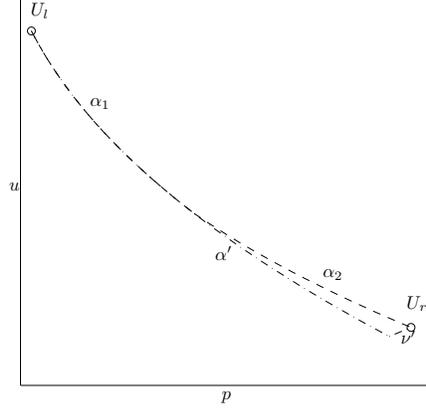


FIGURE 9. The interaction $\alpha_1 + \alpha_2 \rightarrow \alpha' + \nu'$.

lies above α' and there is only one possible outcome of this interaction, see Fig. 9. We have that

$$|\alpha'| - |\alpha_1| - |\alpha_2| = -|\nu'|,$$

from which we get

$$\Delta F = -|\nu'|, \quad \Delta Q_1 \leq 0, \quad \Delta Q_2 \leq |\nu'| F_\gamma,$$

where $\Delta F := F_{n+1} - F_n$ and $\Delta Q_i := Q_{i,n+1} - Q_{i,n}$. Thus,

$$\Delta G \leq |\nu'|(-1 + 3C_2 F_\gamma) \leq |\nu'| \left(-1 + \frac{C}{3}\right) \leq |\nu'| \left(-1 + \frac{1}{3}\right) \leq 0.$$

By the symmetry property $\Delta G \leq 0$ also across the interaction $\beta_1 + \beta_2$.

(ii) $\alpha + \mu$ (and $\nu + \beta$): There are two possible outcomes of this interaction.

- $\alpha + \mu \rightarrow \mu' + \beta'$: In this case U_r is to the left of the 3-shock curve starting at U_l , see Fig. 10(a). From [16] we find that there exists a \tilde{C} depending only on p_{\min} , p_{\max} and $\bar{\gamma}$ such that

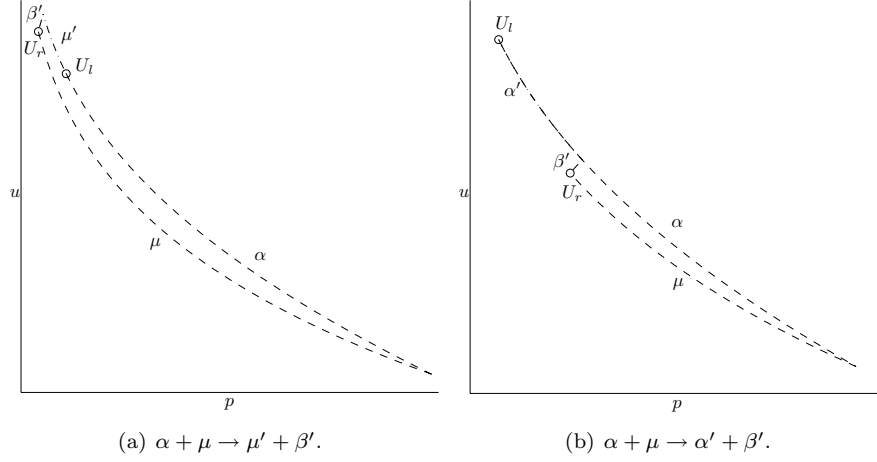
$$|\mu'| \leq |\mu|, \quad |\beta'| - |\alpha| \leq -\tilde{C}|\beta'| \leq -C|\beta'|.$$

Recall that C is defined as minimum over all \tilde{C} . This gives us

$$\begin{aligned} \Delta F &= -C|\beta'|, \\ \Delta Q_1 &\leq |\beta'| F_n \leq \frac{5}{3}|\beta'| L_0, \\ \Delta Q_2 &\leq |\beta'| F_\gamma, \end{aligned}$$

and we find

$$\begin{aligned} \Delta G &\leq |\beta'| \left(-C + 3C_1(\bar{\gamma} - 1)\frac{5}{3}L_0 + 3C_2 F_\gamma\right) \\ &\leq |\beta'| \left(-C + \frac{5}{3}\frac{C}{3} + \frac{C}{3}\right) \leq 0. \end{aligned}$$

FIGURE 10. The interaction $\alpha + \mu$.

- $\alpha + \mu \rightarrow \alpha' + \beta'$: In this case U_r is to the right of the 3-shock curve starting at U_l , see Fig. 10(b). Then there exists a constant $\tilde{C} \geq C$ so that

$$|\alpha'| + |\beta'| - |\alpha| \leq -\tilde{C} |\beta'| \leq -C |\beta'|.$$

As above we find

$$\begin{aligned} \Delta F &= -C |\beta'|, \\ \Delta Q_1 &\leq |\beta'| F_n \leq \frac{5}{3} |\beta'| L_0, \\ \Delta Q_2 &\leq |\beta'| F_\gamma, \end{aligned}$$

thus, $G \leq 0$.

Due to symmetry, $\Delta G \leq 0$ across the interaction $\nu + \beta$.

- (iii) $\mu + \alpha$ (and $\beta + \nu$): There are two possible outcomes of this interaction.

- $\mu + \alpha \rightarrow \mu' + \beta'$: In this case U_r is to the left of the 3-shock curve starting at U_l , see Fig. 11(a). There exists a $\tilde{C} \geq C$ so that

$$(4.2) \quad |\mu'| \leq |\mu|, \quad |\beta'| - |\alpha| \leq -\tilde{C} |\beta'| \leq -C |\beta'|.$$

Thus, $\Delta G \leq 0$ by the same calculation as we just did for $\alpha + \mu$.

- $\mu + \alpha \rightarrow \alpha' + \beta'$: In this case U_r is to the right of the 3-shock curve starting at U_l , see Fig. 11(b). For this interaction we use the same approach as in [16] and replace the interaction by a new one. There exists two waves, $\bar{\beta}$ and $\bar{\alpha}$, so that

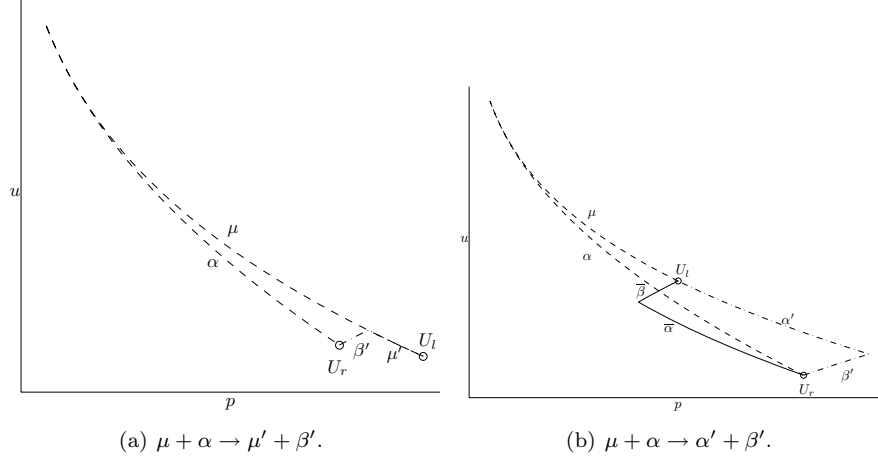
$$|\bar{\alpha}| + |\bar{\beta}| - |\alpha| \leq -\tilde{C} |\bar{\beta}| \leq -C |\bar{\beta}|,$$

and

$$\bar{\beta} + \bar{\alpha} \rightarrow \alpha' + \beta'.$$

We write the interaction as

$$\mu + \alpha \xrightarrow{\Delta G_1} [\bar{\beta} + \bar{\alpha}] \xrightarrow{\Delta G_2} \alpha' + \beta',$$

FIGURE 11. The interaction $\mu + \alpha$.

where the square brackets indicate that the two waves interact at the second step, unlike the first step where we just replace the waves. For the first step we find using the above estimate that

$$\begin{aligned} \Delta F &= -C |\bar{\beta}|, \\ \Delta Q_1 &\leq |\bar{\alpha}| |\bar{\beta}| + |\bar{\beta}| \sum_i |\alpha_i| \leq |\bar{\beta}| F_n \leq \frac{5}{3} |\bar{\beta}| L_0, \\ \Delta Q_2 &\leq |\bar{\beta}| F_\gamma, \end{aligned}$$

where α_i are all 1-shock waves that are approaching $\bar{\beta}$, that is, all 1-shock waves to the right of the diamond. From this we find that $\Delta G_1 \leq 0$ at the first step when passing from $\mu + \alpha$ to $\bar{\beta} + \bar{\alpha}$, regardless of the introduced approaching waves. The interaction at the second step is of type Bb-ii and by the estimate (4.3) below we have $\Delta G_2 \leq 0$.

We have now proved that the Glimm functional is decreasing for both steps, thus, $\Delta G \leq 0$.

Due to symmetry, $\Delta G \leq 0$ across the interaction $\beta + \nu$.

All the constants \tilde{C} in the above estimates consist of one constant from the estimates in [16], let us call this C_0 , and one constant due to the transformation into estimates using p to measure the wave strengths. From [16] we have $C_0 > 0$, thus, $\tilde{C} > 0$ for all the above estimates and $0 < C \leq 1$ since C is the minimum of all \tilde{C} and 1.

4.2.2. Type Bb: Different families, no contact discontinuity.

- (i) $\nu + \mu \rightarrow \mu' + \nu'$: This interaction has only one outcome, see Fig. 12(a), and we obtain

$$|\mu'| \leq |\mu|, \quad |\nu'| \leq |\nu|,$$

thus $\Delta G \leq 0$.

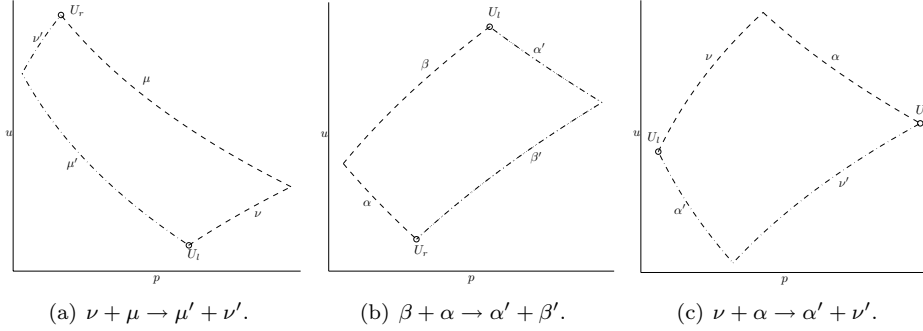


FIGURE 12. The interactions of type Bb

- (ii) $\beta + \alpha \rightarrow \alpha' + \beta'$: This interaction has only one outcome, see Fig. 12(b), and we obtain

$$(4.3) \quad |\alpha'| - |\alpha| \leq C_1(\bar{\gamma} - 1)|\alpha||\beta|, \quad |\beta'| - |\beta| \leq C_1(\bar{\gamma} - 1)|\alpha||\beta|,$$

where C_1 is a constant depending only on p_{\min} , p_{\max} and $\bar{\gamma}$, see Remark 4.1. From these estimates we find

$$\Delta F \leq 2C_1(\bar{\gamma} - 1)|\alpha||\beta|,$$

$$\Delta Q_1 \leq C_1(\bar{\gamma} - 1)|\alpha||\beta|F_n - |\alpha||\beta| \leq \frac{5}{3}C_1(\bar{\gamma} - 1)|\alpha||\beta|L_0 - |\alpha||\beta|,$$

$$\Delta Q_2 \leq C_1(\bar{\gamma} - 1)|\alpha||\beta|F_\gamma.$$

Thus,

$$\begin{aligned} \Delta G &\leq C_1(\bar{\gamma} - 1)|\alpha||\beta| \left(2 + \frac{5}{3}3C_1(\bar{\gamma} - 1)L_0 - 3 + 3C_2F_\gamma \right) \\ &\leq C_1(\bar{\gamma} - 1)|\alpha||\beta| \left(\frac{5}{3}\frac{C}{3} + \frac{C}{3} - 1 \right) \leq 0. \end{aligned}$$

Remark 4.1. In Nishida–Smoller [16], where the strength of the waves are measured using the Riemann invariants r and s , interaction Bb-ii is divided into three different cases with different estimates. However, when transforming these estimates into estimates using p to measure the strength of the waves, we get the same estimate for all the three cases. Similar to C , the constant C_1 is computed from the estimate in [16] and the transformation back from Riemann invariants, and it does only depend on p_{\min} , p_{\max} and $\bar{\gamma}$.

- (iii) $\nu + \alpha \rightarrow \alpha' + \nu'$ (and $\beta + \mu \rightarrow \mu' + \beta'$): There is only one outcome for this interaction, see Fig. 12(c), and we find that

$$|\alpha'| - |\alpha| = -q, \quad |\nu'| - |\nu| = q,$$

where q is a positive constant. We get that

$$\Delta F = -q, \quad \Delta Q_1 \leq 0, \quad \Delta Q_2 \leq qF_\gamma,$$

and furthermore,

$$\Delta G \leq q(-1 + 3C_2F_\gamma) \leq q \left(-1 + \frac{C}{3} \right) \leq 0.$$

Due to symmetry, $\Delta G \leq 0$ across the interaction $\beta + \mu$.

4.2.3. *Type Bc: With a contact discontinuity.* Interactions of this type do not occur in [16] and we prove all estimates.

- (i) $\zeta + \mu$ (and $\nu + \zeta$): In general we do not know which of the curves μ with γ_r or μ' with γ_l lies above the other, or whether they cross, and therefore there are two possible outcomes of this interaction, see Fig. 13. Recall that contact discontinuities are denoted by asterisks in the figures.

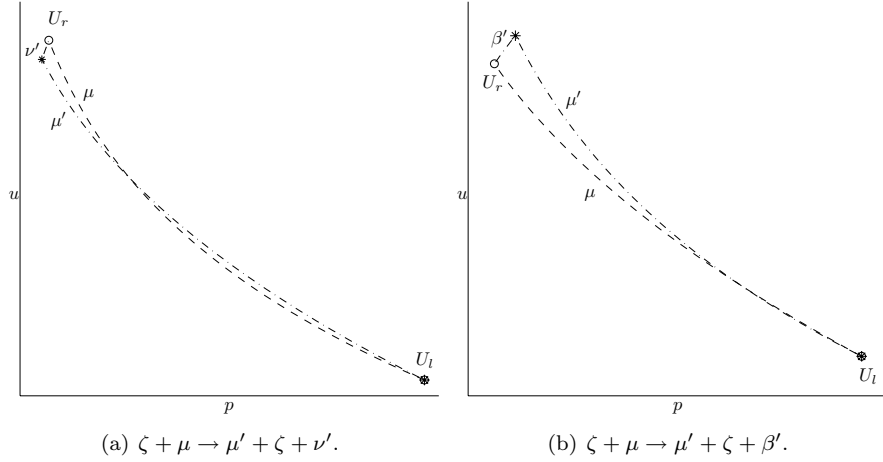


FIGURE 13. The interaction $\zeta + \mu$.

- $\zeta + \mu \rightarrow \mu' + \zeta + \nu'$: In this case U_r lies above μ' , see Fig. 13(a). We have that $|\mu'| - |\mu| = |\nu'|$, and want an estimate on $|\nu'|$. Let \bar{u} denote the point on μ' where $p = p_r$ and apply Lemma 2.2 on the two rarefaction waves μ and μ' on the interval from $p_l = p_1$ to p_r , then

$$u_r - \bar{u} \leq c_2 |\mu| |\zeta|.$$

From the mean value theorem we have $|u_r - \bar{u}| = |r'(p_*, p_l, \gamma)| |p_r - \tilde{p}|$ for some $p_* \in (\tilde{p}, p_r)$ where the derivative is with respect to the first variable. Recall from property (iv) that $|r'(p_*, p_l, \gamma)| \geq r'_{\min}$ where r'_{\min} is a constant only depending on p_{\min} , p_{\max} and $\bar{\gamma}$. We get

$$|\nu'| = |p_r - \tilde{p}| \leq \frac{1}{r'_{\min}} |u_r - \bar{u}| \leq \frac{c_2}{r'_{\min}} |\mu| |\zeta|.$$

This proves the estimate

$$(4.4) \quad |\mu'| - |\mu| = |\nu'| \leq C_2 |\mu| |\zeta|,$$

where C_2 is defined by (3.6). Using this estimate we find

$$\begin{aligned} \Delta F &= 0, \\ \Delta Q_1 &= 0, \\ \Delta Q_2 &\leq C_2 |\mu| |\zeta| F_\gamma - |\mu| |\zeta|, \end{aligned}$$

which gives

$$\Delta G \leq C_2 |\mu| |\zeta| (3C_2 F_\gamma - 3) \leq C_2 |\mu| |\zeta| \left(\frac{C}{3} - 3 \right) \leq 0.$$

- $\zeta + \mu \rightarrow \mu' + \zeta + \beta'$: In this case U_r lies below μ' , see Fig. 13(b). We have $|\mu'| - |\mu| \leq 0$. Let \bar{u} be the point on μ with $p = \tilde{p}$ and apply Lemma 2.2 to μ and μ' on the interval from $p_l = p_1$ to \tilde{p} , then

$$\tilde{u} - \bar{u} \leq c_2 |\zeta| |\mu'| \leq c_2 |\zeta| |\mu|.$$

From the mean value theorem, for a $p_* \in (p_r, \tilde{p})$, and property (v), we get

$$\begin{aligned} |\beta'| &= |p_r - \tilde{p}| = \frac{1}{|s'(\tilde{p}, p_*, \gamma_r)|} |\tilde{u} - u_r| \\ &\leq \frac{1}{s'_{\min}} |\tilde{u} - \bar{u}| \leq \frac{c_2}{s'_{\min}} |\mu| |\zeta|, \end{aligned}$$

where the derivative is with respect to the first variable. This proves the estimates

$$(4.5) \quad |\mu'| - |\mu| \leq 0, \quad |\beta'| \leq C_2 |\mu| |\zeta|,$$

where C_2 is defined by (3.6). We get

$$\begin{aligned} \Delta F &\leq C_2 |\mu| |\zeta|, \\ \Delta Q_1 &\leq C_2 |\mu| |\zeta| F_n \leq \frac{5}{3} C_2 |\mu| |\zeta| L_0, \\ \Delta Q_2 &\leq C_2 |\mu| |\zeta| F_\gamma - |\mu| |\zeta|, \end{aligned}$$

which gives

$$\begin{aligned} \Delta G &\leq C_2 |\mu| |\zeta| \left(1 + \frac{5}{3} 3C_1 (\bar{\gamma} - 1) L_0 + 3C_2 F_\gamma - 3 \right) \\ &\leq C_2 |\mu| |\zeta| \left(\frac{5}{3} \frac{C}{3} + \frac{C}{3} - 2 \right) \leq 0. \end{aligned}$$

By symmetry it follows that $\Delta G \leq 0$ across the interaction $\nu + \zeta$.

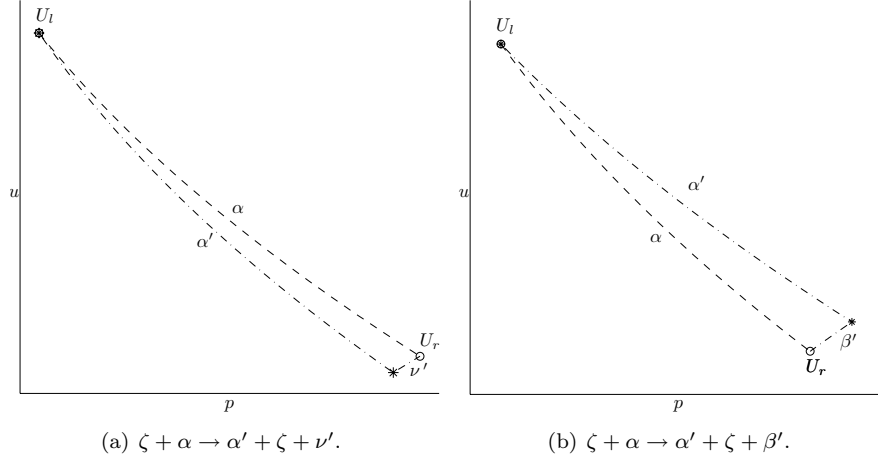
- (ii) $\zeta + \alpha$ (and $\beta + \zeta$): We do not know in general which of the curves α with γ_r or α' with γ_l lies above the other, therefore this interaction has two possible outcomes. Since this interaction is very similar to the interaction between a contact discontinuity and a rarefaction wave discussed above, we do not include all details.

- $\zeta + \alpha \rightarrow \alpha' + \zeta + \nu'$: In this case U_r is above α' , see Fig. 14(a). We have that

$$|\alpha'| - |\alpha| \leq 0, \quad |\nu'| \leq C_2 |\alpha| |\zeta|,$$

where C_2 is defined by (3.6). This follows by applying Lemma 2.2 to α and α' similar to what we did for the interaction $\zeta + \mu \rightarrow \mu' + \zeta + \beta'$. We get

$$\begin{aligned} \Delta F &\leq 0, \\ \Delta Q_1 &\leq 0, \\ \Delta Q_2 &\leq C_2 |\alpha| |\zeta| F_\gamma - |\alpha| |\zeta|, \end{aligned}$$

FIGURE 14. The interaction $\zeta + \alpha$.

which gives

$$\Delta G \leq C_2 |\alpha| |\zeta| (3C_2 F_\gamma - 3) \leq C_2 |\alpha| |\zeta| \left(\frac{C}{3} - 3 \right) \leq 0.$$

- $\zeta + \alpha \rightarrow \alpha' + \zeta + \beta'$: In this case U_r is below α' , see Fig. 14(b). We have that

$$|\alpha'| - |\alpha| = |\beta'| \leq C_2 |\alpha| |\zeta|,$$

where C_2 is defined by (3.6). This estimate is obtained using Lemma 2.2 on α and α' , similar to what we did for the interaction $\zeta + \mu \rightarrow \mu' + \zeta + \nu'$. From this estimate we find

$$\Delta F \leq 2C_2 |\alpha| |\zeta|,$$

$$\Delta Q_1 \leq C_2 |\alpha| |\zeta| F_n \leq \frac{5}{3} C_2 |\alpha| |\zeta| L_0,$$

$$\Delta Q_2 \leq C_2 |\alpha| |\zeta| F_\gamma - |\alpha| |\zeta|,$$

which gives

$$\begin{aligned} \Delta G &\leq C_2 |\alpha| |\zeta| \left(2 + \frac{5}{3} 3C_1 (\bar{\gamma} - 1) L_0 + 3C_2 F_\gamma - 3 \right) \\ &\leq C_2 |\alpha| |\zeta| \left(\frac{5}{3} \frac{C}{3} + \frac{C}{3} - 1 \right) \leq 0. \end{aligned}$$

Due to symmetry, $\Delta G \leq 0$ across the interaction $\beta + \zeta$.

4.3. Type C: Three waves entering the diamond.

4.3.1. *Type Ca: No contact discontinuities.* The interactions of this type are also present for the p -system and are covered by [16], although the detailed estimates are not given there. We choose to include the discussion of this type of interactions in detail since we measure the waves in p and since the methods are useful for later interactions. Note the increase of complexity one gets for the later interactions

involving a contact discontinuity. Recall that regular parentheses are used to indicate which edge the waves enter through, while square brackets are used to indicate which waves interact at each step.

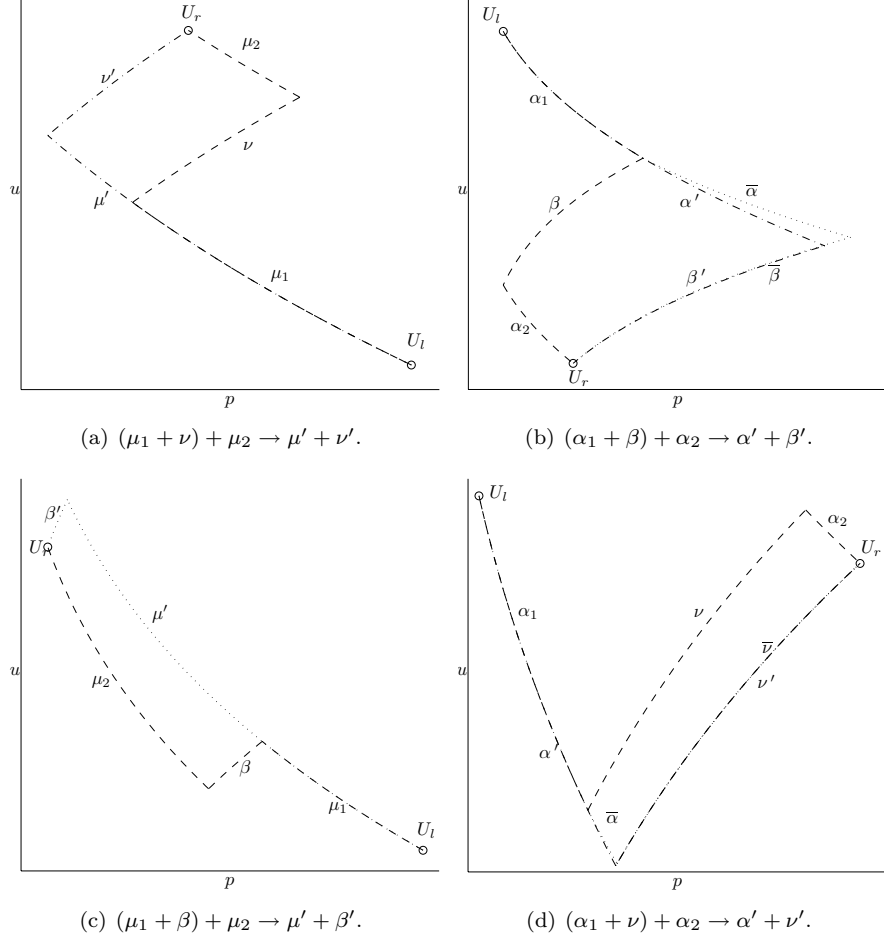


FIGURE 15. Some interactions of type Ca.

- (i) $(\mu_1 + \nu) + \mu_2 \rightarrow \mu' + \nu'$ (and $\nu_1 + (\mu + \nu_2) \rightarrow \mu' + \nu'$): This interaction has only one outcome, see Fig. 15(a), and we divide it into two steps,

$$\mu_1 + [\nu + \mu_2] \xrightarrow{\Delta G_1} \mu_1 + \bar{\mu} + \bar{\nu} \xrightarrow{\Delta G_2} \mu' + \nu'.$$

We have $\Delta G_1 \leq 0$ because the interaction at the first step is of type Bb-i. From property (iv) and property (vii) it follows that $\mu_1 + \bar{\mu} = \mu'$ and $\bar{\nu} = \nu'$, therefore $\Delta G_2 = 0$.

By symmetry it follows that $\Delta G \leq 0$ across $\nu_1 + (\mu + \nu_2)$.

- (ii) $(\alpha_1 + \beta) + \alpha_2 \rightarrow \alpha' + \beta'$ (and $\beta_1 + (\alpha + \beta_2) \rightarrow \alpha' + \beta'$): There is only one outcome of this interaction, see Fig. 15(b), and we divide it into two steps,

$$\alpha_1 + [\beta + \alpha_2] \xrightarrow{\Delta G_1} \alpha_1 + \bar{\alpha} + \bar{\beta} \xrightarrow{\Delta G_2} \alpha' + \beta'.$$

We have $\Delta G_1 \leq 0$ because the interaction at the first step is of type Bb-ii. Due to properties (viii) and (ix) we have

$$|\alpha'| - |\alpha_1| - |\bar{\alpha}| \leq 0, \quad |\beta'| - |\bar{\beta}| \leq 0,$$

and it follows that $\Delta G_2 \leq 0$.

By symmetry we have $\Delta G \leq 0$ across $\beta_1 + (\alpha + \beta_2)$.

- (iii) $(\mu_1 + \beta) + \mu_2 \rightarrow \mu' + \beta'$ (and $\nu_1 + (\alpha + \nu_2) \rightarrow \alpha' + \nu'$): There is only one possible outcome of this interaction, see Fig. 15(c), and we divide it into two steps,

$$\mu_1 + [\beta + \mu_2] \xrightarrow{\Delta G_1} \mu_1 + \bar{\mu} + \bar{\beta} \xrightarrow{\Delta G_2} \mu' + \beta'.$$

The first interaction is of type Bb-iii, thus $\Delta G_1 \leq 0$. From property (iv) and property (vii) it follows that $\mu_1 + \bar{\mu} = \mu'$, therefore we must also have $\bar{\beta} = \beta'$, and then $\Delta G_2 = 0$.

It follows from symmetry that $\Delta G \leq 0$ across $\nu_1 + (\alpha + \nu_2)$.

- (iv) $(\alpha_1 + \nu) + \alpha_2 \rightarrow \alpha' + \nu'$ (and $\beta_1 + (\mu + \beta_2) \rightarrow \mu' + \beta'$): This interaction has only one possible outcome, see Fig. 15(d), and we divide it into two steps,

$$\alpha_1 + [\nu + \alpha_2] \xrightarrow{\Delta G_1} \alpha_1 + \bar{\alpha} + \bar{\nu} \xrightarrow{\Delta G_2} \alpha' + \nu'.$$

Since the first interaction is of type Bb-iii, we have $\Delta G_1 \leq 0$. Property (iv) and property (viii) imply that

$$|\alpha'| - |\alpha_1| - |\bar{\alpha}| = -q, \quad |\nu'| - |\bar{\nu}| = q,$$

for a $q > 0$, and it follows that $\Delta G_2 \leq 0$.

From symmetry we have that $\Delta G \leq 0$ across $\beta_1 + (\mu + \beta_2)$.

- (v) $(\mu + \beta) + \alpha$ (and $\beta + (\alpha + \nu)$): This interaction has two possible outcomes.

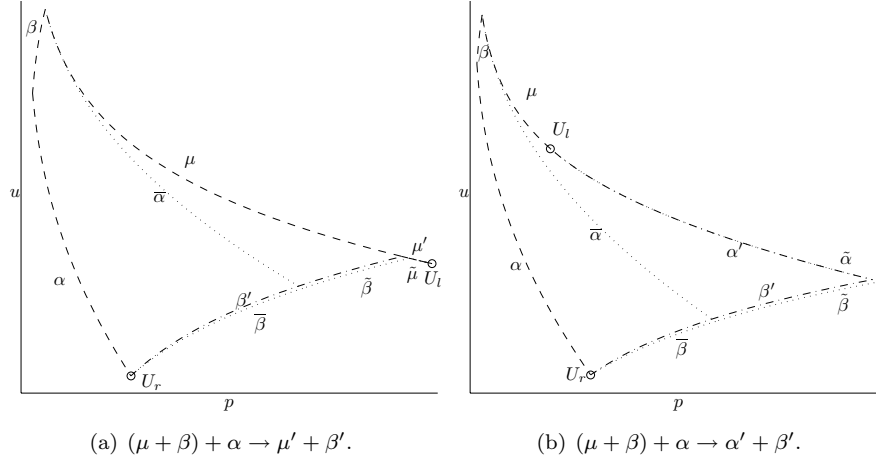


FIGURE 16. The interaction $(\mu + \beta) + \alpha$.

- $(\mu + \beta) + \alpha \rightarrow \mu' + \beta'$: In this case U_r is to the left of the 3-shock curve starting at U_l , see Fig. 16(a). We divide the interaction into three steps,

$$\mu + [\beta + \alpha] \xrightarrow{\Delta G_1} [\mu + \bar{\alpha}] + \bar{\beta} \xrightarrow{\Delta G_2} \tilde{\mu} + \tilde{\beta} + \bar{\beta} \xrightarrow{\Delta G_3} \mu' + \beta',$$

where we have $\Delta G_1 \leq 0$ because the interaction at the first step is of type Bb-ii, and $\Delta G_2 \leq 0$ because the second interaction is of type Ba-iii. From property (vi) and property (ix) we know that the intersection between $\bar{\alpha}$ and $\bar{\beta}$ is to the right of β' , but still $|\bar{\beta}| \leq |\beta'|$. However, from property (iv) and property (ix) it follows that $\tilde{\beta}$ starts to the left of β' and we have

$$|\mu'| - |\tilde{\mu}| = q, \quad |\beta'| - |\bar{\beta}| - |\tilde{\beta}| = -q,$$

from which we obtain $\Delta G_3 \leq 0$.

- $(\mu + \beta) + \alpha \rightarrow \alpha' + \beta'$: In this case U_r is to the right of the 3-shock curve starting at U_l , see Fig. 16(b). We divide the interaction into three steps,

$$\mu + [\beta + \alpha] \xrightarrow{\Delta G_1} [\mu + \bar{\alpha}] + \bar{\beta} \xrightarrow{\Delta G_2} \tilde{\alpha} + \tilde{\beta} + \bar{\beta} \xrightarrow{\Delta G_3} \alpha' + \beta'.$$

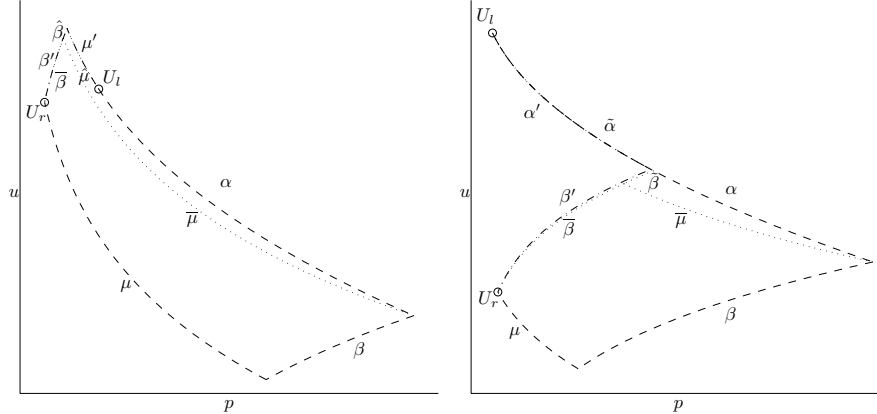
Again we have $\Delta G_1 \leq 0$ and $\Delta G_2 \leq 0$ because the interactions at the first and second step are of type Bb-ii and Ba-iii, respectively. Due to property (vi) and property (ix), the intersection between $\bar{\alpha}$ and $\bar{\beta}$ is to the right of β' . Therefore, we have from property (ix) that the intersection between $\tilde{\alpha}$ and $\tilde{\beta}$ is to the right of the intersection between α' and β' , and

$$|\alpha'| - |\tilde{\alpha}| \leq 0, \quad |\beta'| - |\bar{\beta}| - |\tilde{\beta}| \leq 0,$$

hence $\Delta G_3 \leq 0$.

By symmetry we have $\Delta G \leq 0$ across $\beta + (\alpha + \nu)$.

- (vi) $(\alpha + \beta) + \mu$ (and $\nu + (\alpha + \beta)$): This interaction has two outcomes.



(a) $(\alpha + \beta) + \mu \rightarrow \mu' + \beta'$.

(b) $(\alpha + \beta) + \mu \rightarrow \alpha' + \beta'$.

FIGURE 17. The interaction $(\alpha + \beta) + \mu$.

- $(\alpha + \beta) + \mu \rightarrow \mu' + \beta'$: In this case U_r is to the left of the 3-shock wave starting at U_l , see Fig. 17(a). We divide this interaction into three steps,

$$\alpha + [\beta + \mu] \xrightarrow{\Delta G_1} [\alpha + \bar{\mu}] + \bar{\beta} \xrightarrow{\Delta G_2} \tilde{\mu} + \tilde{\beta} + \bar{\beta} \xrightarrow{\Delta G_3} \mu' + \beta',$$

where $\Delta G_1 \leq 0$ and $\Delta G_2 \leq 0$ since the interactions at the first and second step are of type Bb-iii and Ba-ii, respectively. By property (vi) we know that $\bar{\mu}$ is lying below α , and together with property (ix), this implies that the intersection between $\bar{\mu}$ and $\bar{\beta}$ is to the right of β' . From property (iv) and property (ix) we then get

$$|\mu'| - |\tilde{\mu}| = q, \quad |\beta'| - \left| \tilde{\beta} \right| - |\bar{\beta}| = -q,$$

and it follows that $\Delta G_3 \leq 0$.

- $(\alpha + \beta) + \mu \rightarrow \alpha' + \beta'$: In this case U_r is to the right of the 3-shock wave starting at U_l , see Fig. 17(b). We divide this interaction into three steps,

$$\alpha + [\beta + \mu] \xrightarrow{\Delta G_1} [\alpha + \bar{\mu}] + \bar{\beta} \xrightarrow{\Delta G_2} \tilde{\alpha} + \tilde{\beta} + \bar{\beta} \xrightarrow{\Delta G_3} \alpha' + \beta,$$

where $\Delta G_1 \leq 0$ and $\Delta G_2 \leq 0$ because the interactions at the first and second step are of type Bb-iii and Ba-ii, respectively. By properties (vi) and (ix) we have that the intersection between $\bar{\mu}$ and $\bar{\beta}$ is to the right of β' . Furthermore, the intersection between $\hat{\alpha}$ and $\hat{\beta}$ is then by property (viii) and property (ix) to the right of the intersection between α' and β' , thus

$$|\alpha'| - |\tilde{\alpha}| \leq 0, \quad |\beta'| - \left| \tilde{\beta} \right| - |\bar{\beta}| \leq 0,$$

and it follows that $\Delta G_3 \leq 0$.

Due to symmetry, $\Delta G \leq 0$ across $\nu + (\alpha + \beta)$.

Before we carry on with the last two interactions of this type, we prove the following proposition.

Proposition 4.2. *If U_r is below the outgoing 1-wave for the interaction*

$$\mu + \nu + \alpha, \quad \text{or} \quad \alpha + \nu + \mu,$$

then the interaction can be replaced by

$$(4.6) \quad \hat{\mu} + \hat{\alpha}, \quad \text{or} \quad \hat{\alpha} + \hat{\mu},$$

respectively, where

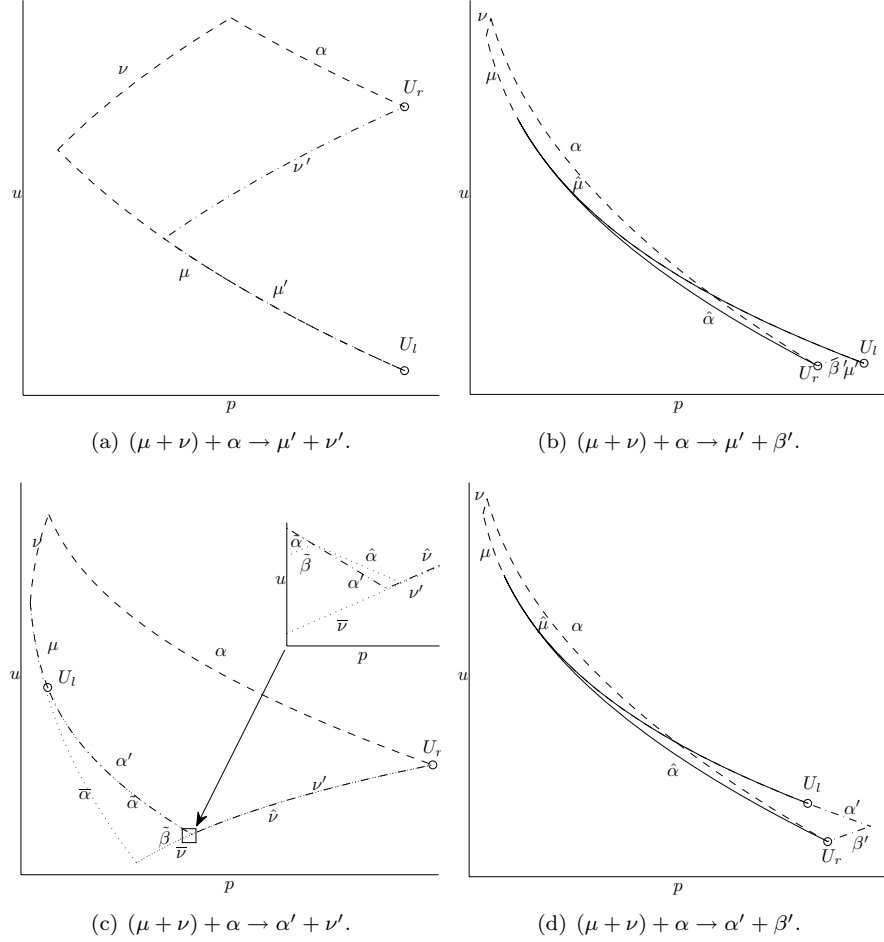
$$(4.7) \quad |\hat{\mu}| \leq |\mu|, \quad |\hat{\alpha}| \leq |\alpha|,$$

and $\Delta G \leq 0$ for the replacement.

Proof. Let us start with the second interaction. For U_r to be below the outgoing 1-wave, μ has to cross α . From property (iv) it then follows that U_l can be connected to U_r by following the wave α until the intersection point and then following μ from the intersection point to U_r . Obviously, the estimates in (4.7) are then satisfied and from these it follows that $\Delta G \leq 0$.

Also for the first interaction α and μ have to intersect if U_r is below the outgoing 1-wave. We are looking for a 1-shock wave, $\hat{\alpha}$, which ends at U_r and starts somewhere on μ . By property (viii) it follows that $\hat{\alpha}$ has to start to the left of the intersection point between μ and α , but to the right of the starting point of α . Thus, there exist a $\hat{\mu}$ and an $\hat{\alpha}$ so that (4.7) is satisfied and the interaction can be replaced by $\hat{\mu} + \hat{\alpha}$. From (4.7) we obtain $\Delta G \leq 0$. \square

- (vii) $(\mu + \nu) + \alpha$ (and $\beta + (\mu + \nu)$): This interaction has four possible outcomes.

FIGURE 18. The interaction $(\mu + \nu) + \alpha$.

- $(\mu + \nu) + \alpha \rightarrow \mu' + \nu'$: In this case U_r is above μ' and to the left of the 3-rarefaction curve starting at U_l , see Fig. 18(a). Observe that $|\mu'| \leq |\mu|$ and $|\nu'| \leq |\alpha|$. It then follows that

$$\begin{aligned}\Delta F &= -|\alpha|, \\ \Delta Q_1 &\leq 0, \\ \Delta Q_2 &\leq |\nu'| F_\gamma \leq |\alpha| F_\gamma,\end{aligned}$$

and we obtain $\Delta G \leq 0$.

- $(\mu + \nu) + \alpha \rightarrow \mu' + \beta'$: In this case U_r is below μ' and to the left of the 3-shock curve starting at U_l , see Fig. 18(b). By Proposition 4.2 we can replace this interaction by a new one,

$$\mu + \nu + \alpha \xrightarrow{\Delta G_1} [\hat{\mu} + \hat{\alpha}] \xrightarrow{\Delta G_2} \mu' + \beta',$$

where $\Delta G_1 \leq 0$. Moreover, the interaction at the second step is of type Ba-iii, thus $\Delta G_2 \leq 0$.

- $(\mu + \nu) + \alpha \rightarrow \alpha' + \nu'$: In this case U_r is above α' and to the right of the 3-rarefaction wave starting at U_l , see Fig. 18(c). We divide this interaction into four steps,

$$\begin{aligned} \mu + [\nu + \alpha] &\xrightarrow{\Delta G_1} [\mu + \bar{\alpha}] + \bar{\nu} \\ &\xrightarrow{\Delta G_2} \tilde{\alpha} + [\tilde{\beta} + \bar{\nu}] \\ &\xrightarrow{\Delta G_3} \tilde{\alpha} + \hat{\alpha} + \hat{\nu} \\ &\xrightarrow{\Delta G_4} \alpha' + \nu', \end{aligned}$$

where the interaction at the first step is of type Bb-iii, thus $\Delta G_1 \leq 0$. Furthermore, $\Delta G_2 \leq 0$ and $\Delta G_3 \leq 0$ because the interactions at the second and third step are both of type Ba-iii. From properties (iv) and (viii) we obtain

$$|\alpha'| - |\tilde{\alpha}| - |\hat{\alpha}| = -q, \quad |\nu'| - |\hat{\nu}| = q,$$

thus $\Delta G_4 \leq 0$.

- $(\mu + \nu) + \alpha \rightarrow \alpha' + \beta'$: In this case U_r is below α' and to the right of the 3-shock wave starting at U_l , see Fig. 18(d). From Proposition 4.2 we know that the interaction can be replaced by $\hat{\mu} + \hat{\alpha}$,

$$\mu + \nu + \alpha \xrightarrow{\Delta G_1} [\hat{\mu} + \hat{\alpha}] \xrightarrow{\Delta G_2} \alpha' + \beta',$$

where $\Delta G_1 \leq 0$. The interaction at the second step is of type Ba-iii and therefore $\Delta G_2 \leq 0$.

By symmetry we have $\Delta G \leq 0$ across $\beta + (\mu + \nu)$.

(viii) $(\alpha + \nu) + \mu$ (and $\nu + (\mu + \beta)$): This interaction has four possible outcomes.

- $(\alpha + \nu) + \mu \rightarrow \mu' + \nu'$: In this case U_r is above μ' and to the left of the 3-rarefaction wave starting at U_l , see Fig. 19(a). We divide this interaction into two steps,

$$\alpha + [\nu + \mu] \xrightarrow{\Delta G_1} \alpha + \bar{\mu} + \bar{\nu} \xrightarrow{\Delta G_2} \mu' + \nu',$$

where the interaction at the first step is of type Bb-i, thus $\Delta G_1 \leq 0$. By property (vi) we have that $\bar{\mu}$ lies below α , and therefore $|\nu'| \leq |\bar{\nu}|$. Since also $|\mu'| \leq |\bar{\mu}|$, we get $\Delta G_2 \leq 0$.

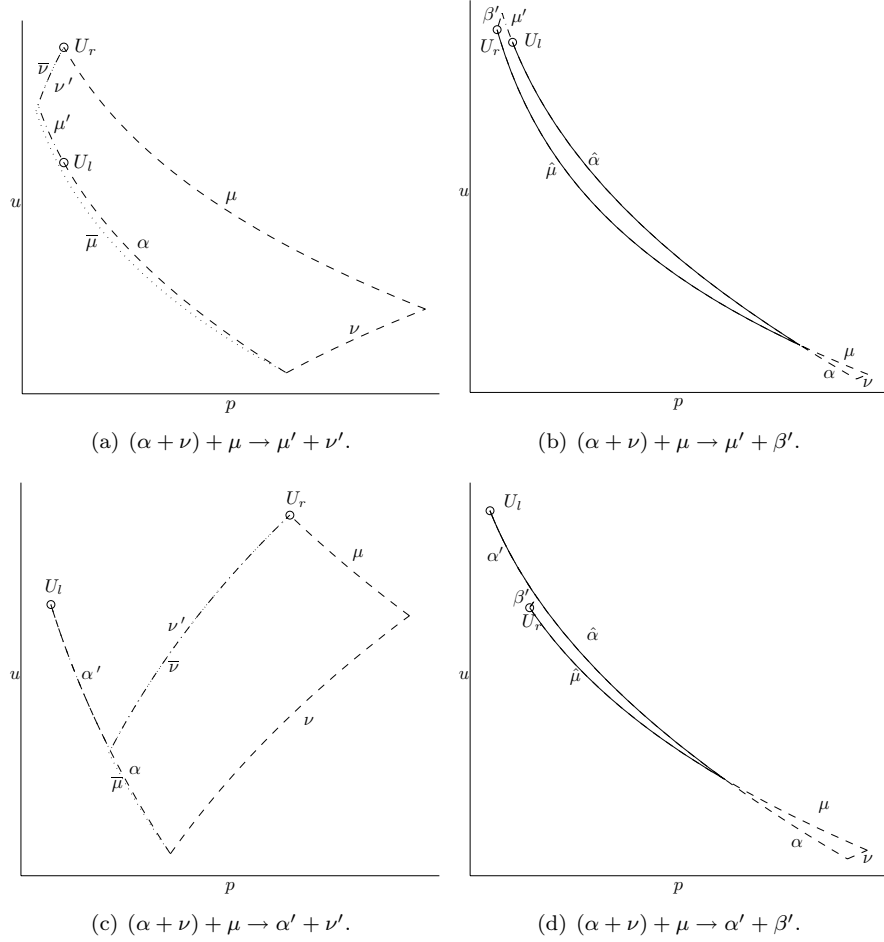
- $(\alpha + \nu) + \mu \rightarrow \mu' + \beta'$: In this case U_r is below μ' and to the left of the 3-shock wave starting at U_l , see Fig. 19(b). According to Proposition 4.2 the interaction can be replaced by a new one,

$$\alpha + \nu + \mu \xrightarrow{\Delta G_1} [\hat{\alpha} + \hat{\mu}] \xrightarrow{\Delta G_2} \mu' + \beta',$$

where $\Delta G_1 \leq 0$. Furthermore, $\Delta G_2 \leq 0$ because the interaction at the second step is of type Ba-ii.

- $(\alpha + \nu) + \mu \rightarrow \alpha' + \nu'$: In this case U_r is above α' and to the right of the 3-rarefaction wave starting at U_l , see Fig. 19(c). This interaction is divided into two steps,

$$\alpha + [\nu + \mu] \xrightarrow{\Delta G_1} \alpha + \bar{\mu} + \bar{\nu} \xrightarrow{\Delta G_2} \alpha' + \nu',$$

FIGURE 19. The interaction $(\alpha + \nu) + \mu$.

where the first interaction is of type Bb-i, thus $\Delta G_1 \leq 0$. We have $|\alpha'| \leq |\alpha|$. Since $\bar{\mu}$ lies below α by property (vi), we furthermore have $|\nu'| \leq |\bar{\nu}|$, and thus, $\Delta G_2 \leq 0$.

- $(\alpha + \nu) + \mu \rightarrow \alpha' + \beta'$: In this case U_r is below α' and to the right of the 3-shock wave starting at U_l , see Fig. 19(d). Again we can replace the interaction by a new one,

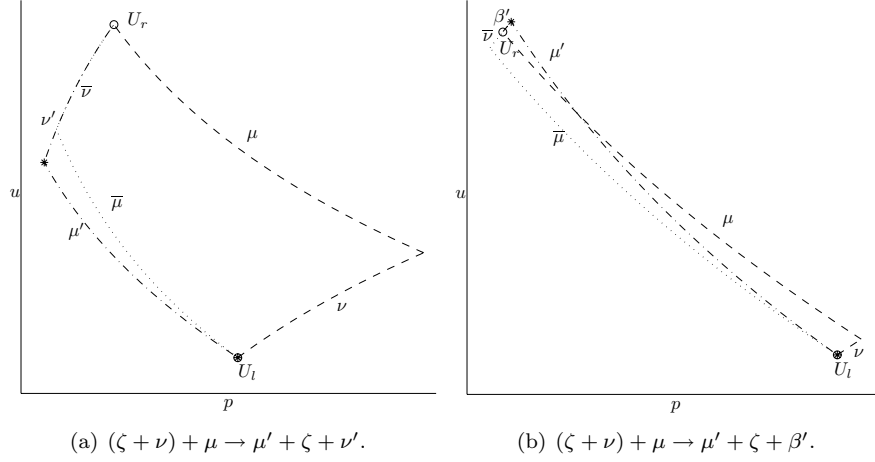
$$\alpha + \nu + \mu \xrightarrow{\Delta G_1} [\hat{\alpha} + \hat{\mu}] \xrightarrow{\Delta G_2} \alpha' + \beta',$$

where $\Delta G_1 \leq 0$ by Proposition 4.2. At the second step we have an interaction of type Ba-ii, thus $\Delta G_2 \leq 0$.

It follows from symmetry that $\Delta G \leq 0$ across $\nu + (\mu + \beta)$.

4.3.2. *Type Cb: A contact discontinuity as the leftmost or rightmost wave.* All these interactions have two possible outcomes.

- (i) $(\zeta + \nu) + \mu$ (and $\nu + (\mu + \zeta)$):

FIGURE 20. The interaction $(\zeta + \nu) + \mu$.

- $(\zeta + \nu) + \mu \rightarrow \mu' + \zeta + \nu'$: In this case U_r lies above μ' , see Fig. 20(a). We divide the interaction into two steps

$$\zeta + [\nu + \mu] \xrightarrow{\Delta G_1} \zeta + \bar{\mu} + \bar{\nu} \xrightarrow{\Delta G_2} \mu' + \zeta + \nu'.$$

The interaction at the first step is of type Bb-i and thus $\Delta G_1 \leq 0$. If the intersection between $\bar{\mu}$ and $\bar{\nu}$ is below μ' , then $|\mu'| \leq |\bar{\mu}|$ and $|\nu'| \leq |\bar{\nu}|$ and $\Delta G_2 \leq 0$. If the intersection is above μ' , then $|\mu'| - |\bar{\mu}| = |\nu'| - |\bar{\nu}|$ and by using Lemma 2.2 on $\bar{\mu}$ and μ' we get

$$|\mu'| - |\bar{\mu}| \leq C_2 |\bar{\mu}| |\zeta|, \quad |\nu'| - |\bar{\nu}| \leq C_2 |\bar{\mu}| |\zeta|,$$

and hence, $\Delta G_2 \leq 0$.

- $(\zeta + \nu) + \mu \rightarrow \mu' + \zeta + \beta'$: In this case U_r lies below μ' , see Fig. 20(b). We divide the interaction into two steps,

$$\zeta + [\nu + \mu] \xrightarrow{\Delta G_1} \zeta + \bar{\mu} + \bar{\nu} \xrightarrow{\Delta G_2} \mu' + \zeta + \beta'.$$

The interaction at the first step is of type Bb-i and we have $\Delta G_1 \leq 0$. Furthermore, we have $|\beta'| \leq |\bar{\mu}| - |\mu'|$ and applying Lemma 2.2 on $\bar{\mu}$ and μ' we obtain

$$|\mu'| - |\bar{\mu}| \leq 0, \quad |\beta'| \leq C_2 |\mu'| |\zeta| \leq C_2 |\bar{\mu}| |\zeta|,$$

from which we get $\Delta G_2 \leq 0$.

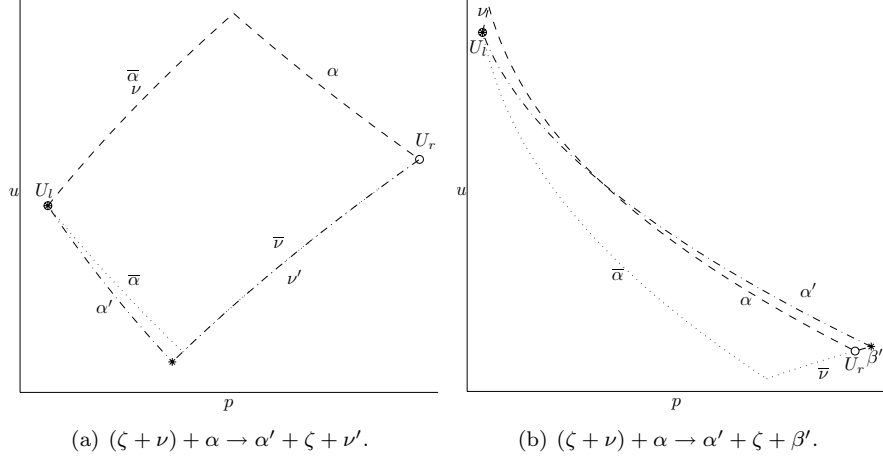
Due to symmetry, $\Delta G \leq 0$ across $\nu + (\mu + \zeta)$.

(ii) $(\zeta + \nu) + \alpha$ (and $\beta + (\mu + \zeta)$):

- $(\zeta + \nu) + \alpha \rightarrow \alpha' + \zeta + \nu'$: In this case U_r is above α' , see Fig. 21(a). We divide the interaction into two steps,

$$\zeta + [\nu + \alpha] \xrightarrow{\Delta G_1} \zeta + \bar{\alpha} + \bar{\nu} \xrightarrow{\Delta G_2} \alpha' + \zeta + \nu'.$$

At the first step we have an interaction of type Bb-iii, thus $\Delta G_1 \leq 0$. If the intersection between $\bar{\alpha}$ and $\bar{\nu}$ is above α' as in Fig. 21(a), then we

FIGURE 21. The interaction $(\zeta + \nu) + \alpha$.

have

$$|\alpha'| - |\bar{\alpha}| = -q, \quad |\nu'| - |\bar{\nu}| = q,$$

which results in $\Delta G_2 \leq 0$. If the intersection is below, we use Lemma 2.2 on $\bar{\alpha}$ and α' , and get

$$|\alpha'| - |\bar{\alpha}| \leq C_2 |\zeta| |\bar{\alpha}|, \quad |\nu'| - |\bar{\nu}| \leq 0,$$

therefore, $\Delta G_2 \leq 0$.

- $(\zeta + \nu) + \alpha \rightarrow \alpha' + \zeta + \beta'$: In this case U_r is below α' , see Fig. 21(b). We divide the interaction into two steps,

$$\zeta + [\nu + \alpha] \xrightarrow{\Delta G_1} \zeta + \bar{\alpha} + \bar{\nu} \xrightarrow{\Delta G_2} \alpha' + \zeta + \beta'.$$

Since the interaction at the first step is of type Bb-iii we have $\Delta G_1 \leq 0$, and by construction $|\beta'| \leq |\alpha'| - |\bar{\alpha}|$. We apply Lemma 2.2 on $\bar{\alpha}$ and α' and find

$$|\alpha'| - |\bar{\alpha}| \leq C_2 |\zeta| |\bar{\alpha}|, \quad |\beta'| \leq C_2 |\zeta| |\bar{\alpha}|,$$

thus $\Delta G_2 \leq 0$.

By symmetry we have $\Delta G \leq 0$ across $\beta + (\mu + \zeta)$.

- (iii) $(\zeta + \beta) + \mu$ (and $\nu + (\alpha + \zeta)$):

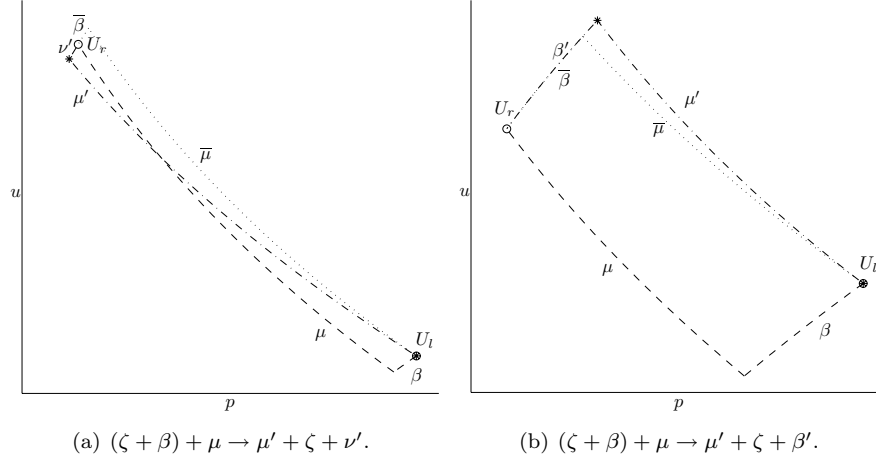
- $(\zeta + \beta) + \mu \rightarrow \mu' + \zeta + \nu'$: In this case U_r is above μ' , see Fig. 22(a). Two steps are enough,

$$\zeta + [\beta + \mu] \xrightarrow{\Delta G_1} \zeta + \bar{\mu} + \bar{\beta} \xrightarrow{\Delta G_2} \mu' + \zeta + \nu',$$

where the interaction at the first step is of type Bb-iii, thus $\Delta G_1 \leq 0$. We have $|\nu'| \leq |\mu'| - |\bar{\mu}|$ and apply Lemma 2.2 on $\bar{\mu}$ and μ' . We get

$$|\mu'| - |\bar{\mu}| \leq C_2 |\bar{\mu}| |\zeta|, \quad |\nu'| \leq C_2 |\bar{\mu}| |\zeta|,$$

and it follows that $\Delta G_2 \leq 0$.


 FIGURE 22. The interaction $(\zeta + \beta) + \mu$.

- $(\zeta + \beta) + \mu \rightarrow \mu' + \zeta + \beta'$: In this case U_r is below μ' , see Fig. 22(b). This interaction is divided into two steps,

$$\zeta + [\beta + \mu] \xrightarrow{\Delta G_1} \zeta + \bar{\mu} + \bar{\beta} \xrightarrow{\Delta G_2} \mu' + \zeta + \nu,$$

where $\Delta G_1 \leq 0$ because the interaction at the first step is of type Bb-iii. If the intersection between $\bar{\mu}$ and $\bar{\beta}$ is above μ' , it follows from property (ix) that

$$|\mu'| - |\bar{\mu}| = q, \quad |\beta'| - |\bar{\beta}| = -q,$$

thus, $\Delta G_2 \leq 0$. If the intersection is below, as in Fig. 22(b), it follows from property (ix) that $|\mu'| \leq |\bar{\mu}|$. We then use Lemma 2.2 on $\bar{\beta}$ and β' and obtain

$$|\mu'| - |\bar{\mu}| \leq 0, \quad |\beta'| - |\bar{\beta}| \leq C_2 |\zeta| |\bar{\beta}|,$$

thus, $\Delta G_2 \leq 0$.

Due to symmetry, $\Delta G \leq 0$ across $\nu + (\alpha + \zeta)$.

(iv) $(\zeta + \beta) + \alpha$ (and $\beta + (\alpha + \zeta)$):

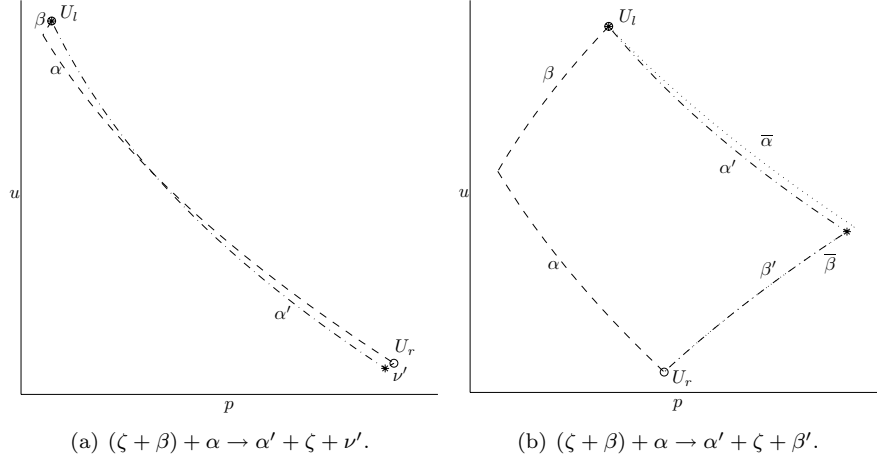
- $(\zeta + \beta) + \alpha \rightarrow \alpha' + \zeta + \nu'$: In this case U_r is above α' , see Fig. 23(a). We can divide the interaction into steps by the same approach as above, but this is not necessary for this interaction. We have $|\alpha'| - |\alpha| \leq -|\nu'|$, thus

$$\begin{aligned} \Delta F &= |\alpha'| - |\alpha| - |\beta| \leq -|\nu'|, \\ \Delta Q_1 &\leq 0, \\ \Delta Q_2 &\leq |\nu'| F_\gamma, \end{aligned}$$

which yields $\Delta G \leq 0$.

- $(\zeta + \beta) + \alpha \rightarrow \alpha' + \zeta + \beta'$: In this case U_r is below α' , see Fig. 23(b). Again we divide into two steps

$$\zeta + [\beta + \alpha] \xrightarrow{\Delta G_1} \zeta + \bar{\alpha} + \bar{\beta} \xrightarrow{\Delta G_2} \alpha' + \zeta + \beta',$$

FIGURE 23. The interaction $(\zeta + \beta) + \alpha$.

where the interaction at the first step is of type Bb-iii with $\Delta G_1 \leq 0$. If the intersection between $\bar{\alpha}$ and $\bar{\beta}$ is above α' , as in Fig. 23(b), it follows from property (viii) and property (ix) that

$$|\alpha'| - |\bar{\alpha}| \leq 0, \quad |\beta'| - |\bar{\beta}| \leq 0,$$

hence, $\Delta G_2 \leq 0$. If the intersection is below, we have $|\alpha'| - |\bar{\alpha}| = |\beta'| - |\bar{\beta}|$ and by applying Lemma 2.2 to the 1-shock curves we obtain

$$|\alpha'| - |\bar{\alpha}| \leq C_2 |\bar{\alpha}| |\zeta|, \quad |\beta'| - |\bar{\beta}| \leq C_2 |\bar{\alpha}| |\zeta|.$$

From these estimates we obtain $\Delta G_2 \leq 0$.

By symmetry we have $\Delta G \leq 0$ across the interaction $\beta + (\alpha + \zeta)$.

4.3.3. Type Cc: A contact discontinuities as the middle wave.

(i) $(\mu_1 + \zeta) + \mu_2$ (and $\nu_1 + (\zeta + \nu_2)$): This interaction has two possible outcomes.

- $(\mu_1 + \zeta) + \mu_2 \rightarrow \mu' + \zeta + \nu'$: In this case U_r is above μ' , see Fig. 24(a). We divide the interaction into two steps,

$$\mu_1 + [\zeta + \mu_2] \xrightarrow{\Delta G_1} \mu_1 + \bar{\mu} + \zeta + \bar{\nu} \xrightarrow{\Delta G_2} \mu' + \zeta + \nu'.$$

The interaction at the first step is of type Bc-i, thus $\Delta G_1 \leq 0$. Note that μ_1 , $\bar{\mu}$ and μ' all have $\gamma = \gamma_l$, and $\bar{\nu}$ and ν' have $\gamma = \gamma_r$. By property (iv) and property (vii) we therefore have $\mu_1 + \bar{\mu} = \mu'$ and $\bar{\nu} = \nu'$, thus $\Delta G_2 = 0$.

- $(\mu_1 + \zeta) + \mu_2 \rightarrow \mu' + \zeta + \beta'$: In this case U_r lies below μ' , see Fig. 24(b). This interaction is divided into two steps,

$$\mu_1 + [\zeta + \mu_2] \xrightarrow{\Delta G_1} \mu_1 + \bar{\mu} + \zeta + \bar{\beta} \xrightarrow{\Delta G_2} \mu' + \zeta + \beta'.$$

The interaction at the first step is of type Bc-i with $\Delta G_1 \leq 0$. Furthermore, μ_1 , $\bar{\mu}$ and μ' all have the same γ , and so do $\bar{\beta}$ and β' . Property (iv) and property (vii) then imply that $\mu_1 + \bar{\mu} = \mu'$, therefore we also have that $\bar{\beta} = \beta'$, and it follows that $\Delta G_2 = 0$.

Due to symmetry, $\Delta G \leq 0$ across the interaction $\nu_1 + (\zeta + \nu_2)$ as well.

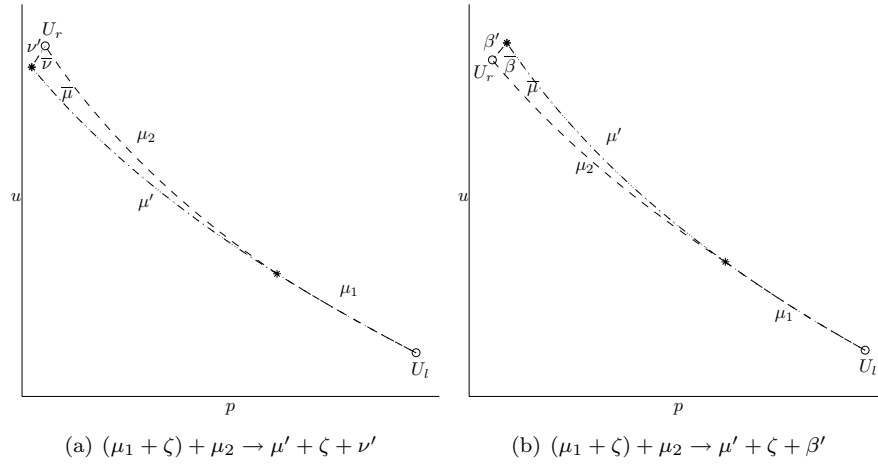


FIGURE 24. The interaction $(\mu_1 + \zeta) + \mu_2$.

(ii) $(\alpha_1 + \zeta) + \alpha_2$ (and $\beta_1 + (\zeta + \beta_2)$): This interaction has two possible outcomes.

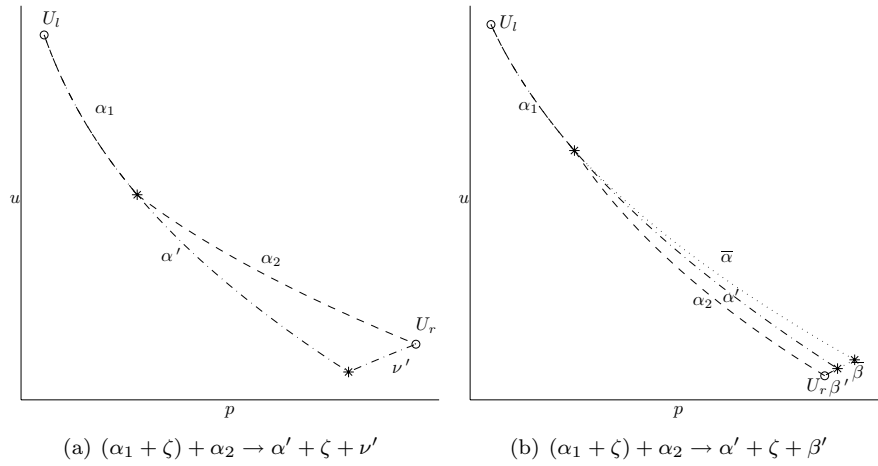


FIGURE 25. The interaction $(\alpha_1 + \zeta) + \alpha_2$.

- $(\alpha_1 + \zeta) + \alpha_2 \rightarrow \alpha' + \zeta + \nu'$: In this case U_r is above α' , see Fig. 25(a). No extra steps are needed because we have

$$|\alpha'| - |\alpha_1| - |\alpha_2| = -|\nu'|,$$

which gives us

$$\Delta F = -|\nu'|,$$

$$\Delta Q_1 \leq 0,$$

$$\Delta Q_2 \leq |\nu'| F_\gamma - |\zeta| |\alpha_2| \leq |\nu'| F_\gamma,$$

and

$$\Delta G \leq |\nu'|(-1 + 3C_2F_\gamma) \leq |\nu'| \left(-1 + \frac{C}{3} \right) \leq 0.$$

- $(\alpha_1 + \zeta) + \alpha_2 \rightarrow \alpha' + \zeta + \beta'$. In this case U_r is below α' , see Fig. 25(b). In this case we need two steps,

$$\alpha_1 + [\zeta + \alpha_2] \xrightarrow{\Delta G_1} \alpha_1 + \bar{\alpha} + \zeta + \bar{\beta} \xrightarrow{\Delta G_2} \alpha' + \zeta + \beta'.$$

The interaction at the first step is of type Bc-ii, thus $\Delta G_1 \leq 0$. Note that $\bar{\alpha}$ and α' have the same γ , and so do $\bar{\beta}$ and β' . It therefore follows from property (viii) and property (ix) that the intersection point between $\bar{\alpha}$ and $\bar{\beta}$ is to the right of the intersection point between α' and β' . This yields

$$|\alpha'| - |\alpha_1| - |\bar{\alpha}| \leq 0, \quad |\beta'| - |\bar{\beta}| \leq 0,$$

and we obtain $\Delta G_2 \leq 0$.

By symmetry it follows that $\Delta G \leq 0$ across the interaction $\beta_1 + (\zeta + \beta_2)$.

Before discussing the last interactions of this type, we prove a useful proposition.

Proposition 4.3. *If U_r is below the outgoing 1-wave for the interactions*

$$\mu + \zeta + \alpha, \quad \text{or} \quad \alpha + \zeta + \mu,$$

and if

$$\zeta + \alpha \rightarrow \bar{\alpha} + \zeta + \bar{\nu}, \quad \text{or} \quad \zeta + \mu \rightarrow \bar{\mu} + \zeta + \bar{\nu},$$

respectively, then U_l can be connected to U_r by

$$(4.8) \quad \hat{\mu} + \hat{\alpha} + \zeta, \quad \text{or} \quad \hat{\alpha} + \hat{\mu} + \zeta,$$

respectively, where

$$(4.9) \quad |\hat{\mu}| \leq |\mu|, \quad \text{and} \quad |\hat{\alpha}| \leq |\alpha|,$$

and $\Delta G \leq 0$ for the replacement.

Proof. For the first interaction we are looking for a 1-shock wave, $\hat{\alpha}$, with $\gamma = \gamma_l$ that is starting somewhere at μ and ending at $\hat{U} = (p_r, u_r, \gamma_l)$. From property (viii) it follows that $\hat{\alpha}$ cannot reach \hat{U} if it starts to the left of $\bar{\alpha}$. Moreover, since U_r lies below any 1-wave starting at U_l , so does \hat{U} , and therefore $\hat{\alpha}$ has to start to the right of U_l . This proves that there exists a $\hat{\mu}$ and an $\hat{\alpha}$ so that U_l is connected to U_r by the first interaction of (4.8) and so that (4.9) is satisfied. From (4.9) it follows that $\Delta G \leq 0$ for the replacement.

For the second interaction consider the backward 1-rarefaction curve from \hat{U} . By property (iv) this wave will stay above $\bar{\mu}$ and, since \hat{U} lies below any 1-wave starting at U_l , the backward rarefaction curve must intersect α . Thus, there exists a $\hat{\mu}$ and an $\hat{\alpha}$ so that U_l is connected to U_r by the second interaction of (4.8) and so that (4.9) is satisfied. Furthermore, it follows from (4.9) that $\Delta G \leq 0$ for the replacement. \square

- (iii) $(\mu + \zeta) + \alpha$ (and $\beta + (\zeta + \nu)$): This interaction has four different outcomes.

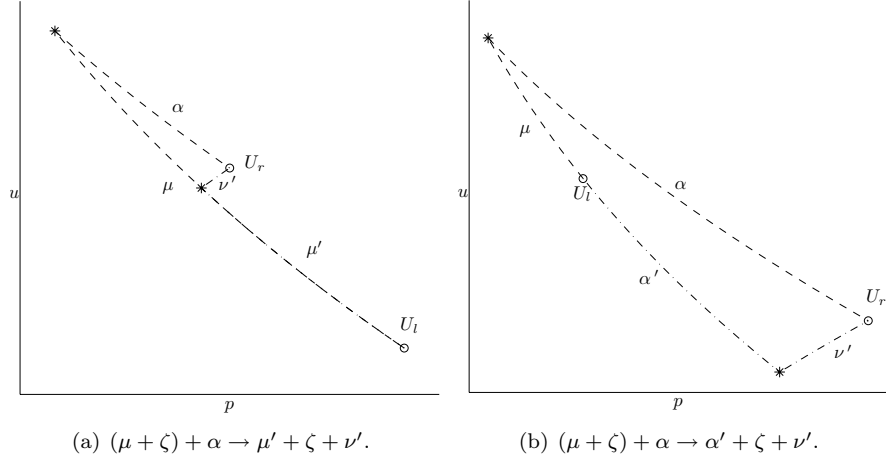


FIGURE 26. Two outcomes of the interaction $(\mu + \zeta) + \alpha$.

- $(\mu + \zeta) + \alpha \rightarrow \mu' + \zeta + \nu'$: In this case U_r is above μ and to the left of the 3-rarefaction curve starting at U_l , see Fig. 26(a). We have $|\mu'| \leq |\mu|$ and $|\nu'| \leq |\alpha|$, thus

$$\begin{aligned} \Delta F &= -|\alpha|, \\ \Delta Q_1 &\leq 0, \\ \Delta Q_2 &\leq |\nu'| F_\gamma \leq |\alpha| F_\gamma, \end{aligned}$$

which gives

$$\Delta G \leq |\alpha| (-1 + 3C_2 F_\gamma) \leq |\alpha| \left(-1 + \frac{C}{3} \right) \leq 0.$$

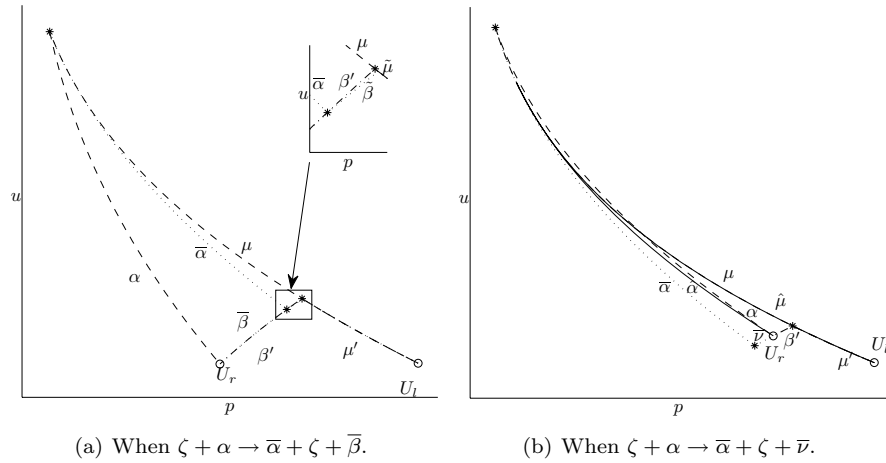


FIGURE 27. The interaction $(\mu + \zeta) + \alpha \rightarrow \mu' + \zeta + \beta'$.

- $(\mu + \zeta) + \alpha \rightarrow \mu' + \zeta + \beta'$: In this case U_r is below μ' and to the left of the 3-shock curve starting at U_l , see Fig. 27. This interaction needs several steps, and it is natural to let ζ and α interact first. We do not know what type of outgoing 3-wave this interaction gives, and we will have to look at each case separately. Assume first that $\zeta + \alpha \rightarrow \bar{\alpha} + \zeta + \bar{\beta}$, as in Fig. 27(a), then we have

$$\begin{aligned} \mu + [\zeta + \alpha] &\xrightarrow{\Delta G_1} [\mu + \bar{\alpha}] + \zeta + \bar{\beta} \\ &\xrightarrow{\Delta G_2} \tilde{\mu} + \tilde{\beta} + \zeta + \bar{\beta} \\ &\xrightarrow{\Delta G_3} \mu' + \zeta + \beta'. \end{aligned}$$

The interaction at step one is of type Bc-ii, therefore $\Delta G_1 \leq 0$. At the second step the interaction is of type Ba-iii, thus $\Delta G_2 \leq 0$. We do not know whether $\tilde{\beta}$ starts to the left or the right of β' because the two waves have different γ 's. If $\tilde{\beta}$ starts to the right, as in Fig. 27(a), we have for a $q > 0$ that

$$|\mu'| - |\tilde{\mu}| \leq q, \quad |\beta'| - |\tilde{\beta}| - |\bar{\beta}| = -q,$$

which gives

$$\Delta F = -q, \quad \Delta Q_1 \leq 0, \quad \Delta Q_2 \leq qF_\gamma,$$

and it follows that $\Delta G_3 \leq 0$. If $\tilde{\beta}$ starts to the left of β' , we claim that

$$(4.10) \quad |\mu'| - |\tilde{\mu}| \leq 0, \quad |\beta'| - |\bar{\beta}| - |\tilde{\beta}| \leq C_2 |\tilde{\beta}| |\zeta|,$$

which gives us

$$\begin{aligned} \Delta F &\leq C_2 |\tilde{\beta}| |\zeta|, \\ \Delta Q_1 &\leq C_2 |\tilde{\beta}| |\zeta| F_n, \\ \Delta Q_2 &\leq C_2 |\tilde{\beta}| |\zeta| F_\gamma - |\tilde{\beta}| |\zeta|, \end{aligned}$$

and furthermore that

$$\Delta G_3 \leq C_2 |\tilde{\beta}| |\zeta| (1 + 3C_1(\bar{\gamma} - 1)F_n + 3C_2F_\gamma - 3) \leq 0.$$

Thus, we just have to prove (4.10). We introduce a 3-shock curve with $\gamma = \gamma_r$, β^* , that starts somewhere on μ and ends at the same point as $\tilde{\beta}$ ends. Since β^* has the same γ as β' , it follows from property (ix) that β^* starts to the right of β' , thus $|\beta'| - |\tilde{\beta}| - |\bar{\beta}| \leq |\beta^*| - |\tilde{\beta}|$. Moreover, β^* and $\tilde{\beta}$ have different γ 's and ends at the same point, therefore we can apply Lemma 2.2 on the two shock waves and obtain $|\beta^*| - |\tilde{\beta}| \leq C_2 |\tilde{\beta}| |\zeta|$. Since the estimate on the rarefaction waves follows directly from the construction, we have proved (4.10).

Assume now that $\zeta + \alpha \rightarrow \bar{\alpha} + \zeta + \bar{\nu}$, this is illustrated in Fig. 27(b). By Proposition 4.3 we can replace the interaction by a new one,

$$\mu + \zeta + \alpha \xrightarrow{\Delta G_1} [\hat{\mu} + \hat{\alpha}] + \zeta$$

$$\begin{aligned} & \xrightarrow{\Delta G_2} \tilde{\mu} + \tilde{\beta} + \zeta \\ & \xrightarrow{\Delta G_3} \mu' + \zeta + \beta', \end{aligned}$$

where $\Delta G_1 \leq 0$. The interaction at the second step is of type Ba-iii, thus $\Delta G_2 \leq 0$. If $\tilde{\beta}$ starts to the right of β' , we have for a $q > 0$ that

$$|\mu'| - |\tilde{\mu}| = q, \quad |\beta'| - |\tilde{\beta}| = -q,$$

which gives $\Delta G_3 \leq 0$. If $\tilde{\beta}$ starts to the right of β' , we have $|\mu'| - |\tilde{\mu}| \leq 0$. Furthermore, since $\tilde{\beta}$ and β' ends at the same point, but have different γ 's, it follows by applying Lemma 2.2 that

$$|\beta'| - |\tilde{\beta}| \leq C_2 |\tilde{\beta}| |\zeta|,$$

and we get $\Delta G_3 \leq 0$. Figure 27(b) do not show $\tilde{\beta}$ since it lies very close to β' .

- $(\mu + \zeta) + \alpha \rightarrow \alpha' + \zeta + \nu'$: In this case U_r is above α' and to the right of the 3-rarefaction curve starting at U_l , see Fig. 26(b). Since

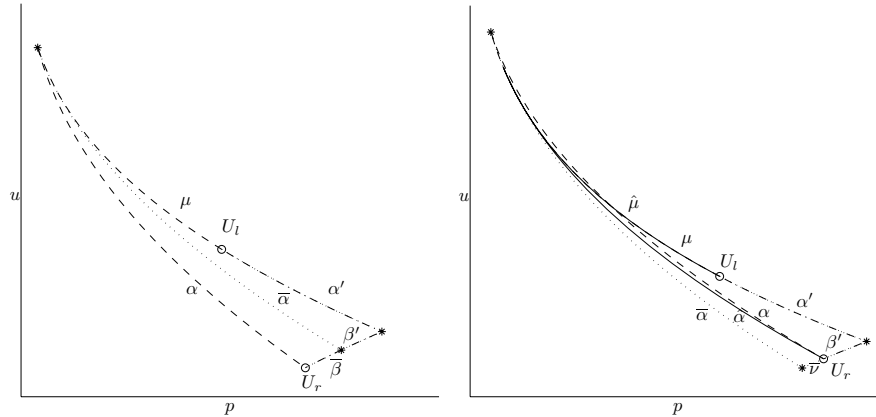
$$|\alpha'| + |\nu'| \leq |\alpha|, \quad \text{or} \quad |\alpha'| - |\alpha| \leq -|\nu'|,$$

we have

$$\Delta F = -|\nu'|, \quad \Delta Q_1 \leq 0, \quad \Delta Q_2 \leq |\nu'| F_\gamma,$$

which gives

$$\Delta G \leq |\nu'| (-1 + 3C_2 F_\gamma) \leq |\nu'| \left(-1 + \frac{C}{3} \right) \leq 0.$$



(a) When $\zeta + \alpha \rightarrow \bar{\alpha} + \zeta + \bar{\beta}$.

(b) When $\zeta + \alpha \rightarrow \bar{\alpha} + \zeta + \bar{\nu}$.

FIGURE 28. The interaction $(\mu + \zeta) + \alpha \rightarrow \alpha' + \zeta + \beta'$.

- $(\mu + \zeta) + \alpha \rightarrow \alpha' + \zeta + \beta'$: In this case U_r is below α' and to the right of the 3-shock curve starting at U_l , see Fig. 28. Again we do not know what type of outgoing 3-wave we get if ζ and α interact, and we need to

consider each case separately. Assume first that $\zeta + \alpha \rightarrow \bar{\alpha} + \zeta + \bar{\beta}$, as illustrated in Fig. 28(a), then we need four steps,

$$\begin{aligned} \mu + [\zeta + \alpha] &\xrightarrow{\Delta G_1} [\mu + \bar{\alpha}] + \zeta + \bar{\beta} \\ &\xrightarrow{\Delta G_2} \tilde{\alpha} + [\tilde{\beta} + \zeta + \bar{\beta}] \\ &\xrightarrow{\Delta G_3} \tilde{\alpha} + \hat{\alpha} + \zeta + \hat{\beta} \\ &\xrightarrow{\Delta G_4} \alpha' + \zeta + \beta'. \end{aligned}$$

The interaction at the first step is of type Bc-ii, thus $\Delta G_1 \leq 0$. At the second step the interaction is of type Ba-iii and $\Delta G_2 \leq 0$. If $\tilde{\beta}$ starts to the right of β' , the remaining steps can be skipped because then

$$|\alpha'| - |\tilde{\alpha}| \leq 0, \quad |\beta'| - |\tilde{\beta}| - |\bar{\beta}| \leq 0,$$

and going straight to the last step we get $\Delta G_* \leq 0$. If $\tilde{\beta}$ starts to the left of β' , we need one more step² and the interaction at the third step is of type Cc-ii, thus $\Delta G_3 \leq 0$. The waves $\tilde{\alpha}$, $\hat{\alpha}$ and α' all have $\gamma = \gamma_l$ and $\hat{\beta}$ and β' have $\gamma = \gamma_r$. Combining properties (viii) and (ix) it follows that

$$|\alpha'| - |\tilde{\alpha}| - |\hat{\alpha}| \leq 0, \quad |\beta'| - |\hat{\beta}| \leq 0,$$

and we have $\Delta G_4 \leq 0$. The waves $\tilde{\alpha}$ and $\tilde{\beta}$ are not denoted in Fig. 28(a) because they lie very close to α' and β' .

Assume now that $\zeta + \alpha \rightarrow \bar{\alpha} + \zeta + \bar{\nu}$, see Fig. 28(b). According to Proposition 4.3, we can replace the interaction with a new one,

$$\begin{aligned} \mu + \zeta + \alpha &\xrightarrow{\Delta G_1} [\hat{\mu} + \hat{\alpha}] + \zeta \\ &\xrightarrow{\Delta G_2} \tilde{\alpha} + \tilde{\beta} + \zeta \\ &\xrightarrow{\Delta G_3} \alpha' + \zeta + \beta', \end{aligned}$$

where $\Delta G_1 \leq 0$. At the second step we have an interaction of type Ba-iii with $\Delta G_2 \leq 0$. If $\tilde{\beta}$ starts to the right of β' , we have

$$|\alpha'| - |\tilde{\alpha}| \leq 0, \quad |\beta'| - |\tilde{\beta}| \leq 0,$$

hence $\Delta G_3 \leq 0$. If $\tilde{\beta}$ starts to the left of β' , we have $|\alpha'| - |\tilde{\alpha}| = |\beta'| - |\tilde{\beta}|$. Furthermore, since $\tilde{\beta}$ and β' ends at the same point, but have different γ 's, it follows by applying Lemma 2.2 that

$$|\beta'| - |\tilde{\beta}| \leq C_2 |\tilde{\beta}| |\zeta|,$$

and therefore $\Delta G_3 \leq 0$.

By symmetry it follows that $\Delta G \leq 0$ across the interaction $\beta + (\zeta + \nu)$.

(iv) $(\alpha + \zeta) + \mu$ (and $\nu + (\zeta + \beta)$): This interaction has four different outcomes.

²Here we could compare $\tilde{\beta}$ to an auxiliary curve β^* with $\gamma = \gamma_r$, similar to what we did before, but since only one more step is needed, we chose this approach.

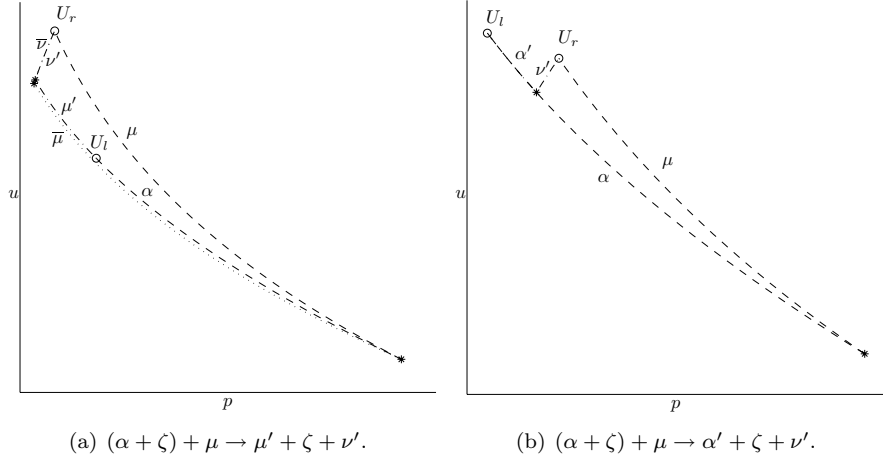


FIGURE 29. Two outcomes of the interaction $(\alpha + \zeta) + \mu$.

- $(\alpha + \zeta) + \mu \rightarrow \mu' + \zeta + \nu'$: In this case U_r is above μ' and to the left of the 3-rarefaction wave starting at U_l , see Fig. 29(a). We divide the interaction into two steps,

$$\alpha + [\zeta + \mu] \xrightarrow{\Delta G_1} \alpha + \bar{\mu} + \zeta + \bar{\nu} \xrightarrow{\Delta G_2} \mu' + \zeta + \nu',$$

where the interaction at the first step is of type Bc-i, thus $\Delta G_1 \leq 0$. Since $\bar{\mu}$ has to lie below α by property (vi), the outgoing 3-wave of the first step is a rarefaction wave. From this it follows that

$$|\mu'| - |\bar{\mu}| \leq 0, \quad |\nu'| - |\bar{\nu}| \leq 0,$$

and therefore $\Delta G_2 \leq 0$.

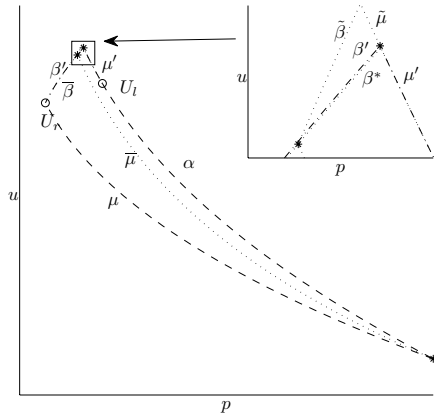


FIGURE 30. $(\alpha + \zeta) + \mu \rightarrow \mu' + \zeta + \beta'$.

- $(\alpha + \zeta) + \mu \rightarrow \mu' + \zeta + \beta'$: In this case U_r is below μ' and to the left of the 3-rarefaction wave starting at U_l , see Fig. 30. If ζ and μ interact we again

do not know the type of the outgoing 3-wave we get, and we choose to look at the two cases separately. Assume first that the outgoing 3-wave is a shock wave as illustrated in Fig. 30. Then we need three steps,

$$\begin{aligned} \alpha + [\zeta + \mu] &\xrightarrow{\Delta G_1} [\alpha + \bar{\mu}] + \zeta + \bar{\beta} \\ &\xrightarrow{\Delta G_2} \tilde{\mu} + \tilde{\beta} + \zeta + \bar{\beta} \\ &\xrightarrow{\Delta G_3} \mu' + \zeta + \beta'. \end{aligned}$$

The interaction at the first step is of type Bc-i with $\Delta G_1 \leq 0$. At the second step we have an interaction of type Ba-ii, thus $\Delta G_2 \leq 0$. If $\tilde{\beta}$ starts to the right of β' , then

$$|\mu'| - |\tilde{\mu}| = q, \quad |\beta'| - |\tilde{\beta}| = -q,$$

and it follows that $\Delta G_3 \leq 0$. If $\tilde{\beta}$ starts to the left of β' , as is the case in Fig. 30, we once again introduce an auxiliary curve β^* , and this curve is indicated in the figure. This curve has $\gamma = \gamma_r$, starts somewhere along μ' , and ends at the same point as $\tilde{\beta}$. By property (ix) the starting point of β^* has to be to the right of β' , thus $|\beta'| - |\tilde{\beta}| - |\bar{\beta}| \leq |\beta^*| - |\tilde{\beta}|$. Moreover, we apply Lemma 2.2 on $\tilde{\beta}$ and β^* , and get $|\beta^*| - |\tilde{\beta}| \leq C_2 |\tilde{\beta}| |\zeta|$. Thus,

$$|\mu'| - |\tilde{\mu}| \leq 0, \quad |\beta'| - |\bar{\beta}| - |\tilde{\beta}| \leq C_2 |\tilde{\beta}| |\zeta|,$$

and $\Delta G_3 \leq 0$.

Assume now that the outgoing 3-wave of the interaction between ζ and μ is a rarefaction wave. According to Proposition 4.3 we can replace the interaction by a new one,

$$\begin{aligned} \alpha + \zeta + \mu &\xrightarrow{\Delta G_1} [\hat{\alpha} + \hat{\mu}] + \zeta \\ &\xrightarrow{\Delta G_2} \tilde{\mu} + \tilde{\beta} + \zeta \\ &\xrightarrow{\Delta G_3} \mu' + \zeta + \beta', \end{aligned}$$

where $\Delta G_1 \leq 0$. The interaction at the second step is of type Ba-ii, thus $\Delta G_2 \leq 0$. If $\tilde{\beta}$ starts to the right of β' , we have

$$|\mu'| - |\tilde{\mu}| = q, \quad |\beta'| - |\tilde{\beta}| = -q,$$

which gives $\Delta G_3 \leq 0$. If $\tilde{\beta}$ starts to the left of β' , we have $|\mu'| - |\tilde{\mu}| \leq 0$. Furthermore, since $\tilde{\beta}$ and β' end at the same point and have different γ 's, it follows by applying Lemma 2.2 that

$$|\beta'| - |\tilde{\beta}| \leq C_2 |\tilde{\beta}| |\zeta|,$$

and we get $\Delta G_3 \leq 0$.

- $(\alpha + \zeta) + \mu \rightarrow \alpha' + \zeta + \nu'$: In this case U_r is above α' and to the right of the 3-rarefaction wave starting at U_l , see Fig. 29(b). We have

$$|\alpha'| + |\nu'| \leq |\alpha|, \quad \text{or} \quad |\alpha'| - |\alpha| \leq -|\nu'|,$$

which gives

$$\Delta F = |\alpha'| - |\alpha| \leq -|\nu'|,$$

$$\Delta Q_1 \leq 0,$$

$$\Delta Q_1 \leq |\nu'| F_\gamma - |\mu| |\zeta| \leq |\nu'| F_\gamma,$$

and

$$\Delta G \leq |\nu'| (-1 + 3C_2 F_\gamma) \leq 0.$$

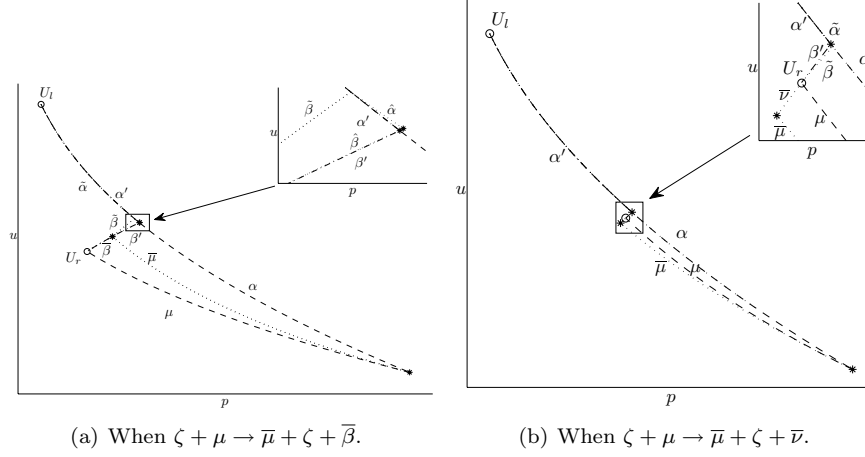


FIGURE 31. The interaction $(\alpha + \zeta) + \mu \rightarrow \alpha' + \zeta + \beta'$.

- $(\alpha + \zeta) + \mu \rightarrow \alpha' + \zeta + \beta'$: In this case U_r is below α' and to the right of the 3-shock wave starting at U_l , see Fig. 31. We divide the interaction into steps,

$$\begin{aligned} \alpha + [\zeta + \mu] &\xrightarrow{\Delta G_1} [\alpha + \bar{\mu}] + \zeta + \bar{\eta} \\ &\xrightarrow{\Delta G_2} \tilde{\alpha} + [\tilde{\beta} + \zeta + \bar{\eta}] \\ &\xrightarrow{\Delta G_3} \tilde{\alpha} + \hat{\alpha} + \zeta + \hat{\beta} \\ &\xrightarrow{\Delta G_4} \alpha' + \zeta + \beta'. \end{aligned}$$

The interaction at the first step is of type Bc-i and $\Delta G_1 \leq 0$. We do not know whether the outgoing 3-wave is a shock wave or a rarefaction wave, but in this case we are able effectively to treat both case at the same time.³ At the second step we have an interaction of type Ba-ii, thus $\Delta G_2 \leq 0$. If $\tilde{\beta}$ starts to the right of β' , as is the case in Fig. 31(b), then

$$|\alpha'| - |\tilde{\alpha}| \leq 0, \quad \begin{cases} |\beta'| - |\tilde{\beta}| \leq 0, & \text{if } \bar{\eta} = \bar{\nu}, \\ |\beta'| - |\tilde{\beta}| - |\bar{\beta}| \leq 0, & \text{if } \bar{\eta} = \bar{\beta}, \end{cases}$$

and going straight to the last step we get $\Delta G_* \leq 0$. However, if $\tilde{\beta}$ starts to the left of β' as in Fig. 31(a), we need more steps. We then let three

³This is the shortest way to do it, although we could for $\eta = \beta$ use Lemma 2.2 and be able to stop after step two (similar to the case $\rightarrow \mu' + \zeta + \beta'$). Moreover, for $\eta = \nu$ we could replace the interaction according to Proposition 4.3.

waves interact at the third step. This is an interaction of type Cc-ii if $\bar{\eta} = \bar{\beta}$ and of type Cc-iv if $\bar{\eta} = \bar{\nu}$, in either case we have $\Delta G_3 \leq 0$ and the outgoing 1- and 3-waves are shock waves. By property (viii) and property (ix) we obtain

$$|\alpha'| - |\tilde{\alpha}| - |\hat{\alpha}| \leq 0, \quad |\beta'| - |\hat{\beta}| \leq 0,$$

thus, $\Delta G_4 \leq 0$.

By symmetry we have $\Delta G \leq 0$ across $\nu + (\zeta + \beta)$.

This ends the discussion of interactions of type Cc, but before we carry on to interactions between four waves, we collect some results that will be useful when discussing the interactions of type Db. During the discussion of Cc-iii and Cc-iv we have shown the following:

Proposition 4.4. *For the interactions*

$$(4.11) \quad \mu + \alpha + \zeta + \beta \rightarrow \epsilon' + \zeta + \beta', \quad \text{and}$$

$$(4.12) \quad \alpha + \mu + \zeta + \beta \rightarrow \epsilon' + \zeta + \beta',$$

where ϵ' is either α' or μ' , the Glimm functional is decreasing, that is, $\Delta G \leq 0$.

Furthermore, we have also proved the following result:

Proposition 4.5. *For the interactions*

$$(4.13) \quad \mu + \alpha + \zeta \rightarrow \epsilon' + \zeta + \beta', \quad \text{and}$$

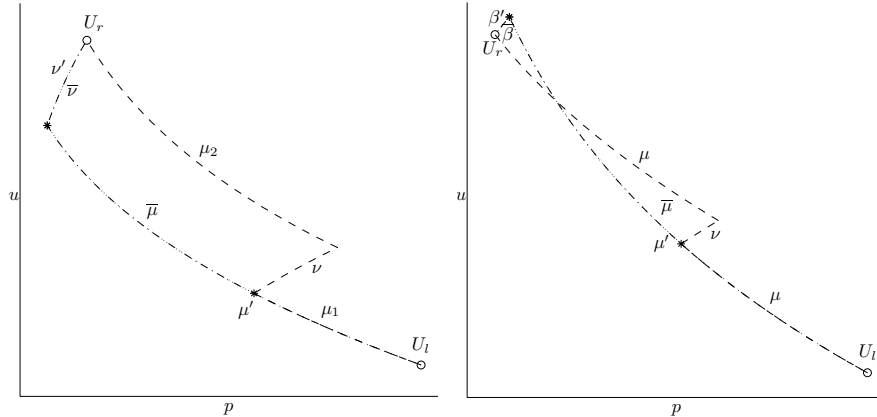
$$(4.14) \quad \alpha + \mu + \zeta \rightarrow \epsilon' + \zeta + \beta',$$

where ϵ' is either α' or μ' , the Glimm functional is decreasing, that is, $\Delta G \leq 0$.

4.4. Type D: Four waves entering the diamond.

4.4.1. *Type Da: Waves of the same family are also of the same type.* The interactions of this type all have two possible outcomes to be considered.

- (i) $(\mu_1 + \zeta + \nu) + \mu_2$ (and $\nu_1 + (\mu + \zeta + \nu_2)$):



(a) $(\mu_1 + \zeta + \nu) + \mu_2 \rightarrow \mu' + \zeta + \nu'$.

(b) $(\mu_1 + \zeta + \nu) + \mu_2 \rightarrow \mu' + \zeta + \beta'$.

FIGURE 32. The interaction $(\mu_1 + \zeta + \nu) + \mu_2$.

- $(\mu_1 + \zeta + \nu) + \mu_2 \rightarrow \mu' + \zeta + \nu'$: In this case U_r lies above μ' , see Fig. 32(a). This interaction is divided into two steps,

$$\mu_1 + [\zeta + \nu + \mu_2] \xrightarrow{\Delta G_1} \mu_1 + \bar{\mu} + \zeta + \bar{\nu} \xrightarrow{\Delta G_2} \mu' + \zeta + \nu'.$$

The interaction at the first step is of type Cb-i, therefore $\Delta G_1 \leq 0$. By property (iv) and property (vii) we have $\mu_1 + \bar{\mu} = \mu'$ and $\bar{\nu} = \nu'$, thus $\Delta G_2 = 0$.

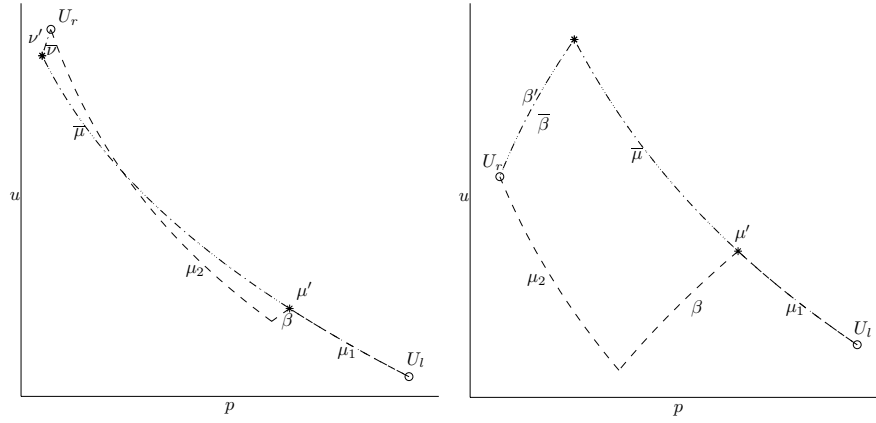
- $(\mu_1 + \zeta + \nu) + \mu_2 \rightarrow \mu' + \zeta + \beta'$: In this case U_r lies below μ' , see Fig. 32(b). Again we need two steps,

$$\mu_1 + [\zeta + \nu + \mu_2] \xrightarrow{\Delta G_1} \mu_1 + \bar{\mu} + \zeta + \bar{\beta} \xrightarrow{\Delta G_2} \mu' + \zeta + \beta'.$$

The first interaction is of type Cb-i, thus $\Delta G_1 \leq 0$. From property (iv) and property (vii) we have $\mu_1 + \bar{\mu} = \mu'$. It then follows that $\bar{\beta} = \beta'$, and therefore $\Delta G_2 = 0$.

Due to symmetry, $\Delta G \leq 0$ across $\nu_1 + (\mu + \zeta + \nu_2)$.

- (ii) $(\mu_1 + \zeta + \beta) + \mu_2$ (and $\nu_1 + (\alpha + \zeta + \nu_2)$):



(a) $(\mu_1 + \zeta + \beta) + \mu_2 \rightarrow \mu' + \zeta + \nu'$.

(b) $(\mu_1 + \zeta + \beta) + \mu_2 \rightarrow \mu' + \zeta + \beta'$.

FIGURE 33. The interaction $(\mu_1 + \zeta + \beta) + \mu_2$.

- $(\mu_1 + \zeta + \beta) + \mu_2 \rightarrow \mu' + \zeta + \nu'$: In this case U_r is above μ' , see Fig. 33(a). Observe that μ_2 crosses μ' , which is possible since the two waves have different γ 's. We divide the interaction into two steps,

$$\mu_1 + [\zeta + \beta + \mu_2] \xrightarrow{\Delta G_1} \mu_1 + \bar{\mu} + \zeta + \bar{\nu} \xrightarrow{\Delta G_2} \mu' + \zeta + \nu',$$

where the interaction at the first step is of type Cb-iii, thus $\Delta G_1 \leq 0$. Due to property (iv) and property (vii) we have that $\mu_1 + \bar{\mu} = \mu'$ and $\bar{\nu} = \nu'$, and it follows that $\Delta G_2 = 0$.

- $(\mu_1 + \zeta + \beta) + \mu_2 \rightarrow \mu' + \zeta + \beta'$: In this case U_r is below μ' , see Fig. 33(b). The interaction is divided into two steps,

$$\mu_1 + [\zeta + \beta + \mu_2] \xrightarrow{\Delta G_1} \mu_1 + \bar{\mu} + \zeta + \bar{\beta} \xrightarrow{\Delta G_2} \mu' + \zeta + \beta',$$

where the interaction at the first step is of type Cb-iii, thus $\Delta G_1 \leq 0$.

Due to property (iv) and property (vii) we have $\mu_1 + \bar{\mu} = \mu'$ and therefore also $\bar{\beta} = \beta'$, thus $\Delta G_2 = 0$.

By symmetry we have $\Delta G \leq 0$ across $\nu_1 + (\alpha + \zeta + \nu_2)$.

(iii) $(\alpha_1 + \zeta + \nu) + \alpha_2$ (and $\beta_1 + (\mu + \zeta + \beta_2)$):

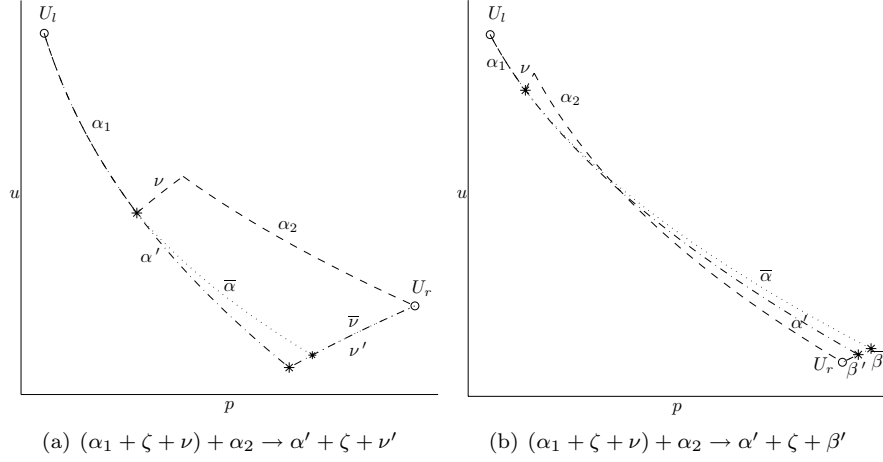


FIGURE 34. The interaction $(\alpha_1 + \zeta + \nu) + \alpha_2$.

- $(\alpha_1 + \zeta + \nu) + \alpha_2 \rightarrow \alpha' + \zeta + \nu'$: In this case U_r is above α' , see Fig. 34(a). Two steps are needed,

$$\alpha_1 + [\zeta + \nu + \alpha_2] \xrightarrow{\Delta G_1} \alpha_1 + \bar{\alpha} + \zeta + \bar{\nu} \xrightarrow{\Delta G_2} \alpha' + \zeta + \nu'.$$

The first interaction is of type Cb-ii, therefore $\Delta G_1 \leq 0$. It follows from property (iv) and property (viii) that

$$|\alpha'| - |\alpha_1| - |\bar{\alpha}| = -q, \quad |\nu'| - |\bar{\nu}| = q,$$

for a $q > 0$, and this gives $\Delta G_2 \leq 0$.

- $(\alpha_1 + \zeta + \nu) + \alpha_2 \rightarrow \alpha' + \zeta + \beta'$: In this case U_r is below α' , see Fig. 34(b). We divide the interaction into two steps,

$$\alpha_1 + [\zeta + \nu + \alpha_2] \xrightarrow{\Delta G_1} \alpha_1 + \bar{\alpha} + \zeta + \bar{\beta} \xrightarrow{\Delta G_2} \alpha' + \zeta + \beta'.$$

The first interaction is of type Cb-ii, therefore $\Delta G_1 \leq 0$. The 1-shock waves α' and $\bar{\alpha}$ have $\gamma = \gamma_l$ and β' and $\bar{\beta}$ have $\gamma = \gamma_r$, therefore it follows from property (viii) and property (ix) that

$$|\alpha'| - |\alpha_1| - |\bar{\alpha}| \leq 0, \quad |\beta'| - |\bar{\beta}| \leq 0,$$

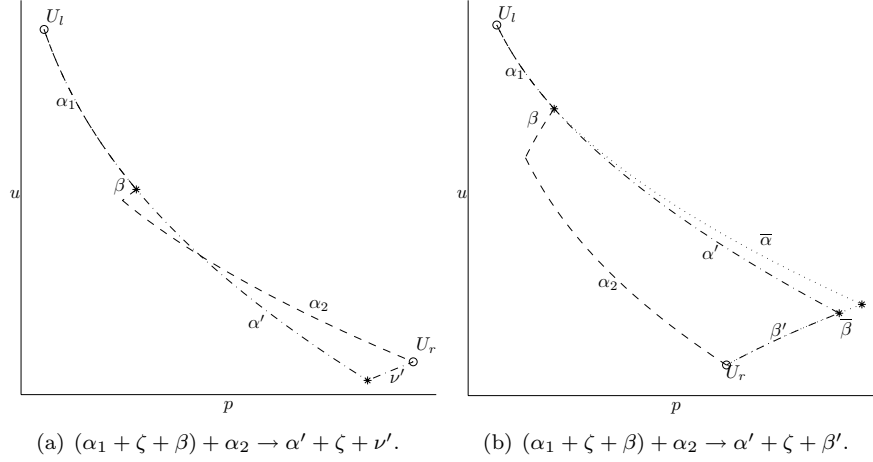
resulting in $\Delta G_2 \leq 0$.

It follows from symmetry that $\Delta G \leq 0$ across $\beta_1 + (\mu + \zeta + \beta_2)$.

(iv) $(\alpha_1 + \zeta + \beta) + \alpha_2$ (and $\beta_1 + (\alpha + \zeta + \beta_2)$):

- $(\alpha_1 + \zeta + \beta) + \alpha_2 \rightarrow \alpha' + \zeta + \nu'$: In this case U_r lies above α' , see Fig. 35(a). Here α_2 crosses α' , which is possible since they have different γ 's. We do not need to divide this interaction because we have

$$|\alpha'| \leq |\alpha_1| + |\alpha_2|,$$


 FIGURE 35. The interaction $(\alpha_1 + \zeta + \beta) + \alpha_2$.

$$|\alpha'| + |\nu'| \leq |\alpha_1| + |\alpha_2| + |\beta|,$$

and from this we find

$$\Delta F = |\alpha'| - |\alpha_1| - |\alpha_2| - |\beta| \leq -|\nu'|,$$

$$\Delta Q_1 \leq 0,$$

$$\Delta Q_2 \leq |\nu'| F_\gamma,$$

which gives us $\Delta G \leq 0$.

- $(\alpha_1 + \zeta + \beta) + \alpha_2 \rightarrow \alpha' + \zeta + \beta'$: In this case U_r lies below α' , see Fig. 35(b). We divide this interaction into two steps,

$$\alpha_1 + [\zeta + \beta + \alpha_2] \xrightarrow{\Delta G_1} \alpha_1 + \bar{\alpha} + \zeta + \bar{\beta} \xrightarrow{\Delta G_2} \alpha' + \zeta + \beta',$$

where the interaction at the first step is of type Cb-iv, thus $\Delta G_1 \leq 0$. Due to property (viii) and property (ix) the intersection between $\bar{\alpha}$ and $\bar{\beta}$ is to the right of the intersection between α' and β' , thus

$$|\alpha'| - |\alpha_1| - |\bar{\alpha}| \leq 0, \quad |\beta| - |\bar{\beta}| \leq 0,$$

and we get $\Delta G_2 \leq 0$.

By symmetry we have $\Delta G \leq 0$ across $\beta_1 + (\alpha + \zeta + \beta_2)$.

4.4.2. *Type Db: Waves of the same family are not of the same type.* Before we discuss each interaction of this type, we state some useful observations in the following propositions.

Proposition 4.6. *If μ and α cross in the interaction*

$$\mu + \zeta + \nu + \alpha, \quad \text{or} \quad \alpha + \zeta + \nu + \mu,$$

then the interaction can be replaced by

$$(4.15) \quad \hat{\mu} + \zeta + \hat{\alpha}, \quad \text{or} \quad \hat{\alpha} + \zeta + \hat{\mu},$$

respectively, where

$$(4.16) \quad |\hat{\mu}| \leq |\mu|, \quad \text{and} \quad |\hat{\alpha}| \leq |\alpha|,$$

and $\Delta G \leq 0$ for this replacement.

Proof. For the first interaction we have to prove that the backward 1-shock curve at U_r crosses μ , and in order to show (4.16), that this intersection is to the right of the starting point of α . By property (viii) a 1-shock with $\gamma = \gamma_r$ that starts to the right of the intersection point between μ and α can never reach U_r . Furthermore, if $\hat{\alpha}$ starts to the left of α , it will always be steeper than α and hence never reach U_r . Thus, there is a $\hat{\alpha}$ starting at μ so that (4.15) connects U_l to U_r and so that (4.16) is satisfied.

Since the slope of a rarefaction wave is independent of the starting point, the proof for the second interaction is easier. Then $\hat{\alpha}$ is the part of α from U_l to the intersection point between α and μ , while $\hat{\mu}$ is the part of μ from the intersection point to U_r . Thus, (4.16) is satisfied, and the interaction can be replaced by (4.15).

For both cases it follows from (4.16) that $\Delta G \leq 0$ for this replacement. \square

Proposition 4.7. *If U_r is to the right of U_l and μ and α do not intersect for the interaction*

$$\mu + \zeta + \nu + \alpha,$$

then the interaction can be replaced by

$$(4.17) \quad \zeta + \hat{\nu} + \hat{\alpha},$$

where, for a positive constant q ,

$$(4.18) \quad |\hat{\alpha}| - |\alpha| = -q, \quad \text{and} \quad |\hat{\nu}| - |\nu| \leq q,$$

and $\Delta G \leq 0$ for this replacement.

Proof. We have from property (viii) and property (iv) that the backward 1-shock curve from U_r has a unique intersection point with the 3-rarefaction curve starting at (p_l, u_l, γ_r) , and that this point is to the right of the starting point of α . Thus, $|\hat{\alpha}| - |\alpha| = -q$ for a positive constant q . Furthermore we find that

$$|\mu| + |\hat{\nu}| + |\hat{\alpha}| = |\nu| + |\alpha|,$$

hence

$$|\hat{\nu}| - |\nu| = -(|\hat{\alpha}| - |\alpha|) - |\mu| = q - |\mu| \leq q,$$

which proves (4.18). Moreover, $\Delta G \leq 0$ follows directly from this estimate. \square

Proposition 4.8. *If U_r is to the left of U_l and μ and α do not intersect for the interaction*

$$\alpha + \zeta + \nu + \mu,$$

then the interaction can be replaced by

$$(4.19) \quad \zeta + \hat{\nu} + \hat{\mu},$$

where

$$(4.20) \quad |\hat{\mu}| - |\mu| \leq 0, \quad \text{and} \quad |\hat{\nu}| - |\nu| \leq |\alpha|,$$

and $\Delta G \leq 0$ for this replacement.

Proof. It follows from property (iv) that $\hat{\mu}$ starts at the point where the 3-rarefaction curve from (p_l, u_l, γ_r) intersects μ . Thus, $|\hat{\mu}| - |\mu| \leq 0$ and furthermore,

$$|\mu| - |\hat{\mu}| + |\hat{\nu}| = |\alpha| + |\nu|,$$

hence, $|\hat{\nu}| - |\nu| = |\alpha| - (|\mu| - |\hat{\mu}|) \leq |\alpha|$. This proves (4.20) from which it follows that $\Delta G \leq 0$ for the replacement. \square

- (i) $(\mu + \zeta + \nu) + \alpha$ (and $\beta + (\mu + \zeta + \nu)$). This interaction has four different outcomes as shown in Fig. 36.

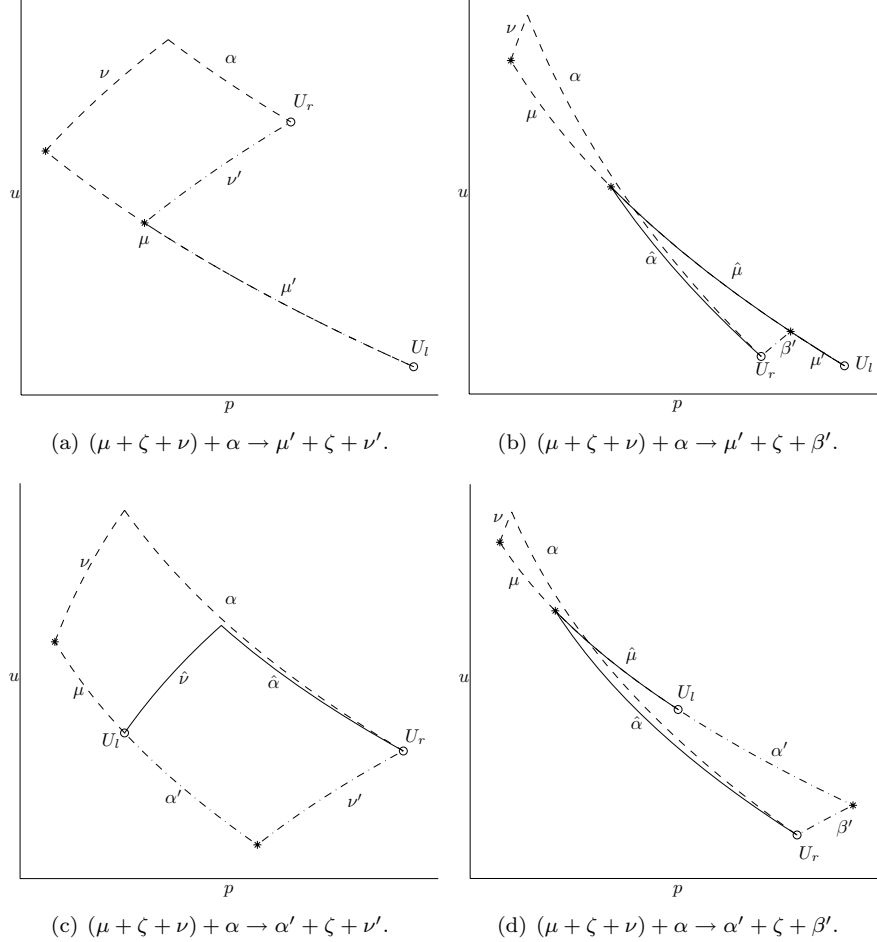


FIGURE 36. The interaction $(\mu + \zeta + \nu) + \alpha$.

- $(\mu + \zeta + \nu) + \alpha \rightarrow \mu' + \zeta + \nu'$: In this case U_r is above μ' and to the left of the 3-rarefaction wave starting at U_l , see Fig. 36(a). We have $|\mu'| \leq |\mu|$ and $|\nu'| - |\nu| \leq |\alpha|$, thus

$$\begin{aligned} \Delta F &= -|\alpha|, \\ \Delta Q_1 &\leq 0, \end{aligned}$$

$$\Delta Q_2 \leq (|\nu'| - |\nu|) \sum_i |\zeta_i| \leq |\alpha| F_\gamma,$$

where ζ_i are all contact discontinuities to the right of the diamond. From this we obtain $\Delta G \leq 0$.

- $(\mu + \zeta + \nu) + \alpha \rightarrow \mu' + \zeta + \beta'$: In this case U_r is below μ' and to the left of the 3-shock wave starting at U_l , thus α has to cross μ , see Fig. 36(b). Then it follows from Proposition 4.6 that the interaction can be replaced by a new one,

$$\mu + \zeta + \nu + \alpha \xrightarrow{\Delta G_1} [\hat{\mu} + \zeta + \hat{\alpha}] \xrightarrow{\Delta G_2} \mu' + \zeta + \beta',$$

where $\Delta G_1 \leq 0$. Since the interaction at the second step is of type Cc-iii, we also have $\Delta G_2 \leq 0$.

- $(\mu + \zeta + \nu) + \alpha \rightarrow \alpha' + \zeta + \nu'$: In this case U_r is above α' and to the right of the 3-rarefaction wave starting at U_l , see Fig. 36(c). Since α and μ cannot intersect, it follows from Proposition 4.7 that the interaction can be replaced by a new one,

$$\mu + \zeta + \nu + \alpha \xrightarrow{\Delta G_1} [\zeta + \hat{\nu} + \hat{\alpha}] \xrightarrow{\Delta G_2} \alpha' + \zeta + \nu',$$

where $\Delta G_1 \leq 0$. At the second step we have an interaction of type Cb-ii, thus $\Delta G_2 \leq 0$.

- $(\mu + \zeta + \nu) + \alpha \rightarrow \alpha' + \zeta + \beta'$: In this case U_r is below α' and to the right of the 3-shock wave starting at U_l , see Fig. 36(d). If α crosses μ , we replace the interaction according to Proposition 4.6,

$$\mu + \zeta + \nu + \alpha \xrightarrow{\Delta G_1} [\hat{\mu} + \zeta + \hat{\alpha}] \xrightarrow{\Delta G_2} \alpha' + \zeta + \beta',$$

where $\Delta G_1 \leq 0$. The interaction at the second step is of type Cc-iii, thus $\Delta G_2 \leq 0$. If, however, α does not cross μ , we use on Proposition 4.7 and replace the interaction by a new one,

$$\mu + \zeta + \nu + \alpha \xrightarrow{\Delta G_1} \zeta + \hat{\nu} + \hat{\alpha} \xrightarrow{\Delta G_2} \alpha' + \zeta + \beta',$$

where $\Delta G_1 \leq 0$. Furthermore, $\Delta G_2 \leq 0$ because the interaction at the second step is of type Cb -ii.

By symmetry we have $\Delta G \leq 0$ across $\beta + (\mu + \zeta + \nu)$.

- (ii) $(\alpha + \zeta + \nu) + \mu$ (and $\nu + (\mu + \zeta + \beta)$): This interaction has four possible outcomes as shown in Fig. 37.

- $(\alpha + \zeta + \nu) + \mu \rightarrow \mu' + \zeta + \nu'$: In this case U_r is above μ' and to the left of the 3-rarefaction curve starting at U_l , see Fig. 37(a). Since α and μ do not cross, we can by Proposition 4.8 replace the interaction by a new one,

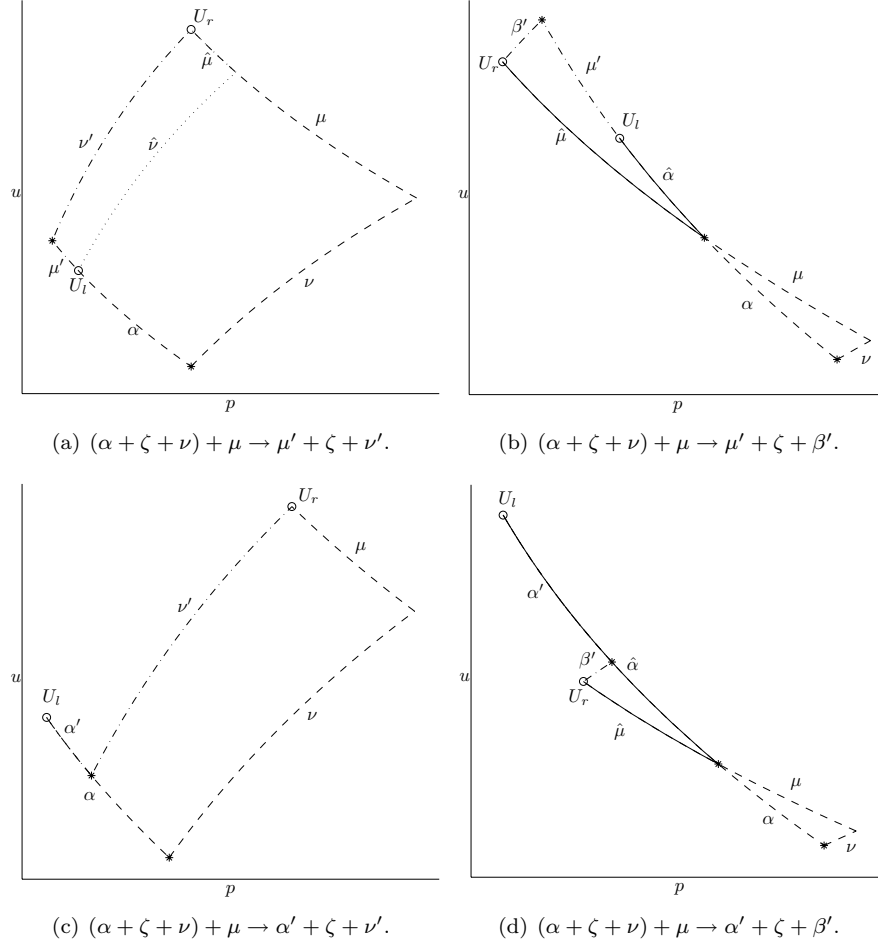
$$\alpha + \zeta + \nu + \mu \xrightarrow{\Delta G_1} [\zeta + \hat{\nu} + \hat{\mu}] \xrightarrow{\Delta G_2} \mu' + \zeta + \nu',$$

where $\Delta G_1 \leq 0$. The second interaction is of type Cb-i, thus $\Delta G_2 \leq 0$.⁴

- $(\alpha + \zeta + \nu) + \mu \rightarrow \mu' + \zeta + \beta'$: In this case U_r is below μ' and to the left of the 3-shock curve starting at U_l , see Fig. 37(b). If α and μ do not intersect, we use Proposition 4.8 as above and replace the interaction,

$$\alpha + \zeta + \nu + \mu \xrightarrow{\Delta G_1} [\zeta + \hat{\nu} + \hat{\mu}] \xrightarrow{\Delta G_2} \mu' + \zeta + \beta',$$

⁴This interaction can also be divided into two steps by letting $\zeta + \nu + \mu$ interact at the first step.


 FIGURE 37. The interaction $(\alpha + \zeta + \nu) + \mu$.

where $\Delta G_1 \leq 0$. Because the interaction at the second step is of type Cb-i, we have $\Delta G_2 \leq 0$. If, however, α and μ do intersect as in Fig. 37(b), we replace the interaction according to Proposition 4.6,

$$\alpha + \zeta + \nu + \mu \xrightarrow{\Delta G_1} [\hat{\alpha} + \zeta + \hat{\mu}] \xrightarrow{\Delta G_2} \mu' + \zeta + \beta',$$

with $\Delta G_1 \leq 0$. Since the interaction at the second step is of type Cc-iv, also $\Delta G_2 \leq 0$.

- $(\alpha + \zeta + \nu) + \mu \rightarrow \alpha' + \zeta + \nu'$: In this case U_r is above α' and to the right of the 3-rarefaction curve starting at U_l , see Fig. 37(c). We have

$$|\alpha'| + |\nu'| + |\mu| = |\alpha| + |\nu|, \quad |\alpha'| - |\alpha| = -q,$$

where $q > 0$, hence,

$$|\nu'| - |\nu| = q - |\mu| \leq q,$$

and

$$\begin{aligned}\Delta F &= |\alpha'| - |\alpha| = -q, \\ \Delta Q_1 &\leq 0, \\ \Delta Q_1 &\leq qF_\gamma,\end{aligned}$$

from which we obtain $\Delta G \leq 0$.

- $(\alpha + \zeta + \nu) + \mu \rightarrow \alpha' + \zeta + \beta'$: In this case U_r is below α' and to the right of the 3-shock curve starting at U_l , see Fig. 37(d). Hence, α and μ have to intersect and by Proposition 4.6 we can replace the interaction

$$\alpha + \zeta + \nu + \mu \xrightarrow{\Delta G_1} [\hat{\alpha} + \zeta + \hat{\mu}] \xrightarrow{\Delta G_2} \mu' + \zeta + \beta',$$

where $\Delta G_1 \leq 0$. The interaction at the second step is of type Cc-iv, thus $\Delta G_2 \leq 0$.

By symmetry we have $\Delta G \leq 0$ across $\nu + (\mu + \zeta + \beta)$.

Yet another proposition is useful before discussing the last two interactions.

Proposition 4.9. *If U_r is below the outgoing 1-wave for the interaction*

$$\mu + \zeta + \beta + \alpha, \quad \text{or} \quad \alpha + \zeta + \beta + \mu,$$

and if

$$\zeta + \beta + \alpha \rightarrow \bar{\alpha} + \zeta + \bar{\nu}, \quad \text{or} \quad \zeta + \beta + \mu \rightarrow \bar{\mu} + \zeta + \bar{\nu},$$

respectively, then U_l can be connected to U_r by

$$(4.21) \quad \hat{\mu} + \hat{\alpha} + \zeta, \quad \text{or} \quad \hat{\alpha} + \hat{\mu} + \zeta,$$

respectively, where

$$(4.22) \quad |\hat{\mu}| \leq |\mu|, \quad \text{and} \quad |\hat{\alpha}| \leq |\alpha|,$$

for the first interaction and

$$(4.23) \quad |\hat{\mu}| \leq |\bar{\mu}|, \quad \text{and} \quad |\hat{\alpha}| \leq |\alpha|,$$

for the second.

Proof. The proof for the first interaction is exactly the same as for the first interaction of Proposition 4.3. Also for the second interaction the arguments are the same as for the second interaction of Proposition 4.3, but due to the extra wave, β , we here only know that the strength of $\hat{\mu}$ is less than the strength of $\bar{\mu}$. \square

- (iii) $(\mu + \zeta + \beta) + \alpha$ (and $\beta + (\alpha + \zeta + \nu)$): This interaction has four possible outcomes.

- $(\mu + \zeta + \beta) + \alpha \rightarrow \mu' + \zeta + \nu'$: In this case U_r is above μ' and to the left of the 3-rarefaction wave starting at U_l , see Fig. 38(a). We have $|\mu'| \leq |\mu|$ and moreover, $|\nu'| \leq |\alpha|$, therefore

$$\begin{aligned}\Delta F &= -|\alpha| - |\beta| \leq -|\alpha|, \\ \Delta Q_1 &\leq 0, \\ \Delta Q_2 &\leq |\nu'| F_\gamma \leq |\alpha| F_\gamma,\end{aligned}$$

which gives $\Delta G \leq 0$.

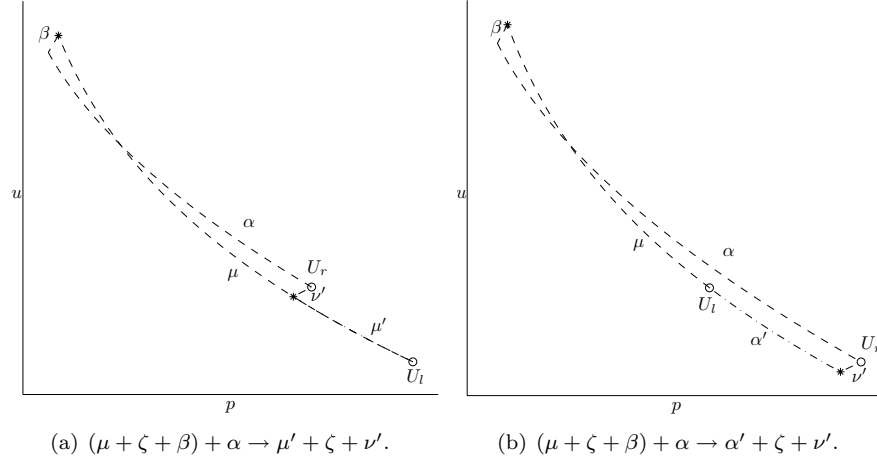


FIGURE 38. Two outcomes of the interaction $(\mu + \zeta + \beta) + \alpha$.

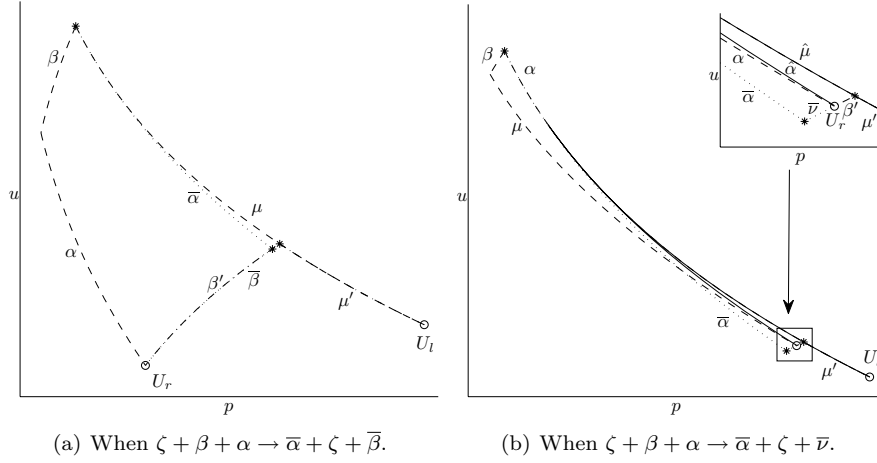


FIGURE 39. $(\mu + \zeta + \beta) + \alpha \rightarrow \mu' + \zeta + \beta'$.

- $(\mu + \zeta + \beta) + \alpha \rightarrow \mu' + \zeta + \beta'$: In this case U_r is below μ' and to the left of the 3-shock wave starting at U_l , see Fig. 39. If $\zeta + \beta + \alpha \rightarrow \bar{\alpha} + \zeta + \bar{\beta}$ as in Fig. 39(a), then we divide the interaction into two steps,

$$\mu + [\zeta + \beta + \alpha] \xrightarrow{\Delta G_1} \mu + \bar{\alpha} + \zeta + \bar{\beta} \xrightarrow{\Delta G_2} \mu' + \zeta + \beta',$$

where $\Delta G_1 \leq 0$ because the interaction at the first step is of type Cb-iv and $\Delta G_2 \leq 0$ follows from Proposition 4.4.

If, however, $\zeta + \beta + \alpha \rightarrow \bar{\alpha} + \zeta + \bar{\nu}$ as in Fig. 39(b), we replace the interaction by $\hat{\mu} + \hat{\alpha} + \zeta$ according to Proposition 4.9,

$$\mu + \zeta + \beta + \alpha \xrightarrow{\Delta G_1} \hat{\mu} + \hat{\alpha} + \zeta \xrightarrow{\Delta G_2} \mu' + \zeta + \beta'.$$

It follows from (4.22) that $\Delta G_1 \leq 0$ and from Proposition 4.5 we have $\Delta G_2 \leq 0$.

- $(\mu + \zeta + \beta) + \alpha \rightarrow \alpha' + \zeta + \nu'$: In this case U_r is above α' and to the right of the 3-rarefaction wave starting at U_l , see Fig. 38(b). We have $|\alpha' - |\alpha| \leq -|\nu'|$, therefore

$$\Delta F = |\alpha'| - |\alpha| - |\beta| \leq -|\nu'|,$$

$$\Delta Q_1 \leq 0,$$

$$\Delta Q_2 \leq |\nu'| F_\gamma,$$

and we obtain $\Delta G \leq 0$.

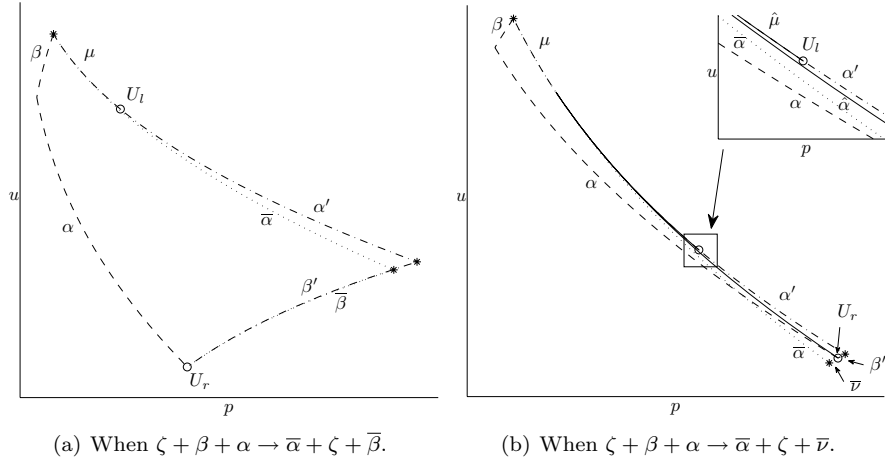


FIGURE 40. $(\mu + \zeta + \beta) + \alpha \rightarrow \alpha' + \zeta + \beta'$.

- $(\mu + \zeta + \beta) + \alpha \rightarrow \alpha' + \zeta + \beta'$: In this case U_r is below α' and to the right of the 3-shock wave starting at U_l , see Fig. 40. If $\zeta + \beta + \alpha \rightarrow \bar{\alpha} + \zeta + \bar{\beta}$ as in Fig. 40(a), then we divide the interaction into two steps,

$$\mu + [\zeta + \beta + \alpha] \xrightarrow{\Delta G_1} \mu + \bar{\alpha} + \zeta + \bar{\beta} \xrightarrow{\Delta G_2} \alpha' + \zeta + \beta',$$

where the interaction at the first step is of type Cb-iv, thus $\Delta G_1 \leq 0$. Furthermore, $\Delta G_2 \leq 0$ follows from Proposition 4.4.

If $\zeta + \beta + \alpha \rightarrow \bar{\alpha} + \zeta + \bar{\nu}$ as in Fig. 40(b), we again replace the interaction according to Proposition 4.9,

$$\mu + \zeta + \beta + \alpha \xrightarrow{\Delta G_1} \hat{\mu} + \hat{\alpha} + \zeta \xrightarrow{\Delta G_2} \alpha' + \zeta + \beta',$$

and get $\Delta G_1 \leq 0$ from (4.22) and $\Delta G_2 \leq 0$ from Proposition 4.5.

Due to symmetry, $\Delta G \leq 0$ across $\beta + (\alpha + \zeta + \nu)$.

- (iv) $(\alpha + \zeta + \beta) + \mu$ (and $\nu + (\alpha + \zeta + \beta)$): This interaction has four different outcomes.

- $(\alpha + \zeta + \beta) + \mu \rightarrow \mu' + \zeta + \nu'$: In this case U_r is above μ' and to the left of the 3-rarefaction curve starting at U_l , see Fig. 41(a). We divide the interaction into two steps,

$$\alpha + [\zeta + \beta + \mu] \xrightarrow{\Delta G_1} \alpha + \bar{\mu} + \zeta + \bar{\nu} \xrightarrow{\Delta G_2} \mu' + \zeta + \nu',$$

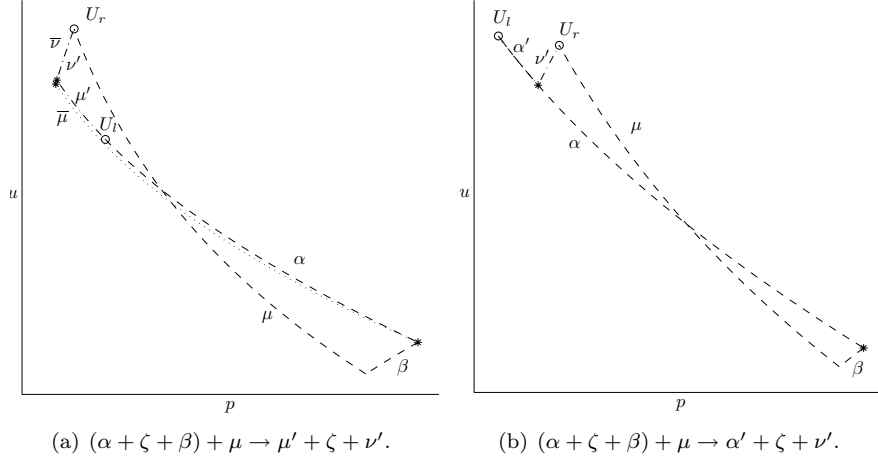


FIGURE 41. Two outcomes of the interaction $(\alpha + \zeta + \beta) + \mu$.

where $\Delta G_1 \leq 0$ since the first interaction is of type Cb-iii. From property (vi) we know that $\bar{\mu}$ lies below α , therefore

$$|\mu'| - |\bar{\mu}| \leq 0, \quad |\nu'| - |\bar{\nu}| \leq 0,$$

and we obtain $\Delta G_2 \leq 0$.

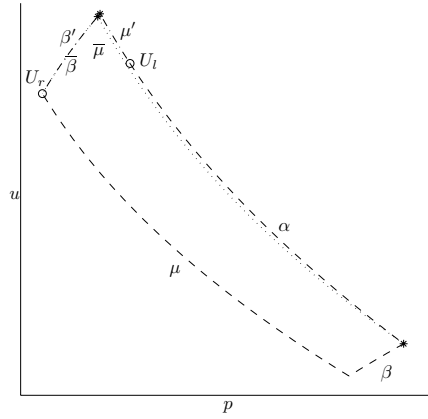


FIGURE 42. $(\alpha + \zeta + \beta) + \mu \rightarrow \mu' + \zeta + \beta'$.

- $(\alpha + \zeta + \beta) + \mu \rightarrow \mu' + \zeta + \beta'$: In this case U_r is below μ' and to the left of the 3-shock curve starting at U_l . We first assume that $\zeta + \beta + \mu \rightarrow \bar{\mu} + \zeta + \bar{\beta}$ as in Fig. 42. Then we divide the interaction into two steps

$$\alpha + [\zeta + \beta + \mu] \xrightarrow{\Delta G_1} \alpha + \bar{\mu} + \zeta + \bar{\beta} \xrightarrow{\Delta G_2} \mu' + \zeta + \beta',$$

where $\Delta G_1 \leq 0$ since the first interaction is of type Cb-iii. Furthermore, it follows from Proposition 4.4 that $\Delta G_2 \leq 0$.

When $\zeta + \beta + \mu \rightarrow \bar{\mu} + \zeta + \bar{\nu}$, we replace the interaction at the second step with a new one according to Proposition 4.9,

$$\begin{aligned} \alpha + [\zeta + \beta + \mu] &\xrightarrow{\Delta G_1} \alpha + \bar{\mu} + \zeta + \bar{\nu} \\ &\xrightarrow{\Delta G_2} \hat{\alpha} + \hat{\mu} + \zeta \\ &\xrightarrow{\Delta G_3} \mu' + \zeta + \beta'. \end{aligned}$$

The first interaction is of type Cb-iii, thus $\Delta G_1 \leq 0$. This step is included because we are only able to relate $\hat{\mu}$ to $\bar{\mu}$, not to μ . From (4.23) we obtain $\Delta G_2 \leq 0$, and $\Delta G_3 \leq 0$ follows from Proposition 4.5.

- $(\alpha + \zeta + \beta) + \mu \rightarrow \alpha' + \zeta + \nu'$: In this case U_r is above α' and to the right of the 3-rarefaction curve starting at U_l , see Fig. 41(b). We observe that $|\alpha'| - |\alpha| \leq -|\nu'|$, thus

$$\begin{aligned} \Delta F &= |\alpha'| - |\alpha| - |\beta| \leq -|\nu'|, \\ \Delta Q_1 &\leq 0, \\ \Delta Q_2 &\leq |\nu'| F_\gamma, \end{aligned}$$

and we have $\Delta G \leq 0$.

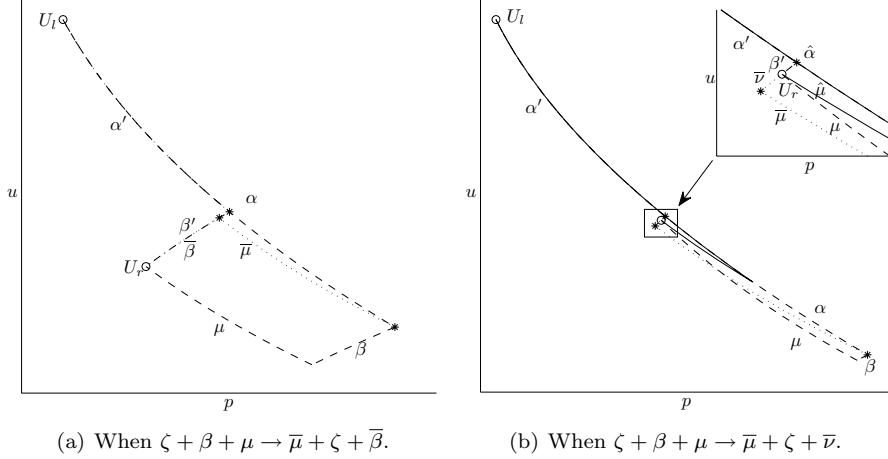


FIGURE 43. $(\alpha + \zeta + \beta) + \mu \rightarrow \alpha' + \zeta + \beta'$.

- $(\alpha + \zeta + \beta) + \mu \rightarrow \alpha' + \zeta + \beta'$: In this case U_r is below α' and to the right of the 3-shock curve starting at U_l . Again we have to look at two cases. Assume first that $\zeta + \beta + \mu \rightarrow \bar{\mu} + \zeta + \bar{\beta}$ as in Fig. 43(a), then we divide the interaction into two,

$$\alpha + [\zeta + \beta + \mu] \xrightarrow{\Delta G_1} \alpha + \bar{\mu} + \zeta + \bar{\beta} \xrightarrow{\Delta G_2} \alpha' + \zeta + \beta',$$

where the interaction at step one is of type Cb-iii, thus $\Delta G_1 \leq 0$. Furthermore, it follows from Proposition 4.4 that $\Delta G_2 \leq 0$.

Assume now that $\zeta + \beta + \mu \rightarrow \bar{\mu} + \zeta + \bar{\nu}$ as in Fig. 43(b). Then we at the second step replace the interaction with a new one according to

Proposition 4.9,

$$\begin{aligned} \alpha + [\zeta + \beta + \mu] &\xrightarrow{\Delta G_1} \alpha + \bar{\mu} + \zeta + \bar{\nu} \\ &\xrightarrow{\Delta G_2} \hat{\alpha} + \hat{\mu} + \zeta \\ &\xrightarrow{\Delta G_3} \alpha' + \zeta + \beta'. \end{aligned}$$

Since the interaction at the first step is of type Cb-iii, we have $\Delta G_1 \leq 0$. Moreover, $\Delta G_2 \leq 0$ follows from (4.23) and $\Delta G_3 \leq 0$ follows from Proposition 4.5.

By symmetry it follows that $\Delta G \leq 0$ across $\nu + (\alpha + \zeta + \beta)$.

5. CONVERGENCE

We have to show that the approximate solution, $U_h(x, t)$ given by (3.4), converges and that the limit is a weak solution of (1.1). From [20, Ch. 19 §C] we know that an approximate solution converges to a weak solution if the approximation is uniformly bounded, has bounded total variation and is locally L^1 Lipschitz continuous in time. Note that the analysis in [20, Ch. 19 §C] to obtain convergence and to show that the limit is a weak solution, only relies on the above conditions and does not require a sufficiently small total variation of the initial data. Furthermore, if we have that the total variation of the approximate solution is bounded, then we can show that it is L^1 Lipschitz continuous in time. Thus, the requirement in the general theory that the total variation of the initial data should be sufficiently small is only needed in order to prove that the total variation of the approximate solution is bounded. Therefore, convergence to a weak solution of (1.1) follows if we can show that the total variations of $U_h(\cdot, t)$ is bounded, and we show this using the decreasing Glimm functional. Then we find the domain \mathcal{U} that contains the approximate solution. As long as \mathcal{U} does not include vacuum, we have that $U_h(x, t)$ is bounded.

Recall from Section 3.3 that the constant C_1 is the constant appearing in estimate (4.3), C_2 is given by (3.6), k by (3.7) and C is the minimum of the constants \tilde{C} appearing in the estimates for interactions of type Ba, cf. Section 4.2.1. Define the constant

$$(5.1) \quad \kappa := \frac{10}{3} s'_{\max} k + 1.$$

Note that all these constants only depend on p_{\min} , p_{\max} and $\bar{\gamma}$. We are now ready to prove that the total variation is bounded.

Lemma 5.1. *If the initial data satisfy*

$$(5.2) \quad (\bar{\gamma} - 1) \text{T.V.}(p_0, u_0) \leq \frac{C}{9kC_1},$$

$$(5.3) \quad \text{T.V.}(\gamma_0) \leq \frac{C}{9C_2},$$

and the approximate solution $U_h(x, t) = (p_h(x, t), u_h(x, t), \gamma_h(x, t))$ obtained by the Glimm scheme is bounded away from vacuum, then

$$(5.4) \quad \text{T.V.}(p_h(\cdot, t), u_h(\cdot, t)) \leq 2\kappa k \text{T.V.}(p_0, u_0),$$

$$(5.5) \quad \text{T.V.}(\gamma_h(\cdot, t)) \leq \text{T.V.}(\gamma_0).$$

Moreover, the solution is always contained in the domain

$$(5.6) \quad \mathcal{U} = \left\{ (p, u, \gamma) \mid \max\{|p - p_-|, |p - p_+|\} \leq 2\kappa k \text{T.V.}(p_0, u_0), \right. \\ \left. \max\{|u - u_-|, |u - u_+|\} \leq 2\kappa \text{T.V.}(p_0, u_0), \gamma \in (1, \bar{\gamma}] \right\},$$

where $p_{\pm} = p_0(\pm\infty)$ and $u_{\pm} = u_0(\pm\infty)$.

Proof. Let J_n be the mesh curve connecting sampling points at the times $(n+1)\Delta t$ and $n\Delta t$, and let $n\Delta t \leq t < (n+1)\Delta t$. First of all, (5.5) is obvious since γ only changes along contact discontinuities, thus

$$(5.7) \quad \text{T.V.}(\gamma_h(\cdot, t)) = F_{\gamma} = \text{T.V.}(\gamma_h(\cdot, 0)) \leq \text{T.V.}(\gamma_0).$$

We furthermore have that

$$(5.8) \quad L(J_0) \leq \text{T.V.}(p_h(\cdot, 0)) + k \text{T.V.}(u_h(\cdot, 0)) \leq k \text{T.V.}(p_h(\cdot, 0), u_h(\cdot, 0)),$$

where J_0 is the mesh curve connecting sampling points at $t = 0$ and $t = \Delta t$. When (5.2) and (5.3) are satisfied, we therefore have

$$(5.9) \quad L(J_0) \leq k \text{T.V.}(p_h(\cdot, 0), u_h(\cdot, 0)) \leq k \text{T.V.}(p_0, u_0) \leq \frac{C}{9C_1(\bar{\gamma} - 1)},$$

$$(5.10) \quad F_{\gamma} = \text{T.V.}(\gamma_h(\cdot, 0)) \leq \text{T.V.}(\gamma_0) \leq \frac{C}{9C_2},$$

hence, the Glimm functional is decreasing and $F(J_n) \leq \frac{5}{3}L(J_0)$ by Lemma 3.3. We use this first to find a bound on $\text{T.V.}(u_h(\cdot, t))$. Since u is increasing along all rarefaction waves and decreasing along all shock waves, we have

$$(5.11) \quad \sum_{\text{rf}} \llbracket u \rrbracket = \sum_{\text{shock}} \llbracket u \rrbracket + u(\infty, \cdot) - u(-\infty, \cdot),$$

where $\llbracket u \rrbracket := |u_r - u_l|$ for a wave connecting U_l to U_r , and rf is short for rarefaction wave. Let $c := |u(\infty, \cdot) - u(-\infty, \cdot)| = |u_+ - u_-|$, then

$$(5.12) \quad \sum_{\text{rf}} \llbracket u \rrbracket \leq \sum_{\text{shock}} \llbracket u \rrbracket + c,$$

and we have

$$\begin{aligned} \text{T.V.}(u_h(\cdot, t)) &= \text{T.V.}(u_h|_{J_n}) = \sum_{\text{rf}} \llbracket u \rrbracket + \sum_{\text{shock}} \llbracket u \rrbracket \leq 2 \sum_{\text{shock}} \llbracket u \rrbracket + c \\ &\leq 2 \sum_{\text{shock}} |s'(\tilde{p}, p_l, \gamma_l)| \llbracket p \rrbracket + c \leq 2s'_{\max} \sum_{\text{shock}} \llbracket p \rrbracket + c \\ &= 2s'_{\max} F_n + c \leq 2s'_{\max} \frac{5}{3} L_0 + c \\ &= \frac{10}{3} s'_{\max} k \text{T.V.}(p_0, u_0) + c \leq \kappa \text{T.V.}(p_0, u_0), \end{aligned}$$

where we have used that $c \leq \text{T.V.}(u_0)$. For $\text{T.V.}(p_h(\cdot, t))$ we find

$$\begin{aligned} \text{T.V.}(p_h(\cdot, t)) &= \text{T.V.}(p_h|_{J_n}) = \sum_{\text{rf}} \llbracket p \rrbracket + \sum_{\text{shock}} \llbracket p \rrbracket \leq k \left(\sum_{\text{rf}} \llbracket u \rrbracket + \sum_{\text{shock}} \llbracket u \rrbracket \right) \\ &= k \text{T.V.}(u_h) \leq \kappa k \text{T.V.}(p_0, u_0), \end{aligned}$$

and moreover,

$$\text{T.V.}(p_h(\cdot, t), u_h(\cdot, t)) = \text{T.V.}(p_h(\cdot, t)) + \text{T.V.}(u_h(\cdot, t))$$

$$(5.13) \quad \leq 2\kappa k T.V.(p_0, u_0).$$

To show the last part of the lemma we use that

$$\sup(y) \leq |y(\infty)| + |y(-\infty)| + T.V.(y),$$

and since $p_h(\pm\infty, \cdot) = p_0(\pm\infty)$, we find

$$\begin{aligned} \sup(p_h - p_0(\infty)) &\leq |p_h(\infty, \cdot) - p_0(\infty)| + |p_h(-\infty, \cdot) - p_0(\infty)| + T.V.(p_h) \\ &= |p_0(\infty) - p_0(-\infty)| + T.V.(p_h) \\ &\leq 2T.V.(p_h) \leq 2\kappa k T.V.(p_0, u_0). \end{aligned}$$

Furthermore,

$$\begin{aligned} \sup(p_h - p_0(-\infty)) &\leq 2\kappa k T.V.(p_0, u_0), \\ \sup(u_h - u_0(\infty)) &\leq 2\kappa T.V.(p_0, u_0), \\ \sup(u_h - u_0(-\infty)) &\leq 2\kappa T.V.(p_0, u_0). \end{aligned}$$

We can do the same for γ , but since $\gamma_h(\cdot, t)$ only takes the same values as $\gamma_h(\cdot, 0)$, we know that γ always lies between 1 and $\bar{\gamma}$. In other words, $U_h(\cdot, t)$ is always contained in \mathcal{U} given by (5.6). \square

Let us now prove that $U_h(x, t)$ is bounded, and in particular, bounded away from vacuum. First of all, the Riemann problems we solve at the first step in the Glimm scheme must have a solutions without vacuum, that is, all jumps in $U_h(x, 0)$ must satisfy (2.27), cf. Lemma 2.4. If the initial data, for any $a_0 \in [-1, 1]$, satisfy

$$(5.14) \quad \begin{aligned} &u_0(y_{r-1}^0-) - u_0(y_{r+1}^0-) \\ &< r(p_0(y_{r-1}^0-), 0, \gamma_0(y_{r-1}^0-)) - r(0, p_0(y_{r+1}^0-), \gamma_0(y_{r+1}^0-)), \quad r \text{ even,} \end{aligned}$$

where $y_r^0 = x_r + a_0 h$, then no vacuum forms at the first step. The approximate solution is contained in \mathcal{U} which is bounded by the total variation of the initial data, thus, by imposing an extra condition on the initial data, we ensure that all $U \in \mathcal{U}$ have $p \geq p_{\min} > 0$.

Lemma 5.2. *If for a $p_{\min} > 0$ the initial data satisfy*

$$(5.15) \quad (\bar{\gamma} - 1)T.V.(p_0, u_0) \leq C_3,$$

where $\tilde{p} = \max\{p_0(\infty), p_0(-\infty)\}$ and

$$(5.16) \quad C_3 := \frac{\bar{\gamma}^{1/2}}{\kappa k r'_{\max}} \left(\tilde{p}^{\frac{\bar{\gamma}-1}{2\bar{\gamma}}} - p_{\min}^{\frac{\bar{\gamma}-1}{2\bar{\gamma}}} \right).$$

Then $p \geq p_{\min}$ for all $U \in \mathcal{U}$. Moreover, the solution obtained using the Glimm scheme is bounded and, in particular, satisfies $0 < p_{\min} \leq p_h(x, t) \leq p_{\max}$.

Proof. For a $p < \min(p_0)$ we have

$$\max\{|p - p(\infty)|, |p - p(-\infty)|\} = \max\{p(\infty), p(-\infty)\} - p = \tilde{p} - p,$$

hence, p is in \mathcal{U} if $\tilde{p} - p \leq 2\kappa k T.V.(p_0, u_0)$. Thus, if

$$(5.17) \quad 2\kappa k T.V.(p_0, u_0) \leq \tilde{p} - p_{\min},$$

for a given p_{\min} so that $0 < p_{\min} \leq \min(p_0)$, then $p \geq p_{\min}$ for all $U \in \mathcal{U}$.

Since condition (5.2) gives restriction on $(\bar{\gamma} - 1)\text{T.V.}(p_0, u_0)$, we reformulate condition (5.17) to do the same. For a $p_0 \geq \tilde{p} \geq p_{\min}$ there is a u_0 so that we can write

$$u(p) = u_0 - r(p, p_0, \bar{\gamma}).$$

From the mean value theorem we get that

$$|\tilde{p} - p_{\min}| = \frac{1}{|u'(\hat{p})|} |u(\tilde{p}) - u(p_{\min})| \geq \frac{1}{r'_{\max}} (u(p_{\min}) - u(\tilde{p})),$$

for $p_{\min} \leq \hat{p} \leq \tilde{p}$. Furthermore,

$$\begin{aligned} u(p_{\min}) - u(\tilde{p}) &= u_0 - \frac{2\bar{\gamma}^{\frac{1}{2}}}{\bar{\gamma} - 1} \left(p_{\min}^{\frac{\bar{\gamma}-1}{2\bar{\gamma}}} - p_0^{\frac{\bar{\gamma}-1}{2\bar{\gamma}}} \right) - u_0 + \frac{2\bar{\gamma}^{\frac{1}{2}}}{\bar{\gamma} - 1} \left(\tilde{p}^{\frac{\bar{\gamma}-1}{2\bar{\gamma}}} - p_0^{\frac{\bar{\gamma}-1}{2\bar{\gamma}}} \right) \\ &= \frac{2\bar{\gamma}^{\frac{1}{2}}}{\bar{\gamma} - 1} \left(\tilde{p}^{\frac{\bar{\gamma}-1}{2\bar{\gamma}}} - p_{\min}^{\frac{\bar{\gamma}-1}{2\bar{\gamma}}} \right), \end{aligned}$$

so that

$$\tilde{p} - p_{\min} \geq \frac{2\bar{\gamma}^{1/2}}{(\bar{\gamma} - 1)r'_{\max}} \left(\tilde{p}^{\frac{\bar{\gamma}-1}{2\bar{\gamma}}} - p_{\min}^{\frac{\bar{\gamma}-1}{2\bar{\gamma}}} \right).$$

Therefore, we have that $p \geq p_{\min} > 0$ for all $p \in \mathcal{U}$ if

$$(5.18) \quad 2\kappa k \text{T.V.}(p_0, u_0) \leq \frac{2\bar{\gamma}^{1/2}}{(\bar{\gamma} - 1)r'_{\max}} \left(\tilde{p}^{\frac{\bar{\gamma}-1}{2\bar{\gamma}}} - p_{\min}^{\frac{\bar{\gamma}-1}{2\bar{\gamma}}} \right),$$

which proves the lemma. \square

We have proved that $U_h(x, t)$ given by (3.4) is bounded and have bounded total variation. Similar to Corollary 19.8 in [20], it can then be proved that $U_h(x, t)$ is locally L^1 Lipschitz continuous in time. As already noted, these are the three conditions needed to ensure that $U_h(x, t)$ converges to a weak solution of (1.1). Hence, we have the following theorem:

Theorem 5.3. *Consider the Cauchy problem for system (1.1) with bounded initial data (1.2) where $\inf(p_0(x)) > 0$ and $1 < \gamma_0(x) < \bar{\gamma}$. Assume that the initial data satisfies (5.14) so that no vacuum occurs initially. If*

$$(5.19) \quad (\bar{\gamma} - 1)\text{T.V.}(p_0, u_0) \leq \min \left\{ \frac{C}{9kC_1}, C_3 \right\},$$

$$(5.20) \quad \text{T.V.}(\gamma_0(x)) \leq \frac{C}{9C_2},$$

then there exists a time global weak entropy solution with bounded total variation of system (1.1).

By the results of Wagner [23], there is a one-to-one correspondence between a weak solution of (1.1) and a weak solution of the system given in Eulerian coordinates,

$$(5.21) \quad \begin{aligned} \rho_t + (\rho u)_x &= 0, \\ (\rho u)_t + (\rho u^2 + p(\rho, \gamma))_x &= 0, \\ (\rho \gamma)_t + (\rho u \gamma)_x &= 0, \end{aligned}$$

where $x \in \mathbb{R}$ is the physical space variable and $t \in (0, \infty)$ denotes time.

Theorem 5.4. *If there exists a global weak solution to system (1.1) with initial data (1.2), then there exists a global weak solution of system (5.21) where $0 < \rho_{\min} \leq \rho(x, t) \leq \rho_{\max} < \infty$.*

6. NUMERICAL RESULTS

We have implemented the Glimm scheme as described in Subsection 3.1 using MATLAB. The random sequence $a(s)$ is generated using the function `rand` and `imagesc` is used to visualize the solution.

We find p_{\max} as described in Subsection 2.3. Instead of using (5.15) to find p_{\min} , we choose a suitable candidate for p_{\min} and then check that this candidate indeed satisfy $p_{\min} \leq p_h(x, t)$ for all x and t . We have chosen

$$(6.1) \quad p_{\min} = \min(p_0(x)) - (p_{\max} - \max(p_0(x))),$$

as our candidate, and for both examples this is a good lower bound on $p(x, t)$. In both examples the initial data satisfy (5.2) and (5.3). Since we also have an upper and a lower bound on $p_h(x, t)$, these initial data satisfy the conditions of Theorem 5.3.

Example 1: Piecewise constant initial data. The initial data in this example are piecewise constant and symmetric. We have one gas with $p = 1.26$, $u = 3.00$ and $\gamma = 1.051$ which is initially trapped between a second gas with $p = 1.30$, $u = 2.99$ and $\gamma = 1.010$. The constants calculated for this example are listed in Table 1, and

TABLE 1. The constants for Example 1.

p_{\max}	p_{\min}	$\bar{\gamma}$	C_1	C_2	C	k
1.3067	1.2534	1.051	15.9703	1.3309	1	1.3309

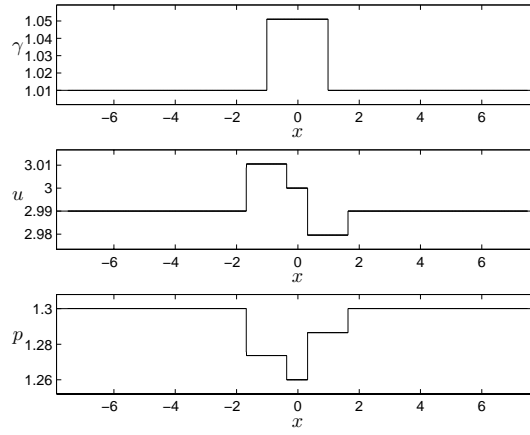
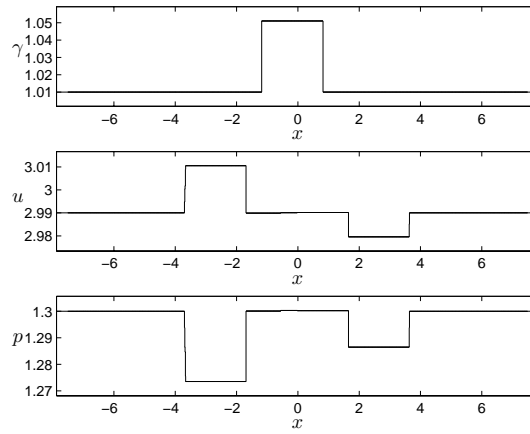
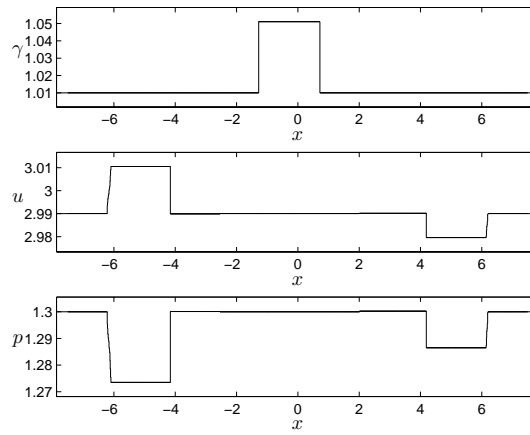
(5.2) and (5.3) are satisfied since

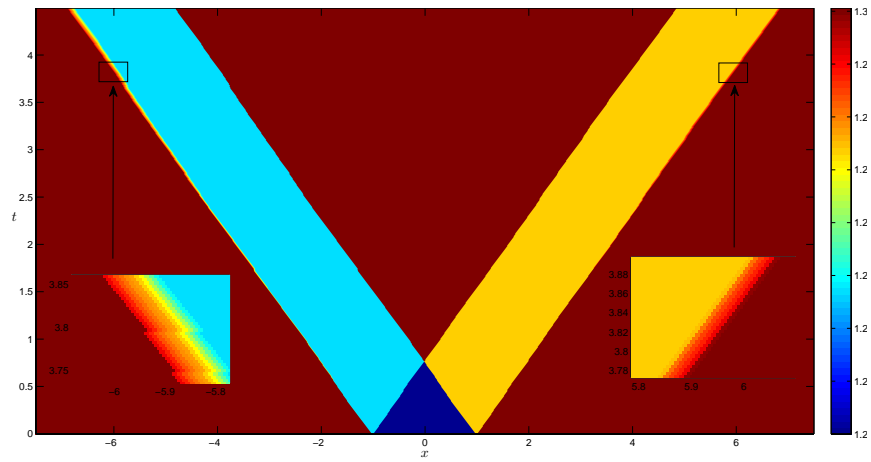
$$(6.2) \quad \text{T.V.}(p_0, u_0) = 0.1 \leq 0.1025 = C/(9kC_1(\bar{\gamma} - 1)),$$

$$(6.3) \quad \text{T.V.}(\gamma_0) = 0.082 \leq 0.0835 = C/(9C_2).$$

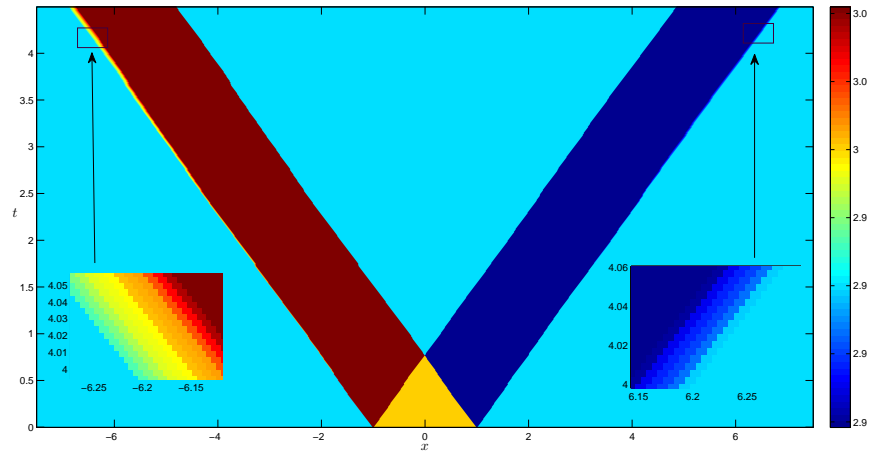
The solution is computed up to the time $T = 4.5$ using $\Delta x = 0.005$ and $\Delta x/\Delta t = 1.3805 = \max |\lambda(U)|$ so that condition (3.1) is satisfied. This corresponds to 1500×1242 mesh points. Figure 44 shows the solution for different times. The solution of the Riemann problem initially situated at $x = -1.0$ consists of a 1-rarefaction wave, a contact discontinuity and a 3-shock wave, while the solution of the Riemann problem at $x = 1.0$ consists of a 1-shock wave, a contact discontinuity and a 3-rarefaction wave. In Fig. 45 one can see how the waves from these two initially Riemann problems evolve in time and space, and how they interact. Moreover, Fig. 46 shows the decreasing Glimm functional for this example.

Example 2: Continuous initial data. In this example the initial data are constant for $x < -1$ and $x > 1$. For $-1 < x < 1$ we have a smooth function connecting the constant states. For p and γ this function is an increasing function based on $\sin x$, while for u the two constant states are equal and connected by a function based on $\cos x$.

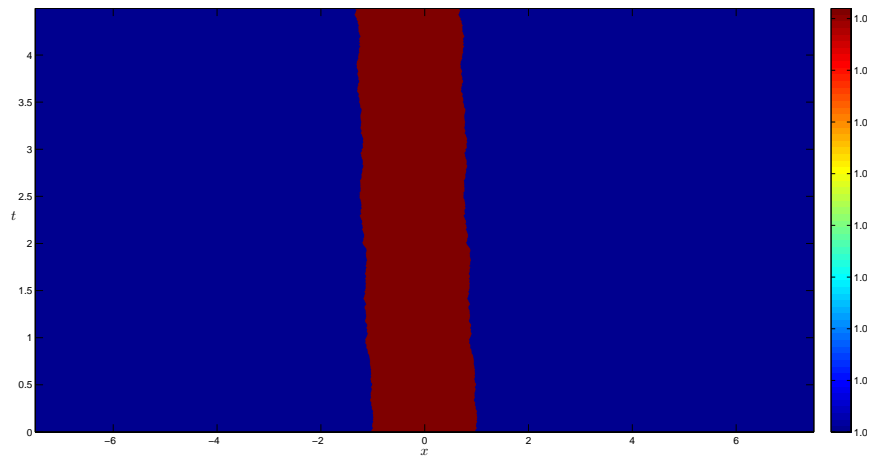
(a) $t = 0.507$.(b) $t = 2.039$.(c) $t = 4.002$.FIGURE 44. $U_h(x, t)$ at different times.



(a) $p_h(x, t)$.



(b) $u_h(x, t)$.



(c) $\gamma_h(x, t)$.

FIGURE 45. The solution $U_h(x, t)$ in the (x, t) -plane.

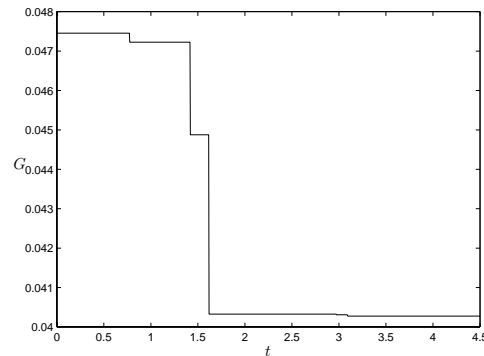


FIGURE 46. The Glimm functional for Example 1.

TABLE 2. The constants for Example 2.

p_{\max}	p_{\min}	$\bar{\gamma}$	C_1	C_2	C	k
1.323	1.277	1.098	15.4427	1.3691	1	1.3691

The constants for this example are listed in Table 2, and (5.2) and (5.3) are satisfied since

$$(6.4) \quad \text{T.V.}(p_0, u_0) = 0.0533 \leq 0.0536 = C/(9kC_1(\bar{\gamma} - 1)),$$

$$(6.5) \quad \text{T.V.}(\gamma_0) = 0.0799 \leq 0.0812 = C/(9C_2).$$

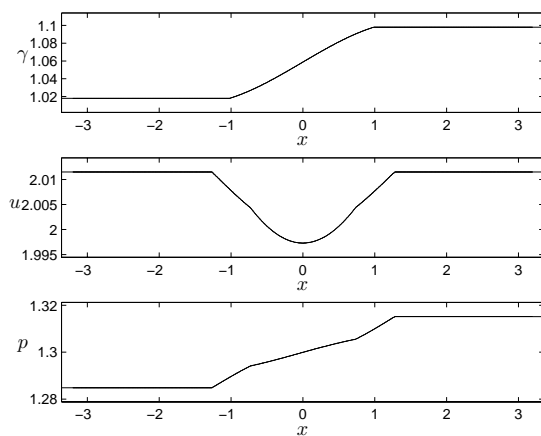
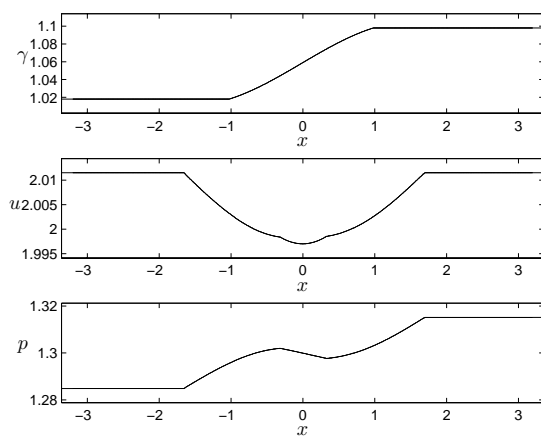
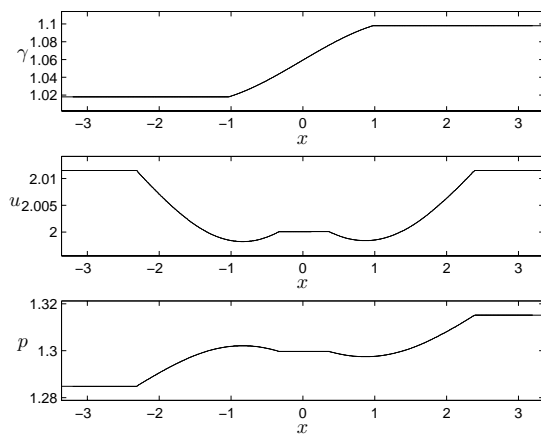
The solution is computed up to the time $T = 1.4$ using $\Delta x = 0.002$ and $\Delta x/\Delta t = 1.4185 = \max |\lambda(U)|$ so that condition (3.1) is satisfied. This corresponds to 1600×992 mesh points. Figure 47 shows the solution at different times, and Fig. 48 shows how the waves from all the initial Riemann problems interact and evolve. Finally, Fig. 49 shows the decreasing Glimm functional for this example.

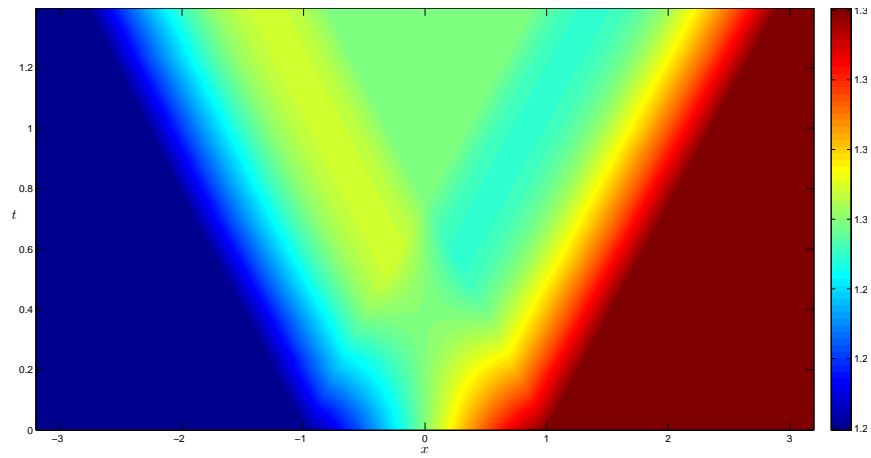
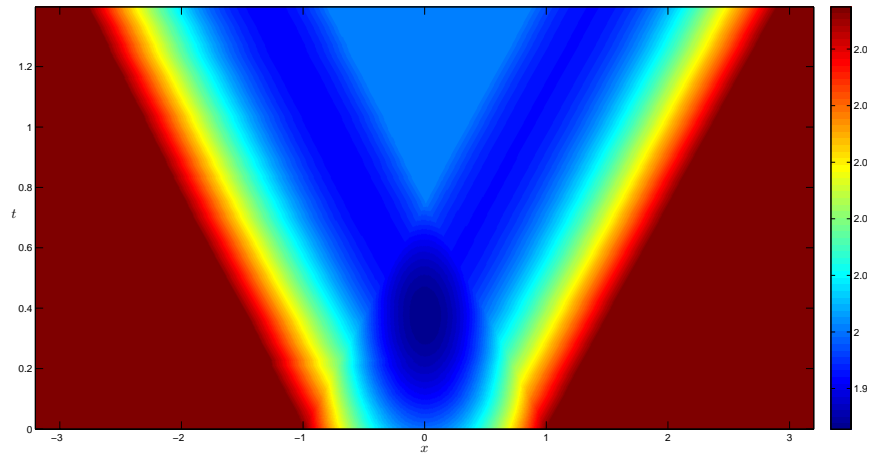
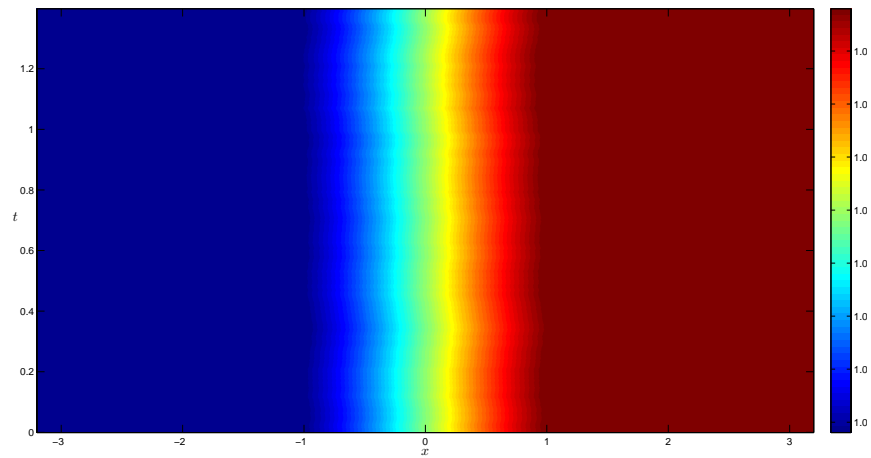
ACKNOWLEDGMENTS

This research was supported in part by the Research Council of Norway.

REFERENCES

- [1] D. Amadori and A. Corli. On a model of multiphase flow. arXiv:math.AP/0605057 v2 7 July 2007.
- [2] F. Asakura. Wave-front tracking for the equation of non-isentropic gas dynamics. *RIMS Kokyuroku*, 1495:78–91, 2006.
- [3] F. Asakura. Wave-front tracking for the equation of isentropic gas dynamics. *Quart. Appl. Math.*, 63(1):20–33, 2005.
- [4] A. Bressan and R. M. Colombo. Unique solutions of 2×2 conservation laws with large data. *Indiana Univ. Math. J.*, 44(3):677–725, 1993.
- [5] C. Chalons and F. Coquel. Navier–Stokes equations with several independent pressure laws and explicit predictor-corrector schemes. *Numer. Math.* 101:451–478, 2005.
- [6] R. J. DiPerna. Existence in the large for quasilinear hyperbolic conservation laws. *Arch. Rational Mech. Anal.*, 52:244–257, 1973.
- [7] S. Evje and K. H. Karlsen. Global existence of weak solutions for a viscous two-phase model. *J. Differential Equations*, to appear.

(a) $t = 0.203$.(b) $t = 0.509$.(c) $t = 1.018$.FIGURE 47. $U_h(x, t)$ at different times.

(a) $p_h(x, t)$.(b) $u_h(x, t)$.(c) $\gamma_h(x, t)$.FIGURE 48. The solution $U_h(x, t)$ in the (x, t) -plane.

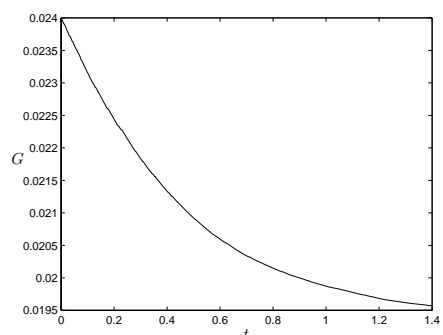


FIGURE 49. The Glimm functional for Example 2.

- [8] H. Fan. On a model of the dynamics of liquid/vapor phase transitions. *SIAM J. Appl. Math.*, 60(4):1270–1301, 2000.
- [9] J. Glimm. Solution in the large for nonlinear hyperbolic systems of equations. *Comm. Pure Appl. Math.*, 18:697–715, 1965.
- [10] D. Hoff. Invariant regions for systems of conservation laws. *Trans. Amer. Math. Soc.*, 289(2):591–610, 1985.
- [11] H. Holden and N. H. Risebro. *Front Tracking for Hyperbolic Conservation Laws*. Springer-Verlag, 2002.
- [12] T.-P. Liu. Solutions in the large for the equations of nonisentropic gas dynamics. *Indiana Univ. Math. J.*, 26(1):147–177, 1977.
- [13] T. P. Liu and J. A. Smoller. On the vacuum state for the isentropic gas dynamics equations. *Adv. in Appl. Math.*, 1(4):345–359, 1980.
- [14] Y. Lu. *Hyperbolic Conservation Laws and the Compensated Compactness Method*. Chapman&Hall/CRC, Boca Raton, 2003.
- [15] T. Nishida. Global solution for an initial boundary value problem for a quasilinear hyperbolic system. *Proc. Japan Acad.*, 44:642–646, 1968.
- [16] T. Nishida and J. A. Smoller. Solution in the large for some nonlinear hyperbolic conservation laws. *Comm. Pure Appl. Math.*, 26:183–200, 1973.
- [17] Y.-J. Peng. Solutions faibles globales pour l'équation d'Euler d'un fluide compressible avec de grandes données initiales. *Comm. Partial Differential Equations*, 17(1-2):161–187, 1992.
- [18] Y.-J. Peng. Solutions faibles globales pour un modèle d'écoulements diphasiques. *Ann. Scuola Norm. Sup. Pisa Cl. Sci. (4)*, 21(4):523–540, 1994.
- [19] D. Serre. *System of Conservation Laws 1: Hyperbolicity, Entropies, Shock Waves*. Cambridge University Press, Cambridge, 1999.
- [20] J. Smoller. *Shock Waves and Reaction-Diffusion Equations*. Springer-Verlag, second edition, 1994.
- [21] J. B. Temple. Solution in the large for the nonlinear hyperbolic conservation laws of gas dynamics. *J. Differential Equations*, 41:96–161, 1981.
- [22] B. Temple and R. Young. The large time stability of sound waves. *Comm. Math. Phys.*, 179(2):417–466, 1996.
- [23] D. H. Wagner. Equivalence of the Euler and Lagrangian equations of gas dynamics for weak solutions. *J. Differential Equations*, 68(1):118–136, 1987.
- [24] W.-A. Yong. A simple approach to Glimm's interaction estimates. *Appl. Math. Lett.*, 12(2):29–34, 1999.
- [25] B. D. Wissmann. Global solutions to the ultra-relativistic Euler equations. arXiv:0705.1333v1 [math.AP] 9 May 2007.

(Holden)

DEPARTMENT OF MATHEMATICAL SCIENCES, NORWEGIAN UNIVERSITY OF SCIENCE AND TECHNOLOGY, NO-7491 TRONDHEIM, NORWAY, AND
CENTRE OF MATHEMATICS FOR APPLICATIONS, UNIVERSITY OF OSLO, P.O. BOX 1053, BLINDERN, NO-0316 OSLO, NORWAY

E-mail address: holden@math.ntnu.no

URL: www.math.ntnu.no/~holden/

(Risebro)

CENTRE OF MATHEMATICS FOR APPLICATIONS, UNIVERSITY OF OSLO, P.O. BOX 1053, BLINDERN, NO-0316 OSLO, NORWAY

E-mail address: nilshr@math.uio.no

URL: www.math.uio.no/~nilshr/

(Sande)

DEPARTMENT OF MATHEMATICAL SCIENCES, NORWEGIAN UNIVERSITY OF SCIENCE AND TECHNOLOGY, NO-7491 TRONDHEIM, NORWAY

E-mail address: hildes@math.ntnu.no

URL: www.math.ntnu.no/~hildes/